

Recent advances in polymer and polymer composite membranes for reverse and forward osmosis processes

Dan Li¹, Yushan Yan³, Huanting Wang²

1. Chemical and Metallurgical Engineering and Chemistry, School of Engineering and Information Technology, Murdoch University, WA, 6150, Australia. Email: l.li@murdoch.edu.au
2. Department of Chemical Engineering, Monash University, VIC, 3800, Australia. Email: huanting.wang@monash.edu
3. Department of Chemical & Biomolecular Engineering, University of Delaware, Newark, DE 19711, USA.

Abstract:

Semipermeable membranes are the core elements for membrane water desalination technologies such as commercial reverse osmosis (RO) process and emerging forward osmosis (FO) process. Structural and chemical properties of the semipermeable membranes determine water flux, salt rejection, fouling resistance, and chemical stability, which greatly impact energy consumption and costs in osmosis separation processes. In recent years, significant progress has been made in the development of high-performance polymer and polymer composite membranes for desalination applications. This paper reviews recent advances in different polymer-based RO and FO desalination membranes in terms of materials and strategies developed for improving properties and performances.

Keywords: Polymer membrane; mixed matrix membrane; reverse osmosis; forward osmosis; desalination

Table of Contents

Nomenclature	44	Formatted: Font color: Auto
1. Introduction	77	Formatted: Font color: Auto
2. Reverse osmosis membranes	1040	Formatted: Font color: Auto
2.1 Polymeric materials	1040	Formatted: Font color: Auto
2.1.1 Cellulosic derivatives	1144	Formatted: Font color: Auto
2.1.2 Polyamide and related polymers	1242	Formatted: Font color: Auto
2.1.2.1 Effect of support materials and microstructures on membrane performances	1343	Formatted: Font color: Auto
2.1.2.2 Modification of active layer towards improved flux and rejection	1444	Formatted: Font color: Auto
2.1.2.3 Modification of active layer towards enhanced fouling resistance	1949	Formatted: Font color: Auto
2.1.2.4 Modification of active layer towards increased chlorine stability	2727	Formatted: Font color: Auto
2.1.3 Polyelectrolytes	3030	Formatted: Font color: Auto
2.1.4 Aquaporin biomimetic membranes	3134	Formatted: Font color: Auto
2.2 Mixed matrix membranes	3535	Formatted: Font color: Auto
2.2.1 Ag and TiO ₂	3636	Formatted: Font color: Auto
2.2.2 Zeolite and silica	3838	Formatted: Font color: Auto
2.2.3 Carbon nanotubes and graphene oxide	4144	Formatted: Font color: Auto
3. Forward osmosis membranes	4444	Formatted: Font color: Auto
3.1 Polymeric membranes	4444	Formatted: Font color: Auto
3.1.1 Cellulosic derivatives	4444	Formatted: Font color: Auto
3.1.2 Polyamide and related polymers	4747	Formatted: Font color: Auto
3.1.2.1 Effect of support properties on membrane performances	4848	Formatted: Font color: Auto
3.1.2.2 Effect of active layer on membrane performances	5154	Formatted: Font color: Auto
3.1.3 Polyelectrolytes	5353	Formatted: Font color: Auto
3.1.4 Others	5555	Formatted: Font color: Auto
3.2 Mixed matrix membranes	5858	Formatted: Font color: Auto
4. Conclusions and future perspectives	5959	Formatted: Font color: Auto
Acknowledgement	6363	Formatted: Font color: Auto

References.....6464

Figure Captions.....8585

Table Captions106106

Formatted: Font color: Auto

Formatted: Font color: Auto

Formatted: Font color: Auto

Nomenclature

AA	acrylic acid
AAPTS	<i>N</i> -[3-(trimethoxysilyl) propyl] ethylenediamine
ABA	poly-(2-methyloxazoline)-poly-(dimethylsiloxane)-poly-(2-methyloxazoline)
AEPPS	<i>N</i> -aminoethyl piperazine propane sulfonate
AL-DS	a mode of active layer facing the draw solution; also called as pressure retarded osmosis (PRO)
AL-FS	a mode of active layer facing the feed solution; also called as forward osmosis mode (FO)
AQP	aquaporin
BWRO	brackish water reverse osmosis
CA	cellulose acetate
CAP	cellulose acetate propionate
CFIC	chloroformyloxyisophthaloyl chloride
CLSM	confocal laser scanning microscopy
CNTs	carbon nanotubes
CP	concentration polarization
CSA	camphorsulfonic acid
CTA	cellulose triacetate
CTAC	cetyltrimethylammonium chloride
DABA	3,5-diamino- <i>N</i> -(4-aminophenyl) benzamide
DMAc	dimethylacetamide
DMMPD	<i>N,N'</i> -dimethyl- <i>m</i> -phenylenediamine
DOTAP	1,2-dioleoyl-3-trimethylammonium-propane (chloride salt)
DOPC	1,2-dioleoyl- <i>sn</i> -glycero-3-phosphocholine
DTAB	dodecyl trimethyl ammonium bromide
<i>E. coli</i>	<i>Escherichia coli</i>
FO	forward osmosis
GMA	glycidyl methacrylate
gMH	g/m ² . h
HTI	Hydration Technologies Inc.
ICP	internal concentration polarization

iCVD	initiated chemical vapour deposition
IP	interfacial polymerization
IPC	isophthaloyl chloride
IU	imidazolidinyl urea
LbL	layer-by-layer
LCST	lower critical solution temperature
L-DOPA	3-(3,4-dihydroxyphenyl)-L-alanine
LMH	L/m ² . h
MMMs	mixed matrix membranes
MOF	porous metal-organic framework
MPD	<i>m</i> -phenylenediamine
MWCNTs	multi-walled carbon nanotubes
NIPAM	<i>N</i> -isopropylacrylamide
NMP	<i>N</i> -methylpyrrolidone
<i>o</i> -ABA-TEA	<i>o</i> -aminobenzoic acid-triethylamine salt
PAA	poly(acrylic acid)
PAH	poly(allylamine hydrochloride)
P(Am-co-AA)	poly(acrylamide- <i>co</i> -acrylic acid)
PAI	poly(amide-imide)
PAN	polyacrylonitrile
PBI	polybenzimidazole
PCTE	polycarbonate tracked-etched
PD	<i>p</i> -phenylene diamine
PDA	polydopamine
PDADMAC	poly(diallyl-dimethylammonium chloride)
PEG	polyethylene glycol
PEI	polyethyleneimine
PES	polyethersulfone
PESU-co-sPPSU	sulfonated copolymer made of polyethersulfone and polyphenylsulfone
PET	polyester
PETA	polyethylene terephthalate
PI	polyimide
PIP	piperazine
PLL	poly-L-lysine

PMOXA-PDMS-PMOXA	poly(2-methyloxazoline)- <i>block</i> -poly(dimethylsiloxane)- <i>block</i> -poly(2-methyloxazoline)
PNIPAM	poly(<i>N</i> -isopropylacrylamide)
P(NIPAM-co-Am)	poly(<i>N</i> -isopropylacrylamide- <i>co</i> -acrylamide)
POSS	polyhedral oligomeric silsesquioxane
PPD	<i>p</i> -phenylenediamine
PPENK	poly(phthalazone ether nitrile ketone)
PRO	pressure retarded osmosis
PSf	polysulfone
PSS	poly(sodium 4-styrenesulfonate)
PTA-POD	polytriazole- <i>co</i> -polyoxadiazole
<i>P. putida</i>	<i>Pseudomonas putida</i>
PVA	polyvinyl alcohol
PVDF	polyvinylidene fluoride
PVP	polyvinylpyrrolidone
rGO	reduced graphene oxide
SEM	scanning electron microscopy
SDS	sodium dodecyl sulfate
SLS	sodium lauryl sulfate
SPEK	sulphonated poly(ether ketone)
sPPSU	sulfonated polyphenylsulfone
SPSf	sulfonated polysulfone
S_i	structural parameter
<i>S. aureus</i>	<i>Staphylococcus aureus</i>
SWNTs	single-wall nanotubes
SWRO	seawater reverse osmosis
TBP	tributyl phosphate
TEA	triethylamine
TEOA	triethanolamine
TFC	thin film composite
TFN	thin film nanocomposite
TMC	1,3,5-trimesoylchloride
TPP	triphenyl phosphate
UF	ultrafiltration

1. Introduction

Membrane technology has become a popular option for a wide range of separation, including water and gas, over the past decades. Due to advantageous features using membrane separation, e.g. no or little need for chemicals, easy scale-up, and relatively low energy use, membrane separation has been widely adopted in a range of industries including water desalination. Desalination is a process for removing salts existing in saline water and providing fresh water suitable for human consumption as well as industrial and agricultural purposes, and has been considered as a reliable and effective approach to ease global water scarcity crisis. [1]

Among various membrane-based desalination processes developed thus far, reverse osmosis (RO) membrane process has played a leading role in desalination industry suppressing others because of advantages in combined capital cost and energy consumption. [2-5]

RO desalination is a typical pressure-driven process, in which an external hydraulic pressure is applied as driving force and solutes are excluded by a semipermeable membrane (called RO membrane) (Fig. 1a). [6]

One of significant breakthroughs in RO desalination industry was successful development of cellulose acetate (CA) asymmetric membrane using phase inversion technique and its commercialization. [7-9] Fig.

2a exemplifies a cross-sectional scanning electron microscope (SEM) image of commercial CA asymmetric membrane with a thin solute-rejecting dense layer (~100 nm - 200 nm thickness) and an open porous substructure, [10] both which are made of one polymeric material, on top of a fabric support. Cellulosic derivatives and their fabricated membranes have shown a number of good properties, including hydrophilicity, mechanical strength, wide availability, chlorine tolerance, fouling resistance, and low cost.

However, some drawbacks exist, such as narrow operating pH and temperature ranges, limited resistance to biological attack, and structural compaction at high operating pressure. [10-13] Since the concept of interfacial polymerization (IP) of creating polyamide (PA) thin film composite (TFC) membrane was introduced by Cadotte and co-workers, [14] the later developed products have largely dominated

desalination membrane market and especially their spiral wound configuration has shared over 90% of market sales. [2] As compared with CA asymmetric membranes, PA TFC membranes, consisting of a non-

woven fabric backing, support layer and top active layer (~100 nm thickness) (illustrated in Fig. 2b), endow

Field Code Changed

Field Code Changed

Field Code Changed

Field Code Changed

Field Code Changed

Field Code Changed

Field Code Changed

Field Code Changed

Field Code Changed

Field Code Changed

Field Code Changed

Field Code Changed

Field Code Changed

Field Code Changed

Field Code Changed

Field Code Changed

improved separation performances, including better water flux and salt retention, and wider operating pH and temperature ranges. However, PA is sensitive to chlorine attack and fouling, which requires costly pre-treatment of feed water, thus increasing desalination costs. [15] Commercial PA TFC RO membranes in general exhibit over 98% of sodium chloride rejection rate. On the other side, as a type of “low-pressure” or “loose” RO membranes, nanofiltration (NF) membranes generally show NaCl rejection of ~20 – 80%, but generate higher water permeability and require lower hydraulic pressure than typical RO membranes. [13] NF has also received considerable attention as a promising pre-treatment for RO, and it usually has a similar chemical structure but loose polymer network compared to PA TFC RO membranes. [5]

Current RO desalination plants consume approximately 3 – 6 kWh energy to produce 1 m³ of fresh water, depending on feed salinity and energy source or recovery. Their energy consumption is usually much lower than those of thermal-based desalination processes (e.g. 10 – 16 kWh/m³ and 6 – 12 kWh/m³ in multi-stage flash and multi-effect distillation, respectively). [16-18] It is well known that a high operating pressure is required in RO, varying from 45 bar to even above 80 bar based on feed salinity, in order to overcome osmotic pressure of saline water and achieve desirable water flux. [16] This takes up 65% – 85% of total energy required in a typical seawater RO (SWRO) desalination and thus contributes to over 25% of total water price. [16] Obviously, by reducing energy consumption and improving energy efficiency in RO, there is an opportunity to further lower the cost of fresh water production. To achieve this, one of feasible solutions is to develop RO membranes with superior water flux while maintaining high salt rejection. Cohen-Tanugi *et al.* modelled and demonstrated the design of ultra-permeable membrane, with 3-fold increase of water permeability and similar salt rejection to the counterpart TFC membrane, could lead to 15 –46% less energy consumption and 44–63% fewer pressure vessels in RO. [19] Moreover, other properties of RO membranes, including fouling resistance and chlorine tolerance, also need to be improved.

Field Code Changed
Field Code Changed

Field Code Changed
Field Code Changed

Field Code Changed
Field Code Changed

Field Code Changed
Field Code Changed

Field Code Changed
Field Code Changed

Field Code Changed
Field Code Changed

Field Code Changed
Field Code Changed

Fig. 1. Schematic diagram illustrating the working principles of (a) reverse osmosis (RO) and (b) forward osmosis (FO) processes. Water flows in different directions in RO and FO (indicated by blue arrows); green arrow shows reverse salt diffusion from draw solution to feed in FO. Hydraulic pressure is utilized as driving force in RO, whilst osmotic pressure differential between feed and draw solution serves as driving force in FO. [20]

Field Code Changed

Field Code Changed

In parallel, some emerging technologies have attracted enormous research interest. In particular, forward osmosis (FO) holds promise towards low energy consumption, fouling propensity, and infrastructure requirements. [12, 20-26] Among various applications, FO has shown attractive potential as a pre-treatment for RO, for instance, to dilute feed seawater before RO to reduce osmotic pressure and subsequently energy use of RO. [27] In a typical FO (Fig. 1b), draw solution generates greater osmotic pressure and then drives water from feed through a semipermeable membrane, while rejecting solutes; the water product is separated from diluted draw solution. FO, as an osmotically driven membrane process, can be operated under FO mode or pressure retarded osmosis (PRO) mode. In the later part of this review (Section 3), FO mode (also known as AL-FS) is referred to the process where the support layer of membrane faces the draw solution; whilst PRO mode (also known as AL-DS) means the active layer of membrane faces the draw solution. Similarly, the membrane in FO process (FO membrane) acts as a selective barrier to govern water transport and solute retention, which is essential in controlling separation efficiency and effectiveness. The initial attempt to use RO membrane in FO process encountered some limitations; low flux was observed due to unfavourable properties of the membrane, e.g. thick sponge-like substrate and compact support, largely hindering mass transfer and causing severe internal concentration polarization (ICP) within the support. [28-30] Hydration Technologies, Inc. (HTI) developed the first commercial FO membranes, [31] one of which has a characteristic structure of embedding cellulose triacetate (CTA) within a thin polyester mesh support (Fig. 2c). Those membranes offer significantly better separation performance than commercially available RO membranes. Apart from commercial CTA FO membranes, HTI later launched TFC FO membrane; the flux of its spiral element was more than double than the existing CTA membranes. This is believed to

Field Code Changed

Field Code Changed

Field Code Changed

Field Code Changed

Field Code Changed

Field Code Changed

Field Code Changed

Field Code Changed

Field Code Changed

provide a new benchmark in future studies of FO membranes. [32] Nevertheless, FO membranes with superior water permeability and salt rejection are still being pursued for commercialization.

Field Code Changed
Field Code Changed

FO and RO membranes share some similarity in terms of properties. [33] An ideal RO or FO membrane would possess high water flux, good salt rejection, fouling resistance, chemical stability, and other characteristics, e.g. mechanical strength and thermal stability; all of which are strongly dependent on membrane intrinsic structure and chemistry. FO membranes are expected to have a low structural parameter (Sr), which is correlated to membrane wettability, porosity, tortuosity and thickness of supports, without compromising mechanical strength. Some recent papers have reviewed the development of RO desalination, and they have more or less covered the progress of desalination membranes and materials. [1, 2, 4, 6, 13, 33-44] Meanwhile, recent progress in FO has been highlighted from the aspects of draw solution, system design to membrane fabrication. [12, 20-26, 45-50] Our review paper published in 2010 included the advances of RO desalination membranes up to that time. [51] Since then, a significant amount of work has been conducted in this field. Therefore, the present review intends to provide an overview of the development of different polymer-based materials for fabricating separation membranes, including RO (Section 2) and FO (Section 3), over the past several years. It focuses on material selection, membrane preparation, and their impact on improving membrane properties and performances, *i.e.*, water flux, salt rejection, fouling resistance and chlorine stability. Some discussions are also made to provide insights into future membrane research directions.

Field Code Changed
Field Code Changed

Field Code Changed
Field Code Changed
Field Code Changed
Field Code Changed
Field Code Changed
Field Code Changed
Field Code Changed
Field Code Changed
Field Code Changed
Field Code Changed
Field Code Changed

Fig. 2. Cross-sectional SEM images showing examples of CA RO membrane (a; GE Osmonics CE), PA TFC RO membrane (b; Dow Filmtec SW30 XLE), and CTA FO membrane (c; HTI). [52]

Field Code Changed
Field Code Changed

2. Reverse osmosis membranes

2.1 Polymeric materials

Seen from tremendous efforts made in RO polymeric membranes, [2, 11, 36, 41] researchers have been exploring polymeric materials that are of low cost, and have good mechanical strength and chemical stability, and proper solubility for membrane fabrication. High water permeability and salt selectivity with improved

Field Code Changed
Field Code Changed
Field Code Changed
Field Code Changed
Field Code Changed

antifouling capacity and chlorine resistance are some main targets. Until now, a wide range of polymers have been investigated for their feasibility as membrane materials, including tris(2,4,6-trimethoxyphenyl)polysulfone-methylene quaternary phosphonium-hydroxide, poly(furfuryl alcohol), chitosan, and sulfonated poly(arylene ether sulfone), *etc.*; [53-70] apart from traditional materials, CA and PA. Moreover, special focus has been on the use of polyelectrolyte and biomimetic aquaporin membranes for water processing.

Field Code Changed

Field Code Changed

2.1.1 Cellulosic derivatives

The use of cellulosic polymers for RO membranes started in 1960's. CA desalination membranes were originally made of cellulose diacetate, triacetate (CTA), or their blends in the form of asymmetric configuration. [10, 13] Last several years have seen some research into improving permeability and selectivity of CA relevant membranes. Most of it utilized phase inversion to produce asymmetric structure, in which effort was made to tailor parameters, including polymer concentration, coagulation bath temperature, type of solvent, addition of additives, *etc.*; despite little covering TFC. [71, 72] For instance, the use of a small amount of polyvinylpyrrolidone (PVP) in casting solution and change of coagulation bath temperature from 0 °C to 25 °C facilitated macrovoid formation and in turn water flux. In contrast, higher PVP concentration (6 wt% in casting solution) or coagulation temperature (50 °C) lowered water flux, due to reduction in macrovoids or membrane hydrophilicity. [73] Blending of chitosan into dope solution formed CA membranes with enhanced rejection, e.g. 92.3% (81.5% for the control membrane), and antibacterial activity against *Escherichia coli* (*E. coli*); [74] however, the low flux made the membranes less competitive, especially in comparison to PA TFC membranes. Addition of inorganic materials such as Ag, TiO₂, carbon nanotubes (CNTs), and ZnO in the fabrication of inorganic-organic mixed matrix membranes (MMMs) could provide a degree of freedom to vary membrane porosity, roughness and hydrophilicity, towards improved membrane performance. [71, 75-79] Especially, introducing porous CNTs might not only improve hydrophilic nature of membrane but also provide channels to connect membrane pores, thus dramatically facilitating water permeation without adverse effect on salt rejection. [75, 76] Furthermore, some inheret

Field Code Changed

Field Code Changed

Field Code Changed

Field Code Changed

Field Code Changed

Field Code Changed

Field Code Changed

Field Code Changed

Field Code Changed

Field Code Changed

Field Code Changed

Field Code Changed

Field Code Changed

Field Code Changed

Field Code Changed

Field Code Changed

properties of inorganic particles such as Ag could endow superior antibacterial and antifouling properties to resulting membranes without expense of flux or rejection. [71, 78]

Field Code Changed

Field Code Changed

Field Code Changed

The properties of CA membranes can be also effectively tuned *via* surface modification. The membranes modified by polymethylhydrosiloxane/polydimethylsiloxane exhibited higher water permeability, which was consistent with the increase of membrane hydrophilicity; but they showed a slight decline in mechanical strength. [80] Hydrolysis and subsequent carboxymethylation of CA hollow fibre enhanced membrane hydrophilicity and negative charge with increasing membrane pore size. [81] Its pure water flux (26 LMH) was more than doubled as compared with the pristine CA hollow fibre at an operating pressure of 5 bar; but the membrane had 25% lower removal of NaCl (using 500 ppm NaCl as feed). [81] By improving surface hydrophilicity and charge density, layer-by-layer (LbL) assembly of 15-bilayer sodium alginate/acidic chitosan polyelectrolyte onto CA membrane increased water flux by ~10% up to approximately 31 LMH at an applied pressure of 15 bar, accompanied with lower susceptibility to BSA protein. [82] However, special care is required to control deposition layers, since excessive coating material may worsen separation flux. [82] This applies to membrane surface modifications involving physical or chemical deposition of other materials. [83]

Field Code Changed

Field Code Changed

Field Code Changed

Field Code Changed

Field Code Changed

Field Code Changed

Field Code Changed

Field Code Changed

Field Code Changed

Field Code Changed

Field Code Changed

Field Code Changed

Despite recent improvements on cellulosic derived membranes, the drawbacks arising from the intrinsic properties including narrow operating pH and temperature as well as propensity to biological attack still make such membranes less competitive for desalination application. PA TFC membranes are currently dominating desalination market and their leading role will not change in the near future.

2.1.2 Polyamide and related polymers

At present, polyamide (PA) thin film composite (TFC) RO membranes are widely used in commercial water treatment processes, especially desalination. They are composed of a porous substrate supported by a non-woven fabric and a thin active layer. Significant research efforts have been focused on enhancing water permeation, salt retention, antifouling property and chlorine resistance by optimizing the chemistry and structure of support and active layer. [11, 15, 36, 84]

Field Code Changed

Field Code Changed

Field Code Changed

Field Code Changed

Field Code Changed

2.1.2.1 Effect of support materials and microstructures on membrane performances

In a PA TFC membrane, a porous support usually provides mechanical strength to a thin selective layer for withstanding high hydraulic pressure applied during RO, but has no much capacity rejecting solutes. Experimental and modelling results suggested the importance of selecting a suitable support on water flux and salt rejection of TFC membranes. [85-89] An ideal support is expected to possess good biological, chemical, mechanical and thermal stabilities, with desirable pore structure, surface morphology and chemistry. [85] Changes of support pore structure and chemistry greatly impacted water flux and salt rejection of the membrane; meanwhile they also affected its fouling and scaling propensity. [85, 87] In general, a more permeable and rougher TFC membrane was formed on a highly porous and hydrophobic support; whereas a thinner and smoother PA layer with lower permeability was prepared using a relatively hydrophilic support. [85] For example, the support cast from *N*-methylpyrrolidone (NMP) solution consisting of ≤ 16 wt% PSf had a high porosity, leading to defects in PA active layer during the interfacial polymerization. [90] In addition, by utilizing or generating free functional groups on support surface, covalent bonds might form between active layer and support, resulting in the PA TFC membrane with high separation performance and superior structure stability. [91]

For the support fabrication, the phase inversion method is commonly used to produce asymmetric membranes (such as ultrafiltration (UF) membranes) from polymers such as PSf and polyethersulfone (PES). Factors such as type of solvent, air humidity, processing temperature, concentration of polymer, and use of additive have been shown to influence properties of supports and subsequently performances of resulting TFC membranes. [85, 90, 92, 93] For example, a negative impact on sublayer hydrophilicity, roughness, and water permeability was observed when higher PES concentration of casting solution (*i.e.* 32 wt% vs. 27 wt%) was used. [92] Low air humidity (*e.g.* 20%) induced a denser structure in the top layer of the support. [93] Interestingly, a nanoimprinting process was used to produce patterned PES UF support; its supported patterned TFC membrane exhibited better performance with a capacity minimizing concentration polarization and scaling, as compared with the non-patterned counterpart. [94] Some other materials including poly(tetrafluoroethylene), poly(phthalazone ether nitrile ketone) (PPENK), polyimide (PI), and polyvinylidene fluoride (PVDF) have also gained attention as substitutes. [89, 95-101] For instance, PPENK

Field Code Changed

Field Code Changed

Field Code Changed

Field Code Changed

Field Code Changed

Field Code Changed

Field Code Changed

Field Code Changed

Field Code Changed

Field Code Changed

Field Code Changed

Field Code Changed

Field Code Changed

Field Code Changed

Field Code Changed

Field Code Changed

Field Code Changed

Field Code Changed

Field Code Changed

Field Code Changed

Field Code Changed

Field Code Changed

Field Code Changed

Field Code Changed

Field Code Changed

Field Code Changed

Field Code Changed

Field Code Changed

and PI polymers are well known for their high mechanical strength, chemical resistance and thermal stability (with a relatively high glass transition temperature T_g). [98, 99] The flux of PPENK-supported PA TFC membrane was enhanced by a factor of approximately 4 with almost unchanged Na_2SO_4 rejection (~95%), when the test temperature increased from 20 °C to 80 °C (1000 ppm Na_2SO_4 feed and 10 bar). [99] The PA TFC membrane formed on a PI support was observed with a flux jumping fivefold to 164.6 LMH with a stable rejection rate of >98% after operating temperature was increased from room temperature to 95 °C (2000 ppm NaCl feed and 27.6 bar). [98] These suggested the membranes be potentially suitable for hot water desalination or treatment. In recent years, the incorporation of hydrophilic inorganic particles such as TiO_2 , silica, CNTs, and zeolite into polymeric supports has been attempted to subsequently tailor TFC membrane performances. [92, 102-104] Compared to the pure PSf-supported membrane, the RO membranes using zeolite or silica-embedded PSf nanocomposites as supports could achieve higher initial permeability, less flux decline, and greater salt retention, which revealed better resistance to compaction because of enhanced mechanical stability derived from inherent characteristics of fillers. [102]

2.1.2.2 Modification of active layer towards improved flux and rejection

The active layer of conventional TFC RO desalination membrane is made of crosslinked aromatic PA, which is generally produced after interfacial polymerization (IP) between amines, e.g. 1,3-benzenediamine (MPD), and aromatic acyl chlorides, e.g. trimesoyl chloride (TMC). [13, 15] Chemistry and properties of thin active layer have been shown to strongly affect membrane separation. [105-109] The process parameters including concentrations and types of monomers/solvents/additives, polymerization condition, and curing process need to be optimized to fabricate high-performance TFC membrane. [90, 93, 110-116] It was accepted to select solvents with high surface tension but low viscosity, control MPD protonation and TMC hydrolysis during IP, and alter curing condition. [110] Water flux of PA TFC membrane was most dramatically affected by curing temperature (25 °C - 85 °C), followed by MPD concentration (1% - 2%) and TMC concentration (0.15% - 0.35%) and lastly reaction time (15 s - 60 s). [117] Additives in aqueous phase or organic solvent phase were effective to alter membrane surface morphology and polymeric network, although most likely they do not directly react with monomers. [90, 115, 118-120] In the presence of sodium dodecyl sulfate (SDS) and triethylamine (TEA) in amine solution, the resulting membrane showed increased

Field Code Changed

Field Code Changed

Field Code Changed

Field Code Changed

Field Code Changed

Field Code Changed

Field Code Changed

Field Code Changed

Field Code Changed

Field Code Changed

Field Code Changed

Field Code Changed

Field Code Changed

Field Code Changed

Field Code Changed

Field Code Changed

Field Code Changed

Field Code Changed

Field Code Changed

Field Code Changed

Field Code Changed

Field Code Changed

Field Code Changed

Field Code Changed

Field Code Changed

Field Code Changed

Field Code Changed

Field Code Changed

Field Code Changed

flux from 36 LMH to 54 LMH with 4% higher rejection recorded at 41 bar. [90] Symmetrical and asymmetrical ammonium salts with different solubility and water sorption properties might work as catalysts and surfactants during IP, thus affecting the crosslinking degree. [120, 121] The addition of ammonium salt with larger steric configuration cationic amine group, such as tetrabutylammonium bromide or benzyltriethylammonium chloride, resulted in the TFC membranes with better performance, rougher surface, and greater thickness. [120, 121] By adding inorganic salt LiBr in triethanolamine (TEOA), it might interact with carbonyl of TMC as well as hydroxyl of alcohol amine, thereby affecting TFC membrane performance. The maximum improvement in pure water flux of composite membrane was achieved by over 4 fold at the certain expense of Na_2SO_4 and MgSO_4 rejection when 3 w/v% LiBr existed in amine solution. [122] On the other side, by increasing the amount of tributyl phosphate (TBP) in TMC/isoparaffin up to 0.9 wt%, the water flux of MPD-TMC TFC membrane was as high as ~116 LMH, along with reduced rejection, when the membrane was tested using 2000 ppm NaCl feed at an operating pressure of 15.5 bar. [119] In contrast, the membrane water flux decreased with unchanged rejection by elevating triphenyl phosphate (TPP) content in TMC/isoparaffin solution. This difference was elucidated by their respective interaction with TMC, where the steric hindrance caused by phenyl segments of TPP reduced formation of complex with TMC compared to TBP. [119] Experimental results revealed a significant improvement in water flux of resulting PA TFC membrane by approximately 4 times without considerable retention loss after introducing 2 wt% acetone into TMC/hexane phase. [118] Similarly, by selecting 3 wt% ethyl acetate as co-solvent in TMC/hexane, the TFC membrane exhibited permeate flux of 75 LMH, which was a threefold increase in relative to the counterpart synthesized without using co-solvent; it could also retain a rejection of >99% (2000 ppm NaCl feed and 15 bar). [115]

As discussed above, the active layers of commercial TFC membranes are typically based on crosslinked aromatic PA formed after IP between MPD and TMC. As a basal strategy, great interest has been devoted to selecting or designing monomers or reactants with desirable functionalities and properties for optimizing membrane separation performances. Meanwhile, some other factors have been taken into consideration, e.g. easy commercialization, low cost and environmental friendly property. For instance, TEOA with multi-hydroxyl groups was an easily accessible monomer and chosen to react with acid chloride TMC to produce a

Field Code Changed

Field Code Changed

Field Code Changed

Field Code Changed

Field Code Changed

Field Code Changed

Field Code Changed

Field Code Changed

Field Code Changed

Field Code Changed

Field Code Changed

Field Code Changed

Field Code Changed

Field Code Changed

Field Code Changed

Field Code Changed

Field Code Changed

Field Code Changed

TFC membrane. [122, 123] Table 1 summarizes the selection of monomers or reactants for fabricating TFC membranes in the recent literature; their properties relating to structures and separation performance are also listed for comparison. Although the relationship between structures and performances is complex, it is commonly accepted that water permeability and salt retention of TFC membranes are strongly correlated to active layer structure as well as thickness and morphology. [110] The membranes with ultrathin, highly crosslinked, and good hydrophilic active layers appear to offer superior water flux and salt rejection. For example, by adding triamine monomer, 3,5-diamino-*N*-(4-aminophenyl) benzamide (DABA), the crosslinking degrees of membranes were enhanced, resulting in smoother and thinner active layers with greater hydrophilicity. [124] The flux of as-prepared TFC membrane increased from approximately 37.5 LMH (without DABA) to above 55 LMH (with 0.25 w/v% DABA in MPD solution) by flowing 2000 ppm NaCl feed at an operating pressure of 20 bar, accompanied with a minimal decrease of rejection (~0.3%). [124] The replacement of aromatic amine MPD with aliphatic amines was proven able to improve mobility and flexibility of polymeric chains, and in turn water transport. [125, 126] Especially, by controlling balance of linear-aromatic monomers and their hydrophilicity, e.g. the partial substitution of 1,3-diamino-2-hydroxypropane (DAHP) for MPD in IP reaction, it not only improved water flux but also maintained salt rejection. [126] Other hydrophilic additives, e.g. *o*-aminobenzoic acid-triethylamine salt (*o*-ABA-TEA), 2-(2-hydroxyethyl) pyridine, *m*-aminobenzoic acid-triethylamine salt, or 4-(2-hydroxyethyl) morpholine, might also associate with amines for use to enhance hydrophilicity and reduce crosslinking of active layer. [127, 128] With 2.85 wt% *o*-ABA-TEA in MPD solution and later post-treatment, the as-prepared TFC had promising flux (89.5 LMH) with superior rejection (>98.5%) by feeding 2000 ppm NaCl solution at 15.5 bar; both outperformed the commercial membrane (Fig. 3). [128]

Field Code Changed

Field Code Changed

Field Code Changed

Field Code Changed

Field Code Changed

Field Code Changed

Field Code Changed

Field Code Changed

Field Code Changed

Field Code Changed

Field Code Changed

Field Code Changed

Field Code Changed

Field Code Changed

Field Code Changed

Field Code Changed

Field Code Changed

Field Code Changed

Field Code Changed

Fig. 3. Comparison of membranes in terms of flux and rejection at the feed of 2000, 3000 and 5000 ppm NaCl, corresponding to 0, 30 and 60% recovery for a feed concentration of 2000 ppm NaCl at 15.5 bar (a) and 31.0 bar (b). “High-flux” and “Commercial” are denoted to the PA TFC membrane, which was prepared with 2.85 wt% *o*-aminobenzoic acid-triethylamine (*o*-ABA-TEA) salt and optimal post-treatment, and a

commercial membrane, respectively (modified from the reference [128]).

Field Code Changed

Field Code Changed

On the other side, by utilizing chloroformyloxyisophthaloyl chloride (CFIC) instead of conventional TMC reacting with MPD, a functional bond of urethane (-NHCOO-) was introduced into polymeric network forming new polyamide-urethane TFC membranes, which exhibited attractive rejection, e.g. >92% to boron and >99.4% to NaCl in desalination of synthetic seawater. [129-132] Addition of diacyl chloride (e.g. isophthaloyl chloride or/and terephthaloyl chloride), selection of high amine-diffusive organic solvent (e.g. hexane or heptane) or optimization of curing/post-treatment were able to effectively improve polyamide-urethane TFC permeability while retaining good rejection. [129] In a later work, polyamide-urethane TFC spiral wound elements were fabricated *via* a modified laminating method and additional thermo-sealing to achieve ~99.5% salt rejection and ~1100 L/h permeate flow when facing synthetic seawater feed at 55 bar. [133] Good stability of those spiral wound elements in a pilot test suggested suitability for a single pass SWRO desalination. [133] More recently, poly(amide-urethane@imide) TFC RO membrane, synthesized after reacting polyamide-urethane TFC with *N,N'*-dimethyl-*m*-phenylenediamine (DMMPD), exhibited stable performance in chlorine solution up to 8000 ppm; however the MPD-TMC TFC counterpart suffered more than 15% drop in NaCl rejection and 100 % increment in flux. [134] Note that second round of modification using DMMPD increased thickness of active layer and decreased hydrophilicity of surface; albeit it worked perfectly as a chlorine-resistant protective layer.

Field Code Changed

Field Code Changed

Field Code Changed

Field Code Changed

Field Code Changed

Field Code Changed

Field Code Changed

Field Code Changed

Field Code Changed

Field Code Changed

Table 1. Summary of selection of monomers or reactants for fabricating active layers of TFC membranes and their properties reported in the recent literature.

It is clear that the selection of monomers or additives with proper functionalities and structures effectively alters separation performances of membranes. Importantly, some other properties, such as antifouling and antibacterial capacity, would be greatly improved due to unique characteristics of reactants introduced. [135] More studies are still required to better understand complicated mechanisms governing active layer formation, and in turn optimize selection of chemicals and IP process. To date, some RO membranes with promising performance have been synthesized in the laboratory; [128] however, little progress has been

Field Code Changed

Field Code Changed

Field Code Changed

Field Code Changed

reported on the pilot test of these membranes in water desalination or treatment to affirm their performance and explore commercialization opportunity.

In addition to blending of monomers or introduction of additives during IP, surface modification of commercial TFC membranes by coating or grafting foreign materials is an alternative approach to achieving immediate commercial outcomes because of relatively easy adoption in current membrane manufacturing process. To date, various materials have been examined for suitability, including polyethylenimine (PEI), polyvinyl methyl ether, polyvinyl alcohol (PVA), polyvinyl pyrrolidone, polyether-polyamide block copolymer, *etc.* [136-144] In particular, “smart” polyelectrolyte polymers, comprising segments of *N*-isopropylacrylamide (NIPAM), are distinguished for their unique thermo-responsive property as promising coating materials; the modified TFC membranes had high salt rejection (*i.e.* ~97%) and retained good water flux when coating with a small amount of polyelectrolyte, thanks to improved membrane hydrophilicity compensating polyelectrolyte-induced resistance to water permeation. [137, 142-144] Most importantly, the special thermo-responsive property could significantly improve membrane antifouling capacity and cleaning efficiency. The flux restoration of poly(*N*-isopropylacrylamide-*co*-acrylamide) (P(NIPAM-*co*-Am))-coated membrane after cleaning at 45 °C (higher than lower critical solution temperature, LCST) was 88.5%, which was ~20% greater than that at 40 °C (lower than LCST) or recovery from the fouled pristine commercial RO membrane. [142] Furthermore, such surface coating would protect active layer of RO membrane from exposure to acid and chlorine as a sacrificial material, thus improving its chemical stability. [143] A long-term separation test (200 h) revealed the good stability of P(NIPAM-*co*-Am)-modified TFC with salt rejection and flux of ~98% and 55.5 LMH at 500 ppm NaCl feed and 6.5 bar, respectively. [137] Redox method is facile for use at room temperature to covalently link organic ligands with various functionalities onto membrane surfaces; however, there see some drawbacks, such as slow kinetics, poor surface specificity, and excessive chemical consumption. Freger’s group introduced a “concentration polarization (CP)-enhanced radical graft polymerization” to successfully tighten structure of commercial low pressure RO membranes by selecting different monomers (e.g. 2-hydroxyethyl methacrylate, methyl methacrylate, 2-ethoxyethyl methacrylate, glycidyl methacrylate (GMA), *etc.*) and in turn improve rejection to some

Field Code Changed

Field Code Changed

Field Code Changed

Field Code Changed

Field Code Changed

Field Code Changed

Field Code Changed

Field Code Changed

Field Code Changed

Field Code Changed

Field Code Changed

contaminates. [145-147] The GMA-modified membranes showed lower boron transport rate in brackish water RO (BWRO) range, but this performance was not superior to that of SWRO membranes. [146]

Field Code Changed

Field Code Changed

Field Code Changed

Field Code Changed

2.1.2.3 Modification of active layer towards enhanced fouling resistance

RO membranes usually suffer from membrane fouling, which deteriorates separation performance, increases energy consumption, shortens membrane lifetime and eventually requires membrane replacement. [148]

Field Code Changed

Field Code Changed

This is inevitably translated into higher cost of water processing. Typically, three approaches are suggested to dealing with this problem: (1) pre-treatment prior to RO process removing foulants; (2) chemical or physical cleaning of fouled RO membranes; and (3) development of antifouling membranes. [39, 149-154]

Field Code Changed

Field Code Changed

Field Code Changed

The latter is the focus herein.

Fundamental studies have revealed membrane fouling susceptibility is highly correlated to membrane surface properties, including roughness, charge and hydrophilicity. [151, 155, 156] A more negatively charged, smoother and less hydrophobic membrane surface appears less prone to fouling. [156-159] Causes to fouling are complex and varied largely depending on characteristics of feed water, operation conditions, and properties of membrane surface. These include particle deposition, interaction with microorganisms leading to growth of biofilm, and adsorption of organic compounds onto membrane surface. Based on natures of foulants, fouling occurring in membrane systems can be categorized into several types, e.g. colloidal fouling, inorganic fouling, organic fouling and biofouling. [153] So far, vast laboratory work has been carried out to develop antifouling membranes tested by using organic foulants and microorganisms, which are correlated to their resistance to organic fouling and biofouling; a few have reported other aspects.

Field Code Changed

Field Code Changed

Field Code Changed

Field Code Changed

Field Code Changed

Field Code Changed

Field Code Changed

Field Code Changed

Undoubtedly, selection of proper monomers or additives could be a good route to modify membrane surface properties and subsequently improve fouling resistance. [135, 160-165] For instance, the piperazine (PIP)-isophthaloyl chloride (IPC) TFC membrane exhibited better fouling resistance and reversibility with 40% flux decline and 74% cleaning efficiency, as compared with 51% and 40% of PIP-TMC membrane; thanks to fewer carboxyl groups on PIP-IPC TFC surface which impeding calcium to bond with alginate foulant.

Field Code Changed

Field Code Changed

Field Code Changed

[164] Addition of PVA (e.g. 16%) into amine aqueous solution reduced roughness and enhanced the hydrophilicity of PIP-TMC composite membrane, thus improving antifouling performance and facilitating

Field Code Changed

Field Code Changed

water transport without apparent loss of rejection. [161] After 12 h separation test using BSA foulant in MgSO₄ feed, the fluxes of as-prepared membranes with 0% and 16% PVA decreased by approximately 20% and 10%, respectively. [161] On the other hand, zwitterionic amine monomer, *N*-aminoethyl piperazine propane sulfonate (AEPPS), participated in IP of PIP-TMC. The excellent resistance of resultant membrane to adsorption of BSA foulant and bacteria was observed, ascribed to high membrane hydrophilicity and strong binding capacity of AEPPS to free water. [135] By introducing 1.0 wt% hydrophilic *o*-ABA-TEA amine salt in MPD solution to react with TMC, the TFC membrane exhibited superior water flux of 75.4 LMH accompanied with 99.4% rejection under desalinating synthetic seawater at 55.2 bar. [127, 128, 160] In particular, due to more hydrophilic and negatively charged surface, its water flux decline was ~10% less than the counterpart in the presence of model foulant alginate, demonstrating a better fouling resistance. [160]

Field Code Changed

Field Code Changed

Field Code Changed

Field Code Changed

Field Code Changed

Field Code Changed

Field Code Changed

Field Code Changed

Field Code Changed

Field Code Changed

Field Code Changed

Field Code Changed

Surface modification of commercial TFC membranes could be a more effective solution to fouling problem in terms of less chemical use and low cost, because a very thin coating material on membrane surface would likely provide antifouling properties. [166] In general, extremely hydrophilic polymers are preferred for use during modification. Meanwhile, it needs minimization of polymer thickness and its penetration into active layer; that could largely reduce water permeability because of higher resistance and lower effective mass diffusivity. [127, 138] Particular research interest was in coating of potentially perfect antifouling materials, polyelectrolytes, onto membranes to improve surface smoothness, hydrophilicity and charge density. [137-139, 141, 167] Moreover, polyelectrolytes show ability to self-clean foulants deposited on them *via* changing solution environment, e.g. pH, ion concentration or temperature. As LbL coating with increasing layers of poly(allylamine hydrochloride) (PAH)/poly(sodium 4-styrenesulfonate) (PSS) from 0 to 6, the antifouling capability to BSA, humic acid and dodecyl trimethyl ammonium bromide (DTAB) of modified commercial ES20 RO membrane was improved, attributed to more hydrophilic, smoother, and charged membrane surface. [138] Incorporation of inorganic antimicrobial silver (Ag) particles in poly(acrylic acid)(PAA)/PEI LbL coated commercial RO membranes could further help inactivate up to 95% of bacteria attached within 1 hour of contact time. [168]

Field Code Changed

Field Code Changed

Field Code Changed

Field Code Changed

Field Code Changed

Field Code Changed

Field Code Changed

Field Code Changed

Field Code Changed

Field Code Changed

Field Code Changed

Field Code Changed

Field Code Changed

In recent years, hydrophilic and biocompatible zwitterionic materials, which possess both negatively and positively charged units as well as strong and stable electrostatic bonds with water, have been investigated as novel antifouling materials. [135, 169-175] The zwitterionic carboxylated PEI-coated SWRO membrane presented lower contact angle to 32000 ppm of NaCl solution compared with that to DI water, suggesting higher affinity to NaCl solution and improved antifouling property in seawater condition. [174] As shown in Fig. 4a, the use of amino acid 3-(3,4-dihydroxyphenyl)-L-alanine (L-DOPA) zwitterionic material increased the water permeability of commercial SW30XLE RO membrane, [170, 172] due to remarkably improved surface hydrophilicity; meanwhile salt rejection was retained. Especially, after fouled by BSA/sodium alginate, the fluxes of modified membranes were almost completely recovered by water cleaning; however, only around 85% restoration of initial flux could be achieved by using the pristine commercial RO membrane (Fig. 4b). [170] Their later work further extended this concept to the FO membrane; which successfully reduced 30% fouling. [171] Because of synergistic effect between biocide release and adhesion resistance arising from Ag and polyzwitterion, the disposition of polyelectrolyte multilayers, followed by embedding Ag nanoparticles and coating amphiphilic polyzwitterion top layer onto commercial ES20 RO membrane improved surface anti-adhesion resistance and bactericidal function to *Pseudomonas putida* (*P. putida*). [176] However, its multiple-step preparation might have created barriers to water transport; thus initial water permeability was decreased by ~15%.

Fig. 4. (a) Oxidative polymerization of amino acid 3-(3,4-dihydroxyphenyl)-L-alanine (L-DOPA) and surface adsorption resistance to organic matter imparted by the hydrated zwitterionic coated surface; (b) normalised flux of the original and modified SW30XLE RO membranes (“12 hr SW30XLE” and “24 hr SW30XLE” are referred to the SW30XLE RO membranes with a 12-hr and 24-hr coating) as a function of time during BSA/sodium alginate (100 ppm of each; 18 bar) fouling (the dashed part shows the treatment of water cleaning) (modified from the reference [170]).

It is known that coating materials in physical modification or sorption normally interact with active layer of membrane by van der Waals attraction, electrostatic interaction or hydrogen bonding, which may not be stable in long-term operation. In contrast, chemical grafting with functional species can assist in producing

Field Code Changed

Field Code Changed

Field Code Changed

Field Code Changed

Field Code Changed

Field Code Changed

Field Code Changed

Field Code Changed

Field Code Changed

Field Code Changed

Field Code Changed

Field Code Changed

Field Code Changed

Field Code Changed

Field Code Changed

Field Code Changed

covalent bonds between coating and active layer of membrane; and in turn better chemical and structural stabilities. A range of techniques have been developed, including adoption of chemicals, UV or plasma, to achieve covalent linking of antifouling materials to free functional groups located on TFC membrane surface, such as carboxyl, amine and acyl chloride groups. [177-188]

Field Code Changed
Field Code Changed

Selenium compounds are capable of inhibiting bacterial biofilm grown on membrane surface, because of their ability to catalyze formation of superoxide radicals *via* non-enzymatic processes. Selenium was covalently coated onto RO membrane surface by using selenocystamine, selenium-attached aceto acetoxy ethyl methacrylate, selenocyanatoacetic acid; and the numbers of adhered *Staphylococcus aureus* (*S. aureus*) and *E. coli* cells were dramatically decreased on the modified RO membranes. [155, 189] The virgin RO membrane had a biofouling-induced flux loss of 55%; however, the modification treatment resulted in merely 15%. [190] Moreover, a significant membrane biofilm reduction in synthetic wastewater was observed; revealing utilization of organo-selenium for RO membrane surface treatment was a feasible and effective biofouling control strategy. [189]

Field Code Changed
Field Code Changed
Field Code Changed

Field Code Changed
Field Code Changed

Field Code Changed
Field Code Changed

Similarly to physical coating, chemical grafting of polyelectrolyte moieties and zwitterionic compounds has been extensively explored. As described above, among a variety of polyelectrolytes, those comprising NIPAM unit are of great interest due to their unique temperature responsive property. By using redox-initiated graft polymerization with NIPAM and subsequently with acrylic acid (AA) to modify membrane, water cleaning at 45.0 °C could revert 93% of initial flux to the fouled membrane attributed to phase transition of NIPAM chains; whereas only 82% of initial flux was recorded for the pristine membrane. [191]

Field Code Changed
Field Code Changed

Especially, this redox-initiated surface graft polymerization would reduce the number of chlorine susceptible amine sites in PA after covalently linked with NIPAM or AA; the N-H groups from NIPAM in grafting layer could work as sacrificial groups, thus greatly enhancing membrane stability after exposure to chlorine. [191] In spite of promising results, adjustment of RO feed temperature would be a challenge in implementation and a concern about energy consumption used for cooling/heating cycles. [192, 193] As aforementioned, the characteristics of zwitterionic molecules make them promising antifouling materials; nevertheless they suffer from a certain extent of poor processability. Redox-initiated graft polymerization

Field Code Changed
Field Code Changed
Field Code Changed
Field Code Changed

covalently attached zwitterionic polymer poly(4-(2-sulfoethyl)-1-(4-vinylbenzyl) pyridinium betaine) to commercial XLE RO membrane; the resulting membrane could restore 90% of its initial flux by cycled DI water/brine rinsing, which could be beneficial in a full-scale RO system. [193] Simply by immersing the freshly prepared PIP-TMC membrane into AEPPS aqueous solution, zwitterionic molecules were linked onto membrane surface *via* chemical reaction between acyl chloride of TFC and amine of AEPPS. A significantly better membrane antifouling property to BSA (91.6% and 95.5% flux recovery at pH of 3.7 and 6.0, respectively) was recorded, coupled with almost doubled water flux and unchanged rejection, as compared with the control (75.6% or 88.3% at pH of 3.7 or 6.0). [192] Further work is recommended to investigate the separation efficiency and structural stability of those modified TFC membranes under various operating conditions.

Field Code Changed

Field Code Changed

Field Code Changed

Field Code Changed

UV grafting of reactants has been attractive for use due to low cost, mild reaction requirement as well as easy and feasible incorporation into membrane manufacturing process. [187] Mondal *et al.* reported the temperature responsive property of PNIPAM-modified NF270 membranes prepared using UV-induced graft polymerization method; that above LCST of PNIPAM (e.g. ~40 °C), polymer chains collapsed by releasing water and foulants (Fig. 5a). [194] When the gel moiety was well compressed (after 1st cycle), water fluxes were almost unchanged for several cycles of warm water flushing, suggesting good reusability (Fig. 5b). [194] Note that experimental work by comparing UV-irradiated grafting of AA during and after formation of active layer recommended the former one, since it led to a 29% (130%) improvement of pure water flux (NaCl rejection) using 10 wt% AA under 60 s UV irradiation accompanied with a 97.8% flux recovery in the BSA fouling test. [195] The second approach caused the formation of highly dense PAA grafted layer and decreased pore size of membrane surface; less than 50% flux was able to be maintained after UV modification. [195] This flux decline after UV grafting was also found in other works, due to greater resistance derived from the grafting layer. [153, 194] On the other side, plasma-induced modification exhibits prosperous features including relatively short treatment time, precise control of surface and little membrane structure damage. [153] A range of gases such as oxygen, nitrogen, helium and mixed gases can be used as plasma source to introduce different functional groups or work in conjunction with desired monomers/polymers. For example, NH₃ plasma treatment introduced nitrogen-containing functional groups;

Field Code Changed

Field Code Changed

Field Code Changed

Field Code Changed

Field Code Changed

Field Code Changed

Field Code Changed

Field Code Changed

Field Code Changed

Field Code Changed

Field Code Changed

Field Code Changed

Field Code Changed

Field Code Changed

Field Code Changed

the treated commercial membranes (e.g. NF270, NF90, TFC-S and TFC-SR2) showed enhanced antifouling properties without detrimental effect on separation performance. [177] After atmospheric pressure plasma-induced graft polymerization using monomers methacrylic acid and acrylamide, the corresponding grafted PA membranes had less flux decline (34% and 40%) with better permeability recovery ratios (82% and 76%), in comparison to the commercial ESPA2 RO membrane used on site (46% and 64%) after 24 h real secondary wastewater treatment. [196, 197] The method above basically comprises two steps, plasma activation of surface followed with graft polymerization. Zou *et al.* reported one-step plasma polymerization to modify commercial SW30HR RO membrane with hydrophilic triethylene glycol dimethyl ether (triglyme) polymer; which shows advantages to increase crosslinking density of material, improve uniformity and adhesion of coating, and simplify preparation process in absence of harsh solvent. [198] After accelerated organic fouling test (BSA/alginate), the flux was nearly unchanged with 99.5% restoration by water cleaning; but ~30% flux reduction and 89% flux recovery were observed during the usage of control membrane. [198]

Fig. 5. (a) Schematic representation of temperature responsive properties of poly(*N*-isopropylacrylamide) (PNIPAM) brushes grafted on TFC membrane surface; (b) repeated water flux results of grafted membrane as a function of applied pressure: after each cycle, the membrane was placed in flushed with lukewarm water (40 °C) for cleaning (modified from [194]).

Continuous effort is still being devoted to exploring other effective methods with regards to membrane modification. Initiated chemical vapour deposition (iCVD) method is a dry and solvent-free polymerization technique, which can be carried out at low temperature. As compared with those methods, e.g. UV, plasma, and solution polymerization, it can largely retain functional groups on membrane surface during modification. [166, 199-204] Gleason and co-workers deposited an ultrathin (30 to 300 nm) anti-biofouling coating onto commercial TFC membranes (Fig. 6a-b) using iCVD; the as-prepared membranes exhibited similar salt rejection and maintained 86% of water flux to the pristine commercial RO membrane (Fig. 6c-d), particularly with good fouling resistance (Fig. 6e) and chlorine stability. [201] This method was considered

Field Code Changed

Field Code Changed

Field Code Changed

Field Code Changed

Field Code Changed

Field Code Changed

Field Code Changed

Field Code Changed

Field Code Changed

Field Code Changed

Field Code Changed

Field Code Changed

Field Code Changed

Field Code Changed

Field Code Changed

Field Code Changed

to be scalable and comparable with current membrane fabrication infrastructure, thus showing the potential for promoting energy-efficient RO desalination process. [201]

Field Code Changed

Field Code Changed

Fig. 6. Antifouling zwitterionic coating applied onto commercial RO membranes via iCVD. (a-b) Cross-sectional SEM image of (a) bare and (b) iCVD coated RO membrane; (c) salt rejection and (d) water flux of bare and coated membranes; (e) surface coverage by *V. cyclitrophicus* on bare glass (black) and iCVD zwitterionic surface (orange) and relative fouling index F_1 (blue). The relative fouling index F_1 (blue) is defined as the fraction of surface coverage for the coated surface compared to the bare glass control (modified from the reference [201]).

Field Code Changed

Field Code Changed

Some problems by adopting surface grafting have been noticed despite significant improvements achieved. It usually leads to permanent change of membrane chemistry and structure. Sometimes its impact on membrane performance is too difficult to be accurately predicted. Use of harsh solvents or high temperatures in chemical modification may cause defects and in turn poor separation performance. Moreover, some grafting requires complex and multiple steps, involves intensive chemical use and is time consuming, thus increasing cost and limiting next commercialization. [205] Other drawbacks are also noticed, such as difficult reproducibility and scale up for plasma-induced modification. [153] Note that optimization of chemical use and fabrication protocol is required in both physical coating and chemical grafting to minimize adverse impact of coating on membrane. [195, 198, 206] Although selecting materials, such as polyelectrolytes or hydrogels, as antifouling coatings has been widely agreed because of their characteristics (*i.e.* high hydrophilicity and smoothness), some issues should not neglected. For instance, an excessive amount of such coating on membrane surface can uptake a large amount of water, increase concentration polarization and build up resistance, leading to low flux.

Field Code Changed

Field Code Changed

Field Code Changed

Field Code Changed

Field Code Changed

Field Code Changed

Field Code Changed

Field Code Changed

To date, a majority of work that is relevant to surface modification of commercial TFC membranes towards improved antifouling property has been concentrated on selection of various polymers or monomers; however, the introduction of inorganic materials has been proved considerably effective. [207-213]

Field Code Changed

Field Code Changed

Especially, attaching inorganic particles, including Ag, Cu, Al₂O₃, and graphene oxide (GO), onto membrane surface seems a favourable route to maximize direct contact between particles and foulants for optimal antifouling efficiency, when compared to MMMs (Section 2.2). Ag is one of most commonly adopted biocides; Yin *et al.* developed a method to covalently attach Ag nanoparticles onto PA TFC membrane surface *via* a bridging agent cysteamine. [208] Excellent antibacterial property was demonstrated, with better water flux (69.4 LMH) and comparable salt rejection (93.6%), in relative to the control (49.8 LMH and 95.9%) at 20.7 bar by flowing 2000 ppm NaCl feed solution. [208] Instead of extensive chemical use, a rapid and facile method applied AgNO₃ solution onto the SW30XLE TFC membrane surface, followed by reacting with a reducing agent NaBH₄ and *in situ* forming Ag. [207] Despite a minor loss of water permeability, a dramatic reduction in the number of attached live bacteria and biofilm development on its surface suggested promising antibacterial activity. [207] This simple approach was applicable to coat Cu nanoparticles onto membrane surface as well, which is considered as a cheaper leachable biocidal agent in comparison to Ag. [213] However, due to the fact of Ag or Cu dissolution in aqueous solution, recharge of those nanoparticles onto membrane surface is needed after a certain period of operation; this would increase operational complexity and costs. In contrast, CNTs represent non-depleting biocides. The CNTs treated by ozonolysis could increase their sidewall functionalities and maximize cytotoxic property; and deposition of such antimicrobial CNTs in membranes achieved up to 60% inactivation of attached bacteria in 1 h. [212] In recent years GO nanosheets have seen an upward trend in research as water purification membrane materials, because of their unique transport properties, hydrophilicity, and chemical stability. After LbL deposition of negatively charged GO and positively charged aminated-GO nanosheets onto the TFC membrane, the layer of nanosheets worked as a protective layer against foulant (BSA) and chlorine. Flux reduction of ~15% and rejection decline of ~4% were recorded for the GO-modified TFC membrane after 12 h 100 ppm BSA fouling test and 1 h 6000 ppm chlorine treatment, as compared with around 34% and 50% for the pristine PA TFC, respectively. In particular, by compensating resistance of stacked nanosheets, the unique water transport property and hydrophilicity derived from GO could help largely maintain membrane flux with unchanged NaCl rejection. [210] Attempt in this interesting field of research was also extended to the modification with multiple types of inorganic materials by taking virtues of each component for

Field Code Changed

Field Code Changed

Field Code Changed

Field Code Changed

Field Code Changed

Field Code Changed

Field Code Changed

Field Code Changed

Field Code Changed

Field Code Changed

Field Code Changed

Field Code Changed

Field Code Changed

Field Code Changed

distinguishing overall property. A novel design system by functionalizing the commercial BW30 TFC membrane with GO, Au nanostars and polyethylene glycol (PEG) resulted in enhanced antifouling capacity to CaCO₃ and CaSO₄ (mineral scalants), humic acid (organic matter), and *E. coli* (bacteria), accompanied with increased salt rejection and water flux. [211] In these studies, it is important to strengthen interaction between membrane surface and particles, avoid delamination or early detachment of coating materials from membrane active layer, as well as minimize reduction of separation performance (e.g. flux). Further research is also needed to systematically study their efficiency and stability in treating complex feed and long-term operation. For those heavy metal (Ag and Cu) based antimicrobial coatings, issues including how to well control their leaching or dissolution during RO, maximize lifetime of antifouling membranes, implement recharge after depletion, as well as ensure safety to environment must be well addressed.

Field Code Changed

Field Code Changed

2.1.2.4 Modification of active layer towards increased chlorine stability

PA TFC membranes exhibit excellent separation performance (e.g. water flux and salt rejection); however, they are sensitive to chlorine. [214-217] Chlorine is generally added at the intake to control microorganisms and provide biological disinfection before desalination membrane units. When exposed to chlorine, PA undergoes a number of reactions, which are dependent on chlorination pH, concentration, and duration. The proposed mechanisms include *N*-chlorination, chlorination-promoted hydrolysis, or ring chlorination by direct chlorination or an intermolecular rearrangement. Consequently, changes in chemical composition, hydrophilicity, charge density and surface morphology occur, some of which do not favour separation performance. [218-226] Current SWRO desalination requires chlorination-dechlorination-rechlorination; in which the extra dechlorination and rechlorination steps increase chemical use, energy consumption and operation cost. [1] To solve this problem, one solution is to develop new chlorine-tolerant membrane materials. Indeed it should not be neglected that under well controlled environment, e.g. at pH 9 and 100 ppm of chlorine concentration (Fig. 7), water permeability and salt rejection could both be increased in conjunction with higher hydrophilicity and in turn potentially greater fouling resistance. [225] Therefore, chlorination may potentially be employed as a means to improve PA TFC NF or RO membrane performance if the membranes are stable in such conditions. [218, 225, 227, 228]

Field Code Changed

Field Code Changed

Field Code Changed

Field Code Changed

Field Code Changed

Field Code Changed

Field Code Changed

Field Code Changed

Field Code Changed

Field Code Changed

Field Code Changed

Field Code Changed

Fig. 7. (a) Effect of chlorine concentration (Cl_T) and solution pH on membrane properties by two competing mechanisms of chlorination-promoted hydrolysis and *N*-chlorination; (b) performance of NF90 membranes, both virgin and chlorinated for 100 h at different Cl_T and pH (at 584.4 ppm NaCl feed and 6.89 bar). Salt rejection (%) shown by the numbers in white and water flux (LMH) shown by the numbers in parentheses; NP: membrane failed to perform (modified from the reference [225]).

To eliminate or protect chlorine-sensitive sites of PA and in turn improve membrane chlorine resistance, it is necessary to select suitable monomers in IP reaction of fabricating TFC membranes. [229] Use of secondary amines or attachment of CH_3 or OCH_3 to MPD's phenyl ring enhanced chlorine stability of PA. [216, 230-232] As compared to MPD-TMC derivate, the PA membrane made of 2,6-diaminotoluene and TMC exhibited improved chlorine tolerance with similar desalination performance or even better flux. [230] By introducing primary diamine bearing hexafluoroalcohol groups on phenyl ring, the synthesized TFC membrane could effectively reduce chlorine attack on its PA functional groups. [233] Especially, at pH ~10, the membrane hydrophilicity and charge density were enhanced, thus increasing water flux and salt rejection; the resulting membrane was suggested for suitable use at high pH desalination. [233] The adoption of melamine, which has low toxicity and reactivity featuring a triazine ring structure, resulted in a TFC membrane showing stable performance during 96 h immersion in 200 ppm $NaClO$ solution; however, more than 20% of Na_2SO_4 rejection was compromised when the secondary amine PIP was selected. [234]

Using surface grafting or coating to improve membrane chlorine stability proceeds at a slower pace as opposed to the success achieved in the field of antifouling property. Surface modification is able to improve chlorine resistance of TFC membranes by introducing protective and/or sacrificial layers to minimize chlorine impact on sensitive sites, e.g. amide linkage and end amine groups. [143, 235-238] Liu *et al.* coated P(NIPAM-co-Am) onto the aromatic PA TFC membrane through hydrogen bonding between PA and coating layer, which caused almost no change of salt rejection and water flux recorded after 1 h exposure to 3000 ppm hypochlorite at pH 4. [143] On the other side, the pristine PA membrane encountered 28% and 3% decline of flux and rejection, respectively. [143] A protective and sacrificial coating of novel hydrophilic

Field Code Changed

Field Code Changed

Field Code Changed

Field Code Changed

Field Code Changed

Field Code Changed

Field Code Changed

Field Code Changed

Field Code Changed

Field Code Changed

Field Code Changed

Field Code Changed

Field Code Changed

Field Code Changed

Field Code Changed

Field Code Changed

Field Code Changed

Field Code Changed

Field Code Changed

Field Code Changed

Field Code Changed

Field Code Changed

Field Code Changed

random copolymer poly(methylacryloxyethyl dimethyl benzyl ammonium chloride-*r*-acrylamide-*r*-2-hydroxyethyl methacrylate) crosslinked by glutaraldehyde could maintain its modified membrane selectivity (>96%) until 32 h exposure to 500 ppm NaClO (pH = 7); whereas, a dramatic reduction in salt retention was observed after 3 h and 6 h for the commercial LCLE and BW30 membranes, respectively. [235] By considering stability over long term or under severe chlorination environment, chemical grafting method would be preferable to physical coating by impeding detachment of protective layer. Through unreacted acyl chloride groups of PA, covalent binding of *N,N*-dimethylamino propylamine and subsequently anchoring of sorbitol polyglycidyl ether onto TFC membrane surface efficiently protected it against chlorine attack and improved stability after exposure to 100 ppm free chlorine (pH = 7) up to 38 h. [237] Using silane compounds, stable Si-O-N or Si-O-C chemical structures formed from the amide or carboxyl groups of commercial SWC1 membrane surface could assist in retaining >99% salt rejection of membrane after 12 h chlorine exposure to 2000 ppm NaClO (pH = 7 – 8). [238]

Field Code Changed

Field Code Changed

Field Code Changed

Field Code Changed

Field Code Changed

Field Code Changed

Very often modification targeting at enhanced chlorine stability also brought improvement in antifouling property, due to more hydrophilic and less rough membrane surfaces. [235, 237, 239, 240] Wang's group reported the attempt on improving both chlorine and fouling resistances of RO membrane by introducing a multifunctional *N*-halamine precursor for the first time, [239, 241, 242] e.g. 3-monomethylol-5,5-dimethylhydantoin or 3-allyl-5,5-dimethylhydantoin. A reversible transition between *N*-halamine and N-H group on a hydantoin ring endowed the membranes with regenerable anti-biofouling property and improved chlorine resistance, when coupled with periodical chlorination pre-treatment. [241, 242] The chlorine resistance of treated membranes was improved relative to the pristine membranes, albeit water and salt passage both increased following grafting. Furthermore, the modified membranes showed good sterilization and substantial prevention effects on *E. coli*. To further enhance chlorine durability, imidazolidinyl urea (IU) with six N-H groups was used in modification instead of monofunctional *N*-halamine precursor. [243] As shown in Fig. 8a, in addition to function as *N*-halamine precursor, there is an equilibrium between hydroxymethyl group of IU and methylene glycol, which could then dehydrate to form formyl group inhibiting microbial growth. For the IU-modified membrane, a relatively stable separation performance (>96% rejection and ~80 LMH at 2000 ppm NaCl feed and 15.5 bar) with slight changes in chemical structure and

Field Code Changed

Field Code Changed

Field Code Changed

Field Code Changed

Field Code Changed

Field Code Changed

Field Code Changed

Field Code Changed

Field Code Changed

Field Code Changed

Field Code Changed

Field Code Changed

Field Code Changed

Field Code Changed

surface morphology was recorded in 100 day simulated periodical free chlorine pre-treatment (Fig. 8b). [243] However, the modified membrane suffered ~25% flux reduction possibly due to additional resistance of coating material (Fig. 8b). [243]

Fig. 8. (a) Schematic of antifouling and chlorine resistant properties of imidazolidinyl urea (IU)-modified membrane; (b) water flux and salt rejection (at 2000 ppm NaCl and 15.5 bar) of both virgin and IU-modified membrane during 100 day investigation by simulating periodical free chlorine pre-treatment. [243]

2.1.3 Polyelectrolytes

The route of layer-by-layer (LbL) assembly of polyelectrolytes, *via* alternating coating of cationic and anionic polyelectrolytes onto a charged support (e.g. polymer or ceramic membranes), has been employed to prepare separation membranes. [244-256] In particular, the use of polymeric supports may favour manufacturing of spiral wound membrane module for high pressure RO desalination; attributed to its flexibility and mechanical strength. [257] Dip-coating is most commonly selected method in the membrane preparation apart from spray-coating and spin-coating; [253] this may be considered as a “static” method since polyelectrolyte solution only flows across membrane surface without any permeation through. Some recent studies suggested use of dynamic self-assembly method by passing polyelectrolyte solution through porous support surface under vacuum filtration or cross-flow filtration to produce membranes with enhanced separation performances. [258, 259] For example, the NF membrane, which was prepared by cross-flow dynamic assembly of 3 poly(diallyl-dimethylammonium chloride) (PDADMAC)/PSS bilayers, showed a permeation flux of 60 LMH at 10 bar (2000 ppm Na₂SO₄ feed solution), which was superior to the commercial DL membrane. [259] Its rejection (~82%) could be further improved up to approximately 90% when combining cross-flow dynamic and static assembly. [259]

Selection of constituent polyelectrolytes greatly affects resultant membrane properties, e.g. surface charge, composition, hydrophilicity, thickness, *etc.*, and in turn separation performance, e.g. flux and rejection. [248, 255, 257, 260-265] Some early work fabricated polyelectrolyte multilayer membrane consisting of a large number of successive coatings, e.g. 60 bilayers; which exhibited pure water flux of ~4 LMH and NaCl

Field Code Changed

Field Code Changed

Field Code Changed

Field Code Changed

Field Code Changed

Field Code Changed

Field Code Changed

Field Code Changed

Field Code Changed

Field Code Changed

Field Code Changed

Field Code Changed

Field Code Changed

Field Code Changed

Field Code Changed

Field Code Changed

Field Code Changed

Field Code Changed

Field Code Changed

Field Code Changed

Field Code Changed

Field Code Changed

Field Code Changed

Field Code Changed

rejection of 93.5% at 40 bar. [251] However, this fabrication appears time consuming; most importantly, a large number of coatings increased transport resistance and reduced water permeability. [259] Later work successfully reduced LbL assembled polyelectrolyte multilayers down to merely 4 to 5 by deposition of solution containing salt, e.g. MnCl₂, NaBr or NaCl. [244, 266, 267] However, this indeed sacrificed NaCl rejection to some extent; thus making resultant membranes potentially fit for NF purpose. In comparison to the commercial NF270 membrane, the 4 repeated deposition of PSS/PAH polyelectrolyte solution (containing NaCl) onto PES support resulted in comparable flux of ~20 LMH – 47 LMH with better rejection (~94%) by flowing MgSO₄ solution at 4.8 bar. [266]

Field Code Changed

Field Code Changed

Field Code Changed

Field Code Changed

Field Code Changed

Field Code Changed

Field Code Changed

Field Code Changed

Field Code Changed

Field Code Changed

Another challenge is to improve stability of LbL assembled polyelectrolyte membrane during NF or RO separation. Crosslinking of polyelectrolyte multilayers was effective in reducing swelling of polyelectrolyte and enhancing rejection property. [257, 268, 269] For example, the PAH/PAA multilayered membrane was heated to 180 °C under *vacuo* for 1 h to initiate crosslinking *via* amide bonding between polyelectrolytes, resulting in reduced thickness and dense structure. [257] The thermally crosslinked 10 and 20 bilayers of PAH/PAA polyelectrolyte membranes exhibited good rejection rate of >80% by flowing 2000 ppm NaCl feed at 20 bar; which could further jump to 99% after recycle of concentrate. However, this thermally crosslinking method is not applicable to all types of polyelectrolytes. Furthermore, the flux of crosslinking PAH/PAA membrane was still not satisfactory (less than 10 LMH at 2000 ppm NaCl feed and 20 bar) as compared with the commercial PA TFC membranes; which might be solved by exploring other polyelectrolyte or crosslinking agent. [257]

Field Code Changed

Field Code Changed

Field Code Changed

Field Code Changed

Field Code Changed

Field Code Changed

Field Code Changed

Field Code Changed

2.1.4 Aquaporin biomimetic membranes

In 2007, Kumar *et al.* reported the water productivity of aquaporin (AQP)-containing poly-(2-methyloxazoline)-poly-(dimethylsiloxane)-poly-(2-methyloxazoline) (ABA) vesicles was approximately two orders of magnitude greater as compared to that of the commercial SWRO membranes with a selectivity of ~100%. [270] This evidenced the design of incorporating AQP into membranes would achieve exceptional water permeability with high selectivity; that opens a new avenue to constructing high performance desalination membranes. [270] Most of AQP proteins feature narrow channels and unique

Field Code Changed

Field Code Changed

Field Code Changed

Field Code Changed

charge characteristic. Such channels exclude transport of ions or small molecules but allowing water through. Thanks to high water transport and excellent selectivity of AQP, over the last few years, some membrane designs loaded with AQP proteins have been explored as potential strategies to offset “trade-off” between permeability and selectivity of separation membranes. [27, 40, 271-273] Use of AQP in conjunction with polymersomes or liposomes may also potentially be a modification method to improve membrane separation performance, e.g. modification of UF for NF purpose. [274] Some of prior attempts on inclusion of AQP into separation membranes reported unsatisfactory monovalent salt rejection. [275-278] Their limited stability also raises difficulty in the fabrication of large-scale and defect-free membranes and the continuous separation under hydraulic pressure driven process.

An ideal AQP-incorporated membrane for desalination purpose is expected to possess high permeability and selectivity, coupled with good mechanical and chemical stability. Seen from the schematic (Fig. 9), when using such a biomimetic membrane in hydraulic pressure driven separation, water molecules from feed enter AQP *via* water channel, further transport through protein, and finally exit from porous support. Salts or other molecules are excluded at feed side. For fabricating high performance AQP-incorporated membranes, it requires favorable substrate surface and suitable building blocks for embedment. Supports should be highly porous, thus giving no extra resistance to extremely fast water transport through AQP. Inorganic supports have prosperous mechanical, chemical and thermal features; whilst adoption of organic (polymeric) supports would be preferable, ascribed to their flexible surface and porous structures. On the other side, both lipids and polymers may be used as building blocks to accommodate AQP and construct biomimetic membranes. Advantages were suggested by using amphiphilic block polymer ABA to lipids due to their better mechanical and chemical stability as well as low water permeability. After AQP are incorporated into liposomes or polymersomes, the resultant vesicles (proteoliposomes or proteopolymersomes) are then immobilized *via* different ways, e.g. direct or pressure assisted vesicle fusion, charged induced or magnetic enhanced deposition, and chemical interaction driven vesicle rupturing, [275, 277-282] onto porous support. Another foreign polymer may be added as a part of active layer; it can play a role in protecting AQP vesicles, improving strength and stability of biomimetic membrane during separation. [283] Due to the lower water permeability derived from polymer as compared with that through water channels of AQP, water molecules

Field Code Changed

Field Code Changed

Field Code Changed

Field Code Changed

Field Code Changed

Field Code Changed

Field Code Changed

Field Code Changed

Field Code Changed

Field Code Changed

Field Code Changed

Field Code Changed

Field Code Changed

preferably pass through proteins. Defects need to be avoided between polymer matrix and vesicles; which may make salt molecules escape through and in turn lower rejection. [284]

Fig. 9. Water molecules in the feed solution penetrate the membrane in 3 steps: (1) passing from the feed solution to the vesicles through the aquaporin (AQP) water channel located at the polymer bilayer facing the feed solution, (2) passing from the vesicles to the support through the AQP located at the polymer bilayer facing the support membrane, and (3) penetrating the porous support into the permeate solution. Other solutes in the feed solution will be rejected. [284]

Lipids are regarded as excellent biomimetic components for constructing vesicles. [281, 285] Wang's group compared direct vesicle fusion on a hydrophilic NF-270 membrane and pressure facilitated vesicle fusion on positively charged lipid-modified NF-270 membrane. [277] The latter method was proven necessary to facilitate vesicle fusion and less defect density, despite both methods observed with reduced rejection and flux relative to the pristine control. [277] Moreover, the AQP-immobilized membrane exhibited a poor flux and rejection. This revealed that AQP did not play their function as expected; which was explicated relating to low lipid mobility on the support. Issues when using liposomes in fabricating biomimetic membranes include improving stability of liposomes and promoting non-defect active layer with good stability and strength. Sun *et al.* formed a hydrophobic polymer mesh by crosslinking methacrylate monomers and amine-functionalized proteoliposomes under UV. [274] The as-prepared amine-functionalized proteoliposomes were then immobilized on a PDA-coated microporous PAN flat sheet followed by crosslinking. This resulted in a NF membrane with good stability under hydraulic pressure and strong agitation ascribed to the polymer network within lipid bilayers. [274] As compared to the control without AQP, the membrane with AQP:lipid ratio of 1:100 significantly increased water flux to ~14.5 LMH by 65% and NaCl rejection to 66.2% by 41%, respectively, against 200 ppm salt at 5 bar. [274] Wang *et al.* reported the progress of biomimetic NF membrane by immobilizing positively charged AQP-incorporated DOPC/1,2-dioleoyl-3-trimethylammonium-propane (chloride salt) (DOTAP) vesicles onto a PEI/PSS LbL polyelectrolyte membranes. The as-prepared membrane showed a good flux of 22 LMH with 97% MgCl₂ and 75% NaCl rejection against flowing 500 ppm single salt feed solution at 4 bar; a relatively high performance stability

Field Code Changed

Field Code Changed

Field Code Changed

Field Code Changed

Field Code Changed

Field Code Changed

Field Code Changed

Field Code Changed

Field Code Changed

Field Code Changed

Field Code Changed

Field Code Changed

Field Code Changed

Field Code Changed

Field Code Changed

Field Code Changed

Field Code Changed

was recorded over 36 h. [286] Li and co-workers immobilized PDA-coated proteoliposomes on a PAI support, followed by PEI deposition and its subsequent crosslinking to PAI in water bath to form active layer. [283] The water flux of AQP-embedded membrane was around 2 – 3 times higher than the commercial NTR-7450 and NF-270 flat sheets with comparable rejection under similar testing condition. Most importantly, because the proteoliposomes were completely protected in crosslinked PEI layer which was covalently bonded to the support; good structural stability and AQP activity could be largely sustained under pressure and toxic feed. [283]

Field Code Changed

Field Code Changed

Starting from Kumar and co-workers' prior work, [270] the ABA block copolymers have been widely studied as biomimetic materials to incorporate AQP, due to their lipid-bilayer-like amphiphilic structure as well as chemical, mechanical stability and low water permeability. [281] Duong *et al.* used AQP-incorporated polymer vesicles prepared from disulfide-functionalized ABA to enhance vesicle spreading on gold-coated alumina support *via* covalent interaction between disulfide functionality and gold surface. [282]

Field Code Changed

Field Code Changed

Field Code Changed

Field Code Changed

The created biomimetic layer on top of substrate remarkably enhanced water flux and rejection to the nascent ABA copolymer, proving the activity of AQPs in membrane; but more work needed to reduce defects on the biomimetic membrane. [282] On the other side, ABA copolymers with methacrylate end groups was utilized to cover the flat sheet CA membrane functionalized with acrylate functionality; after UV polymerization the planar biomimetic NF membranes were produced. [281] Increasing ratio of AQP:ABA resulted in higher water flux and rejection, indicating positive role of AQP water channels in water transport.

Field Code Changed

Field Code Changed

Field Code Changed

Field Code Changed

Field Code Changed

Field Code Changed

A promising pure water flux of 171 LMH under 5 bar was given by the CA-supported membrane comprising AQP:ABA ratio of 1:50; however, merely ~33% NaCl rejection was recorded against 200 ppm salt solution. [281] Later work immobilized AQP-loaded hydroxyl-terminated ABA vesicles onto amine-

Field Code Changed

Field Code Changed

Field Code Changed

Field Code Changed

functionalized CA membrane; followed by a polymer coating after *in situ* redox-initiated polymerization of methyl methacrylate and ethylene glycol dimethacrylate at 40 °C. [284] Comparison proved AQP could maintain their transport characteristics under 5 bar and shear force during NF; suggesting it as an effective way offsetting the fragility flaw of conventional biomimetic membranes. [284] This type of membranes was also applicable in FO separation; the elimination of defects may possibly further enhance the salt rejection of membranes. [284] Although block polymers have been used in biomimetic membranes, the compatibility

Field Code Changed

Field Code Changed

Field Code Changed

Field Code Changed

Field Code Changed

Field Code Changed

Field Code Changed

Field Code Changed

between AQP and polymers still requires examination for better understanding. It may also help expand options when selecting good polymer candidate and simplifying preparation process.

Seen from the literature, most of AQP biomimetic membranes exhibited relatively low NaCl rejection; thus they are more suitable for NF separation purpose. In 2012, Tang's group reported the fabrication of PA RO membranes embedded with proteoliposomes *via* IP for the first time. [287] The water permeability and rejection of membrane loaded with inactive AQP are similar to those of the pristine polymeric membrane, suggesting marginal defects created in IP. The resulting membrane with active AQP had a high flux of ~20 LMH (at 5 bar and 584.4 ppm NaCl feed), which was ~40% greater than the commercial brackish RO membrane (BW30), coupled with good NaCl rejection (~97%). [287] Particularly, this type of membranes could be made into an area of >200 cm² with a good mechanical stability under pressure *via* adoption of traditional IP method, [287] thus suggesting commercialization potential for desalination. However, the reported separation performances seem not reach what was expected for the ultra-permeable biomimetic membranes; thus more should look into composition of proteoliposomes and their loading and comparability in PA membranes towards optimization. Some other issues remain in cost, scalability and their properties, e.g. stability and durability.

2.2 Mixed matrix membranes

Apart from organic molecules and biomolecules as modifiers, another strategy is to incorporate inorganic particles into/onto membranes, which can be achieved by either directly coating inorganic materials onto membrane surface or mixing inorganic particles in monomer/polymer solution during membrane fabrication. The later one normally forms mixed matrix membranes (MMMs), by integrating inorganic particles with polymers. Over last few years, remarkable advances have been made in the preparation of polymeric desalination membranes comprising inorganic particles, which demonstrated not only excellent resistance to fouling and chlorine but also provided potential in overriding the "trade-off" between water permeability and solute selectivity. [2, 17, 35, 36, 40, 44, 288-291] The overview of this progress in recent several years is provided in Table 2. As can be seen, research effort has been exerted on embedding a wide range of inorganic fillers with or without porosity (e.g. silica, silver, titanium dioxide, carbon or titanate nanotubes,

Field Code Changed

Field Code Changed

Field Code Changed

Field Code Changed

Field Code Changed

Field Code Changed

Field Code Changed

Field Code Changed

Field Code Changed

Field Code Changed

Field Code Changed

Field Code Changed

Field Code Changed

Field Code Changed

etc.). In addition, it has recently further extended to incorporation of hybrid organic-inorganic material, polyhedral oligomeric silsesquioxanes (POSS). [292-294] Most of studies loaded fillers into aromatic PA thin layer to form MMMs, which are normally referred to “thin film nanocomposite (TFN) membranes”; [104, 295-309] albeit polyelectrolytes, sulfonated poly(arylene ether sulfone), CA, or PES has also been selected as polymeric matrix for study. [310-321] Indeed a number of prior works also reported the incorporation of inorganic particles into sublayers of TFC membranes; which has been covered in Section 2.1.2.1 of this review.

Table 2. Fabrication and properties of recently reported MMMs for water desalination.

2.2.1 Ag and TiO₂

Until now, a considerable effort has been contributed to easing membrane biofouling problem by adding inorganic nanoparticles, such as silver (Ag) and titanium dioxide (TiO₂). Meanwhile, those fillers could tune salt rejection and water flux by either affecting polymerization process or tailoring polymer network arrangement.

Ag is one of most widely studied biocides killing various aquatic microorganisms. [295, 322-325] On the other side, TiO₂ has received much research attention due to its photocatalytic property to decompose organic compounds and bacterial cells, which can potentially be self-cleaned for reducing fouling during membrane separation. [326] Addition of Ag or TiO₂ directly into feed water in desalination industry may need a considerable amount of materials and in turn be not economical; [207] in contrast, development of their incorporated/coated membranes has been regarded as an alternative. Experimental results confirmed nanosized Ag-embedded nanocomposite membranes had improved anti-adhesive property and inhibited bacterial growth effectively. [327, 328] Slow dissolution of Ag might be able to maintain membrane antibacterial efficiency over a relatively long-time testing. [327] Accompanied with TiO₂ nanoparticles, the use of hydrophilic poly(amide-imide) (PAI) caused resultant composite membrane surface hydrated and thus minimize foulant binding to it. As a result, the fouling-induced flux decline to membrane was reduced and the adsorbed foulant BSA could be more readily dislodged by shear force, as compared with the nascent membrane. [311]

Field Code Changed

Field Code Changed

Field Code Changed

Field Code Changed

Field Code Changed

Field Code Changed

Field Code Changed

Field Code Changed

Field Code Changed

Field Code Changed

Field Code Changed

Field Code Changed

Field Code Changed

Field Code Changed

Field Code Changed

Field Code Changed

Field Code Changed

Field Code Changed

Field Code Changed

Field Code Changed

Field Code Changed

High-performance MMMs also require uniform dispersion of nanoparticles in polymeric matrix, which is crucial in impeding formation of non-selective “defects” and maintaining solute rejection. In most studies about fabricating MMMs, synthesized nanoparticles, e.g. TiO₂, are firstly dispersed in solution under ultrasonication before membrane formation; [311, 313, 326] which normally caused agglomeration of nanoparticles. Moreover, lack of good interaction between inorganic particles and organic polymer may seriously contribute to defects and limit enhancement in separation properties of MMMs. Surface organic-functionalization of nanoparticles has attracted significant interest to enhance particle distribution, provide good adhesion to polymer matrix and improve material surface property; [295, 329] which has been widely studied in the field of gas separation membranes. [330] By adopting such a strategy, the functionalization of TiO₂ with an aminosilane *N*-[3-(trimethoxysilyl) propyl] ethylenediamine (AAPTS) (Fig. 10), was utilized to reduce aggregation of nanoparticles in aqueous solution and improve their uniform dispersion in PA active layer. The membrane with a low concentration (*i.e.* 0.005 wt%) of amine-functionalized nanoparticles offered highest salt retention (~54%) with water flux (~12 LMH) at 7.6 bar against 2000 ppm NaCl feed. By increasing addition of particles to 0.1 wt%, the observed flux of TFN was almost doubled as compared with the TFC membrane. [295] Until to the present, there are few efforts devoted to employment of such functionalized inorganic fillers in improving membrane separation for desalination purpose; [331] which could also be an adoptable method when incorporating other types of inorganic fillers in polymeric matrix. Note that when using MMMs embedded with depleting biocide fillers, e.g. Ag, recharge will be infeasible after depletion. Some studies suggested the location of Ag nanoparticles on membrane surface would largely benefit the direct contact between particles and foulants, e.g. bacterial cells, for optimized antimicrobial performance. [207, 208, 332] Meanwhile, it is necessary to well control dissolution of Ag into environment and improve durability of its containing separation membranes. Taken account of those issues, the strategy by direct surface modification of commercial membranes appears preferable (Section 2.1.2.3). [207, 208, 332]

Fig. 10. Schematic of PA TFN membrane fabricated by dispersing *N*-[3-(trimethoxysilyl) propyl] ethylenediamine (AAPTS)-modified TiO₂ nanoparticles in MPD aqueous solution (modified from the

Field Code Changed

Field Code Changed

Field Code Changed

Field Code Changed

Field Code Changed

Field Code Changed

Field Code Changed

Field Code Changed

Field Code Changed

Field Code Changed

Field Code Changed

Field Code Changed

Field Code Changed

Field Code Changed

Field Code Changed

Field Code Changed

Field Code Changed

Field Code Changed

Field Code Changed

Field Code Changed

Field Code Changed

reference [295]).

Field Code Changed

Field Code Changed

2.2.2 Zeolite and silica

Zeolite molecular sieves are well known for their intrinsically unique pore structure, thus providing superior size and shape selectivities. [304-309, 333] The concept on formation of a zeolite-PA MMM *via* IP started from utilization of zeolite A (LTA) nanoparticles with a pore opening of $\sim 4.2 \text{ \AA}$; the resulting MMM was named for the first time as thin film nanocomposite (TFN) membrane by Jeong and co-workers in 2007. [309] The demonstration-scale test exhibited those zeolite-impregnated TFN membranes required lower feed pressure and thus could achieve up to 10% savings in specific energy consumption. [334] NanoH₂O Inc. officially launched high flux and high rejection TFN membrane modules under the brand of *QuantumFlux* in desalination membrane market in 2011. [335] However, they still need improvement in terms of some properties, e.g. boron rejection. [336]

Field Code Changed

Field Code Changed

Field Code Changed

Field Code Changed

Field Code Changed

Field Code Changed

Field Code Changed

Field Code Changed

Field Code Changed

Field Code Changed

Field Code Changed

In zeolite-embedded TFN membranes, the pores in zeolites are believed to act as preferential flow channels only for water molecules (with a diameter of 2.7 \AA) rather than hydrated sodium and chloride ions, resulting in dramatically improved permeability and superior salt rejection. [309] Smaller zeolites were found to impart greater improvement in permeability and suggested more suitable for practical application in fabricating hollow fibre membrane model. [304] The optimized post-treatment of zeolite-incorporated TFN membranes in solution containing glycerol solution, camphorsulfonic acid (CSA)-TEA salt, and sodium lauryl sulfate (SLS) followed by heating could further enhance separation performance. [337] Apart from LTA (NaA), [103, 302] research attempt has also been expanded to other groups of zeolites, such as FAU (*i.e.* NaX and NaY), MFI (*i.e.* silicalite) and EMT. [306, 308, 337-339] Especially, in addition to enhanced permeability and rejection, the selection of silicalite-1 in fabrication of TFN membrane maintained excellent stability in solution containing acid as well as multivalent cation (CaCl_2), thus being suitable for use in practical desalination process, where acidification is implemented for scaling control or/and there are various multivalent cations in a complex feed. [338]

Field Code Changed

Field Code Changed

Field Code Changed

Field Code Changed

Field Code Changed

Field Code Changed

Field Code Changed

Field Code Changed

Field Code Changed

Field Code Changed

Field Code Changed

Field Code Changed

Field Code Changed

Field Code Changed

Field Code Changed

Similarly to Ag or TiO₂-loaded MMMs, it is essential to avoid forming non-selective voids between zeolites and polymer. Dispersion of zeolites in TMC organic solvent during IP could result in a homogeneous

membrane structure (Fig. 11b) with excellent salt rejection, as compared with dispersing zeolites in MPD aqueous solution, which led to gradual growth of macrovoids in sublayer (Fig. 11a). [307] Several strategies have been investigated to further enhance uniform dispersion in PA active layer, including organic-functionalization of zeolite particles and modification of IP process. [302, 308, 339] The TFN membrane embedded with 0.05 w/v% octadecyltrichlorosilane-modified NaA zeolite exhibited better flux and rejection (~41 LMH and 98.5%) when flowing 2000 ppm NaCl feed at 16 bar, than those of unmodified NaA-PA TFN membrane (~29 LMH and 97.8%). This was explained by better dispersion of organic-functionalized zeolite in TMC/hexane and in turn improved its distribution in TFN active layer. [302] A new strategy called “pre-seeding”-assisted synthesis was utilized in TFN membrane fabrication, in which zeolite crystals modified with organic materials were pre-assembled on a MPD-impregnated support as “seeds”, followed by IP. [308] By improving zeolite/polymer interfacial contact, the as-synthesized TFN membrane (≤ 0.4 wt% zeolite in TMC/ethanol/hexane) showed greater flux (17.3 LMH – 31.3 LMH) with comparable salt rejection (>95%) at 2000 ppm NaCl feed and 15 bar, relative to TFC membrane (11.3 LMH and 98.1%). [308]

Field Code Changed

Field Code Changed

Field Code Changed

Field Code Changed

Field Code Changed

Field Code Changed

Field Code Changed

Field Code Changed

Field Code Changed

Field Code Changed

Field Code Changed

Field Code Changed

As compared with hydrophilic inorganic zeolite, porous metal-organic framework (MOF) materials possess similar pore configuration and was reported in fabricating TFN RO membranes for the first time in 2015; [340] although some early attempt was started from solvent resistant NF membranes. [341] ZIF-8 is one of thermally and chemically stable MOF materials, with 11.6 Å cavity cages connected with 3.4 Å pore apertures. The imidazolate linker connecting tetrahedral zinc ions in ZIF-8 potentially improved the compatibility between ZIF-8 and PA. Experimental results revealed that using ZIF-8 (0.4 w/v% in TMC/hexane) increased the water flux of TFN membrane to ~52 LMH, which was 162% higher than that of TFC membrane; whilst high NaCl rejection of ~99% was retained (at 15.5 bar and 2000 ppm NaCl feed). [340] As the same to zeolites, the inclusion of MOF provides degree of freedom to alter TFN membrane performances. In particular, simulation work suggested fast water permeability through ZIF-8, which was several times above that of zeolite. [342] More work is required for better understanding the interaction between PA matrix and porous ZIF, and in turn optimize TFN membrane performances and fabrication.

Field Code Changed

Field Code Changed

Field Code Changed

Field Code Changed

Field Code Changed

Field Code Changed

Field Code Changed

Field Code Changed

Interestingly, MOF can also work as templates to promote pore creation and connectivity in other types of water treatment membranes. [343]

Fig. 11. SEM (left) and TEM images (right) of TFN membrane with 0.1 w/v% zeolites added in MPD aqueous phase (a); and TFN membrane with 0.1 w/v% zeolites added in TMC hexane organic phase (b) (modified from the reference [307]).

Interest in silica-embedded MMMs was initiated from incorporation of nonporous silica; which may alter polymerization and modify polymer structure. Thermal stability and separation performance, in terms of flux and rejection, of TFN membranes were improved by adding small silica content in PA. [299, 344] Introduction of organic-functionalized silica could further improve TFN membranes' resistance against chlorine and fouling. For example, the TFN synthesized using hyperbranched aromatic PA grafted silica with amine groups retained ~15% higher salt rejection with almost unchanged water flux after 24 h exposure to 500 ppm NaOCl, compared with the TFC membrane. [320] With a proper concentration (e.g. 0.03 wt%) of silica treated by 3-aminopropyltriethoxysilane, the TFN exhibited better antifouling property, with approximately 10% less flux decline in BSA fouling test; thanks to hydrophilicity of functionalized silica. [345] In recent years, studies have been broadened to selection of mesoporous silica with pore size of 2 – 50 nm, due to its uniform and controllable mesoporosity, high specific surface area, and good surface hydrophilicity, along with chemical stability, thermal property, and low cost. Moreover, mesoporous silica was considered as a substitute in fabricating TFN membrane for zeolite in which the oriented pores make available water flow path difficult to control. [301] A comparison between the membranes embedded with nonporous silica and MCM-41 porous silica (pore size of 3.85 nm) was presented in Yin's work; which revealed the importance of short flow paths through MCM-41 during water transport (Fig. 12a). [300] By increasing MCM-41 content, the surface properties, including hydrophilicity, roughness and zeta potential, of TFN membranes were all enhanced. The water flux of membrane embedded with 0 wt% – 0.1 wt% (in TMC/hexane) MCM-41 was improved from 28.5 LMH to 46.6 LMH, coupled with stable NaCl and Na₂SO₄ rejection of ~97.9% and 98.5%, respectively (at 20.7 bar and 2000 single salt feed) (Fig. 12b). [300] On the other side, water flux of TFN with 0.1 wt% nonporous silica increased only up to 35.8 LMH, which was

Field Code Changed

Field Code Changed

Field Code Changed

Field Code Changed

Field Code Changed

Field Code Changed

Field Code Changed

Field Code Changed

Field Code Changed

Field Code Changed

Field Code Changed

Field Code Changed

Field Code Changed

Field Code Changed

Field Code Changed

Field Code Changed

Field Code Changed

much lower than that with MCM-41 (46.6 LMH). [300] As mesopore size of selected silica became larger, water permeability of resultant TFN increased whereas salt retention was sacrificed due to additional pathway of mesopores. [345] Loading of silica should also be carefully controlled; excessive amount lowered crosslinking degree of PA, gave rise to defects in TFN and in turn compromised separation performance. [299, 318, 346]

Fig. 12. (a) Schematic illustration of hypothesized mechanism of MCM-41-incorporated TFN membrane (1 shows the feed solution containing NaCl; 2 shows the PA active layer with MCM-41 or nonporous silica; 3 denotes the porous support); (b) water flux and salt rejection of TFN membranes with MCM-41 nanoparticles at 20.7 bar and 2000 ppm NaCl or Na₂SO₄ feed. [300]

2.2.3 Carbon nanotubes and graphene oxide

Carbon nanotubes (CNTs) exhibit excellent mechanical and separation properties, [34, 35] but they require supports to avoid separating apart during pressure-driven RO separation. The concept of MMMs by incorporating CNTs in polymeric matrix is an effective strategy responding to that. CNTs could increase water permeability, salt rejection, fouling resistance and/or chlorine resistance of resulting MMMs by improving smoothness, hydrophilicity and surface charge on membrane surface and altering chemical structure of layer. [297, 315-317, 347, 348] In order to fabricate CNTs-incorporated MMMs, such as PA TFN membranes, organic-functionalization of CNTs with carboxylic or hydroxyl groups is generally required, which can be achieved *via* a treatment using a mixture of sulfuric acid and nitric acid. In the modification, amount of acid/CNTs, reaction temperature and time was found to strongly affect resulting CNTs' dispersibility in solution and polymer as well as the interfacial interaction between inorganic CNTs and organic polymer matrix. [349] The PA TFN membrane prepared from 0.001 wt% CNTs, which were functionalized in a HNO₃: H₂SO₄ mixture with a ratio of 1:3 (v/v) at 65 °C for 4 h, could achieve around 20% increase of flux with a similar NaCl rejection of 91%, compared with TFC membrane by feeding 2000 ppm NaCl at 15.5 bar. [349] Insufficient functionalization, e.g. at 25 °C for 3 h, caused a poor dispersion of CNTs and then agglomeration in TFN membrane; consequently, merely 10% NaCl rejection was recorded. [349] As shown in Fig. 13, water molecules may transport through the channels of CNTs due to capillary

Field Code Changed

Field Code Changed

Field Code Changed

Field Code Changed

Field Code Changed

Field Code Changed

Field Code Changed

Field Code Changed

Field Code Changed

Field Code Changed

Field Code Changed

Field Code Changed

Field Code Changed

Field Code Changed

Field Code Changed

Field Code Changed

Field Code Changed

Field Code Changed

Field Code Changed

Field Code Changed

Field Code Changed

Field Code Changed

Field Code Changed

Field Code Changed

force or slide quickly on their surfaces because of smoother wall surface, thus increasing flux. [350, 351] In spite of large diameter of used CNTs which was enough to allow ion transport with water, the high rejection to hydrated sodium or chlorine ions might be as a result of PA covering CNTs and in turn narrowing opening of CNTs. [349] Proper variation on surface functionalities of CNTs could even further alter the resultant nanocomposite membrane performances. For instance, experimental observation revealed that water flux was improved by over 4 times (from 11.5 LMH to 48.5 LMH) when increasing chain-like zwitterion functionalized CNTs in PA matrix from 0 wt% to 20 wt%; meanwhile, ion rejection ratio was comparable at ~98% (using 1000 ppm Na⁺ feed and an operational pressure of 36.5 bar). [352] The TFN membranes with adding CNTs which were modified with diisobutryl peroxide exhibited a good compatibility between CNTs and PA, with improved hydrophilicity and charge of membrane surface. Increasing the amount of CNTs in MPD aqueous solution from 0 wt% to 0.1 wt% led to a change of water flux from 14.9 LMH to 28.1 LMH with a relatively high rejection of >90% (2000 ppm NaCl feed and 16 bar). The as-prepared TFN membrane demonstrated an improved antifouling property to Ca(HCO₃)₂ and BSA; as well as antioxidative property when exposed to chlorine. [348] Some simulation data suggested separation performance of MMMs with excellently aligned CNTs could reach several orders of magnitude greater than experimental data. [352] However, this has encountered practical difficulty in reaching and requires further research effort.

Field Code Changed

Field Code Changed

Field Code Changed

Field Code Changed

Field Code Changed

Field Code Changed

Field Code Changed

Field Code Changed

Field Code Changed

Field Code Changed

Field Code Changed

Fig. 13. Schematic illustration of fast water transport in CNTs-incorporated nanocomposite membrane.

[349]

Field Code Changed

Field Code Changed

Special research interest has been attracted on application of graphene oxide (GO) in fabrication of water treatment membranes, [353-355] owing to its special inherent properties, e.g. great surface area, large amount of hydrophilic functional groups, good mechanical strength, and ability to inhibit bacterial growth upon direct contact with cells. The coating of GO onto preformed membrane surface has been proven with improved chlorine resistance and antifouling property. [210] However, such coating layer may not be stable over long-term operation and most likely hinder water transport thus sacrificing fast water permeation

Field Code Changed

Field Code Changed

Field Code Changed

Field Code Changed

through membrane. In recent years, inclusion of GO nanosheets in polymer matrix to form RO membranes was started for study. [356, 357] The TFN membrane formed after IP process, in which GO was introduced in reactant solution, was seen not only improved hydrophilicity and surface charge, but also reduced thickness and roughness of surface layer. Thereby, it achieved a maximal water flux of 16.6 LMH, which was ~80% greater than the flux of TFC membrane (at 2000 ppm NaCl feed and 15.5 bar); accompanied with strong anti-biofouling property (to *Pseudomonas aeruginosa*) and chlorine resistance (in 2000 ppm NaOCl solution for 24 h). [358]

Field Code Changed

Field Code Changed

Field Code Changed

Differently from introduction of single type of fillers into MMMs as aforementioned, blending and subsequent incorporation of various inorganic fillers may combine unique merits from each component and potentially strengthen separation properties. [104, 291, 312, 359] For instance, use of TiO₂-coated MWCNTs could cause low agglomeration in casting polymer and good comparability to polymeric matrix. [312] The TiO₂-coated MWCNTs MMM exhibited superior water flux to the pristine polymer membrane and solely MWCNTs or TiO₂-incorporated MMMs. Meanwhile, the best anti-biofouling property was accompanied, which was induced by its favourable hydrophilicity, surface roughness and synergistic photocatalytic activity. [312] Incorporation of TiO₂-decorated rGO into active layer of PA TFN could improve membrane hydrophilicity, decrease surface roughness and in turn enhance separation performance.

Field Code Changed

Field Code Changed

Field Code Changed

Field Code Changed

Field Code Changed

Field Code Changed

Field Code Changed

Field Code Changed

[359] With 0.02 wt% TiO₂/rGO, the TFN membrane showed a flux of 51.3 LMH and NaCl rejection of 99.5% against 2000 ppm NaCl feed at an operation pressure of 15 bar; while the TFC and the TFN with 0.005 wt% TiO₂ or GO exhibited only ≤43.3 LMH and approximately 98%. [359] Moreover, TiO₂/rGO, working as a protective layer, largely increased chlorine resistance of the TFN membrane, ascribed to the chemical interaction between functional groups derived from TiO₂/rGO and PA, which hindered the replacement of hydrogen with chlorine on amide groups. [359] Lee's group reported the mixture of acid-functionalized CNTs and GO as filler materials was able to facilitate good dispersion of larger amount of carbon nanomaterials in polymer matrix, thus improving membrane mechanical property. [291] Until the loading of CNTs/GO reached 0.02 wt%, increasing water flux of TFN membrane did not encounter a decrease of salt rejection, thanks to the surfactant effect of GO; however, the TFN membrane with 0.01 wt% CNTs or GO alone suffered a dramatic decline in NaCl retention. [291] Due to the inclusion of CNTs and GO both of

Field Code Changed

Field Code Changed

Field Code Changed

Field Code Changed

Field Code Changed

Field Code Changed

Field Code Changed

Field Code Changed

Field Code Changed

Field Code Changed

Field Code Changed

Field Code Changed

which can trap free radicals, the resultant TFN membrane had a stable performance with marginal change in rejection and flux after 40 h exposure to chlorine (500 ppm). [291]

Field Code Changed

Field Code Changed

So far, a significant progress has been reported regarding to the synthesis of MMMs with a wide range of inorganic materials. Nevertheless, the majority of them are focusing on the incorporation of single type of fillers. The nanocomposite with multi-components, which has not been well explored yet, may be an effective way to potentially override trade-off tendency between permeability and selectivity with remarkable chemical and fouling resistance. This would be seen as a growing research field in the future. Moreover, to successfully meet the expectation on superior separation derived from MMMs, it is necessary to enhance uniform dispersion of inorganic fillers in polymeric matrix and stability of composite membranes over long-term operation. Better fundamental understanding on the transport mechanism through MMMs will greatly benefit the optimization of membrane design for different water treatment purposes.

3. Forward osmosis membranes

3.1 Polymeric membranes

An ideal FO membrane is expected to consist of an active layer, which features by high water permeability and low reverse solute permeation, and a support layer, which allows high mass transfer and reduces concentration polarization; accompanied with good antifouling property, chemical resistance and mechanical stability. [20] Especially, for desalination purpose, an RO-like active layer is required due to its capacity to rejecting NaCl. FO membranes with NF-characteristic active layer have also been explored, which can be used to treat the feed contaminated by multivalent ions or other large molecules. Among a number of polymeric materials that have been investigated so far in fabricating FO membranes, current research foci are on cellulosic derivatives, PA, polyelectrolytes, *etc.* [12, 23-25]

Field Code Changed

Field Code Changed

3.1.1 Cellulosic derivatives

CTA FO membranes commercialized by HTI, [31] allows greater water flux accompanied with good salt rejection of >95%, in comparison with the use of commercial RO membranes. [30] However, its induced flux in FO process was reported to be much lower than the theoretical value, [360] which is generally

Field Code Changed

Field Code Changed

Field Code Changed

Field Code Changed

Field Code Changed

Field Code Changed

ascribed to external concentration polarization (ECP) and especially internal concentration polarization (ICP). [12, 20] ECP can be reduced by optimizing fluid hydraulic status (e.g. shear and turbulence); whilst ICP is dominated by membrane structure. [361] In recent years, there has been a significant development of CA, CTA or related FO membranes either in the module of flat sheet or hollow fibre; [362-371] which are generally fabricated by phase inversion, followed by heat annealing treatment. Chung's group reported "double-skinned" CA FO membranes comprising two thin selective layers, mechanically supported by a porous sublayer (as shown in Fig. 14). [364, 365, 370] A transition sublayer was also observed between the thin dense layer, which ensured solute rejection and allowed water transport, and the highly porous bulk support. Both experimental and modelling studies have proven the use of polymer membranes with this unique "double-skinned" structure was capable of reducing fouling and ICP phenomenon and enhancing separation performance. [364, 365, 372]

Fig. 14. A schematic diagram and FESEM images of double-skinned CA membrane cast on glass plate and phase transition in water; which is consisting of double selective skins, transition sublayers, and a porous bulk support (CS is denoted as cross-section of membrane). [365]

In the phase inversion preparation of cellulosic derived polymer FO membranes, polymer or solvent type, dope composition, evaporation time, heat annealing, casting substrate, and coagulant bath, *etc.*, greatly affected membrane structures and performances. [362, 365-369, 373, 374] The double-skinned membrane with a small St (54 μm) could be created by casting CA (22.5 wt%)/acetone/NMP solution on a glass plate and immediately dipping it into tap water bath. [364, 365] Even though both selective layers were smooth without any visible pores under SEM characterization, analysis concluded the layer facing air (referred as top layer) was looser than the layer adjacent to glass substrate (referred as bottom layer). By using glass plate during casting, introduction of an intermediate immersion in NMP/water bath before dipping into tap water even further reduced St to 51 μm , indicating lower ICP in FO. [365] Change of glass casting substrate into Teflon one resulted in a relatively dense top layer supported by a fully porous bottom, attributed to unfavourable hydrophilic (polymer) – hydrophobic (substrate) interaction. [365] When substituting CTA for CA in solvent of acetone/NMP during phase inversion, the favourable polymer's hydrophilic interaction to

Field Code Changed
Field Code Changed
Field Code Changed
Field Code Changed
Field Code Changed
Field Code Changed

Field Code Changed
Field Code Changed
Field Code Changed
Field Code Changed

Field Code Changed
Field Code Changed
Field Code Changed
Field Code Changed

Field Code Changed
Field Code Changed

Field Code Changed
Field Code Changed
Field Code Changed
Field Code Changed
Field Code Changed
Field Code Changed
Field Code Changed

Field Code Changed
Field Code Changed

Field Code Changed
Field Code Changed

glass casting substrate was impeded; thus forming a relatively dense top layer, a bottom layer with small pores, as well as a highly open-cell porous sublayer. [366] Use of dioxane/acetone solvent caused appearance of less porous sublayer as well as relatively dense top and bottom layers in the CTA membrane.

Field Code Changed

Field Code Changed

[366] With including acetic acid in dioxane/acetone, it formed complexes with dioxane and acted as a pore forming agent, thus increasing free volume of dense layer and open porosity of sublayer. When using 2 M NaCl and DI water as draw and feed solution, respectively, the CTA flat sheet membrane fabricated from dioxane/acetone/acetic acid (before heat annealing) exhibited higher flux, ~20 LMH; whereas approximately 4 LMH was recorded for that casted from dioxane/acetone. [366] Other pore forming agents, *i.e.* lactic acid,

Field Code Changed

Field Code Changed

maleic acid or zinc chloride, have also been selected for study; which induced an increase of salt penetration along with enhanced flux during separation. [366, 374] Following phase inversion, thermal annealing treatment of freshly prepared membranes was able to tighten voids and rearrange polymer chains thus affecting membrane microstructures and performances. [364, 365, 367, 369] With 15 min heat annealing at

Field Code Changed

Field Code Changed

Field Code Changed

Field Code Changed

Field Code Changed

90 °C, the rejection of CA flat sheet membrane to 200 ppm NaCl feed reached 92% at 5 bar; this was 80% improvement as compared with no heat treatment after phase inversion. [365] Two step heat treatment, including 60 °C for 60 min followed by 95 °C for another 20 min, could significantly reduce pore size and create dense outer skin of CA hollow fibre; thus it was preferred over one step heating at 60 °C for 60 min.

Field Code Changed

Field Code Changed

Field Code Changed

Field Code Changed

Field Code Changed

Field Code Changed

Field Code Changed

As compared with 24.6% (no heat treatment) and 32.7% (one step heat treatment), the membrane NaCl rejection increased up to 90.2% (two step heat treatment); whilst the corresponding membrane pure water flux was reduced by over 90%. [367]

Field Code Changed

Field Code Changed

Research suggested that use of CA favour formation of FO membranes with acceptable water flux but unsatisfactory rejection; on the other side, CTA FO membranes usually exhibited good rejection with deteriorated water flux. [363] To improve separation performance of FO membranes, another effective strategy is to investigate suitability of other cellulosic derived polymeric materials, except conventional CA and CTA. For instance, the content of functional groups in cellulose ester, *e.g.* hydroxyl, acetyl, and propionyl or butyryl, greatly influenced separation characteristics of prepared FO membranes. [375]

Field Code Changed

Field Code Changed

Field Code Changed

Field Code Changed

Cellulose esters with hydrophobic groups exhibited good salt rejection, ascribed to low water solubility and hydrated free volume of polymer; whilst a high degree of hydrophilic groups endowed cellulose ester

membranes with high salt passage. [375] Because of the presence of propionyl functional group in cellulose acetate propionate (CAP), the resultant membrane had small equilibrium water content, salt diffusivity and partition coefficient, thus achieving low reverse salt flux. [363] A dual-layer hollow fibre membrane made of CA and CAP with an almost equal degree of acetyl and propionyl substitution exhibited a water flux of 17.5 LMH associated with a reverse salt flux of 2.5 gMH (g/m². h) in PRO mode by using 2.0 M NaCl and DI water as draw and feed solution. [363] Its overall FO performance was superior to those of CA-based flat sheet or hollow fibre FO membranes. [363, 365, 367]

As can be seen, some improvement has been made in separation performance of cellulosic derived polymer FO membranes. Effort is still being made to contribute to understanding of the correlation between membrane structure and performance. [376] A concept of sublayer-free thin films was demonstrated; that a 71-nm-thick CA membrane could largely minimize IPC, thus achieving superior water flux of ~22 LMH in simulated seawater FO desalination using 2 M NaCl draw solution. [376] Nevertheless, the poor mechanical strength of those thin films is not sufficient for practical application. So far, the majority of studies relating to CA derived membranes have emphasized water permeation and salt retention; little touched other aspects, e.g. antifouling property. [377] It is known that some flaws exist when using cellulosic derived materials, such as limited stability to pH, temperature and microorganisms. [12] Thus systematic experiment is necessary to verify the stability and performance of newly developed CA derived membranes in long-term FO operation under different conditions, *i.e.* by treating complex feed solution, varying pH of draw or feed solution or altering operation temperature.

3.1.2 Polyamide and related polymers

TFC RO membranes have been investigated for FO application; a high salt rejection was observed, but severe ICP and low flux occurred. Currently developed TFC FO membranes have a similar structure to that of TFC RO membranes, a porous support and a selective active layer mostly fabricated *via* an IP reaction. The structure of support has shown to greatly affect formation of active layer and in turn FO membrane performances; whilst it is a crucial factor controlling ICP during FO. On the other side, the reverse salt flux and salt rejection of TFC membrane are mainly governed by instincts of selective layer. The positive effect

Field Code Changed

Field Code Changed

Field Code Changed

Field Code Changed

Field Code Changed

Field Code Changed

Field Code Changed

Field Code Changed

Field Code Changed

Field Code Changed

Field Code Changed

Field Code Changed

Field Code Changed

Field Code Changed

Field Code Changed

Field Code Changed

Field Code Changed

Field Code Changed

arising from superior transport properties of active layer is as important as support structure. Therefore, current research targeting at fabrication of high-performance TFC FO membranes is being driven towards optimization of support structural characteristics and active layer transport properties.

3.1.2.1 Effect of support properties on membrane performances

Table 3 summarizes the recent development of TFC FO membranes made on various supports, including CAP, CTA, PES, and PSf. Their FO performances were also listed in terms of AL-FS mode (FO mode) and AL-DS mode (PRO mode). A TFC FO flat sheet membrane features a thin selective layer atop of a flat porous polymeric support, which is usually fabricated *via* phase inversion with/without a thin non-woven fabric. [378] More recently, nanofiber mat (e.g. prepared *via* electrospinning technique) was suggested as a promising support to minimize ICP, attributed to an intrinsically great porosity and low tortuosity. [379-384] CNTs Bucky-papers were also tested as support candidates due to their good flexibility, strength and porosity; whilst some other low cost and highly porous materials such as metal oxide nanotubes and metal forms were recommended for future research. [385] In parallel to the advances of TFC flat sheet module, hollow fibre configuration was widely studied thanks to its advantages, e.g. high packing density, enhanced flow pattern and self-supported structure. [386, 387] It has been found to produce much higher flux under the same driving force than the flat sheet membrane module. [388-391] The support structure of hollow fibre could be tuned by varying spinning parameters, such as air gap and composition of bore fluid, using dry-jet wet spinning method. [392]

Table 3. Overview of the separation performances and testing conditions of TFC FO membranes fabricated on different support materials.

Similarly to the requisites of supports for fabricating high-performance PA TFC RO membranes, the sublayers of TFC FO membranes should possess a good hydrophilicity, structure stability and mechanical strength. [52, 393] The stability to chemicals, temperature and oxidation as well as resistance to foulants could extend their potential use to other harsh industrial environment apart from desalination. [394-396]

Field Code Changed

Field Code Changed

Field Code Changed

Field Code Changed

Field Code Changed

Field Code Changed

Field Code Changed

Field Code Changed

Field Code Changed

Field Code Changed

Field Code Changed

Field Code Changed

Field Code Changed

Field Code Changed

Field Code Changed

Field Code Changed

Field Code Changed

Furthermore, supports must be thin and highly porous with low tortuosity, thus being able to assist in minimizing degree of ICP. [397] Regarding to that, alteration of support structures and properties was suggested as a route, including reducing thickness, adjusting porous structure and tuning hydrophilicity. This might be achieved by tailoring a series of parameters in support synthesis, e.g. polymer concentration, solvent composition, use of additives or functionalization. [397-403] Use of co-casting technique, simultaneously casting of two layers of polymer solution with double-blade, was able to produce favourable structured supports to reduce ICP; the resultant TFC FO membranes showed enhanced water flux with relatively low reverse salt flux. [404-406] Properties of selected non-woven fabrics underneath polymeric sublayer significantly impacted uptake of polymer solution and their adhesion to polymer. [407] Selecting a fabric with high tortuosity, large thickness and low porosity led to a reduction in the water flux of FO membrane. [407] Moreover, addition of foreign components into substrate casting solution could promote construction of favourable substrate properties. For instance, inclusion of lignin content in PSf substrate enhanced its bulk porosity and reduced S_t , providing shorter diffusion pathway and enhancing TFC membrane performance. [407] Using diethylene glycol as a pore-forming agent in PSf/sulphonated poly(ether ketone)/NMP casting solution, greater porosity and broader pore size distribution were created, which helped decrease resistance of support to solution in FO but maintaining comparable salt reverse flux. [393] Introduction of PEG in CAP substrate preparation could not only enhance pore connectivity and avoid macrovoids, but also establish a favourable interaction with casting glass plate. The observed features of resultant support, highly porous bottom and tight top surface, was suitable for fabricating high performance TFC FO membrane. [408]

A support of TFC membrane with macrovoids (or finger-like) structures was able to facilitate water transport and promote ICP reduction in FO. [397] However, those porous structures might become mechanically weak points and worsen membrane separation under continuous water flow or backwashing in practice. [389, 392] High porosity of support might also increase difficulty in forming an excellent active selective layer with required transport properties. [397] In contrast, the sponge-like structure, consisting of small pores surrounding by dense walls, could be favourable to form an integral thin active layer and exhibited advantageous mechanical stability over the finger-like feature; but, it increased resistance to mass

Field Code Changed

Field Code Changed

Field Code Changed

Field Code Changed

Field Code Changed

Field Code Changed

Field Code Changed

Field Code Changed

Field Code Changed

Field Code Changed

Field Code Changed

Field Code Changed

Field Code Changed

Field Code Changed

Field Code Changed

Field Code Changed

Field Code Changed

Field Code Changed

Field Code Changed

Field Code Changed

Field Code Changed

Field Code Changed

Field Code Changed

transfer. [378, 389, 397] Experimental works suggested the ideal support with a sponge-like thin layer on top of a finger-like sublayer would be crucial in fabricating high performance TFC FO membranes. [29, 378] Recently, nanofiber support layers with a scaffold-like and interconnected porous structure have been shown promising characteristics to overcome the main obstacle of sponge-like structure. [379, 380, 382] The nanofiber-supported PA TFC membranes exhibited much lower St ($\sim 80\mu\text{m}$), in relative to a commercial HTI FO membrane ($St = 620\mu\text{m}$); thus 5-fold increase of flux was observed in FO mode by using 0.5 M NaCl as draw solution and DI water as feed solution. [382]

Chung and co-workers suggested hydrophilicity and thickness of support be more critical factors in controlling water transport; [389, 393, 399] the TFC membrane atop of a hydrophilic and fully sponge-like porous substrate favoured water flux than that supported by a hydrophobic and finger-like porous substrate. A number of hydrophilic materials have been explored for preparing or modifying supports, e.g. sulfonated polysulfone, copolymer made of polyethersulfone and polyphenylsulfone (PESU-co-sPPSU), sulphonated poly(ether ketone), polydopamine (PDA) or PVA. [393, 398, 399, 409-412] Using a support containing PESU-co-sPPSU, the TFC FO membrane exhibited 33.0 LMH water flux in PRO mode, when using DI water and 2 M NaCl as feed and draw solution; this was 19.5 LMH greater than that of FO membrane derived from the nascent support without sulphonated content. [399] Hydrophilic PDA was coated on a PSf support (PDA@PSf), enhancing smoothness and hydrophilicity coupled with reduced pore size and distribution. [410, 411] The PDA@PSf supported PA TFC membrane showed optimal water flux of 24 LMH in PRO mode (2.0 M NaCl and DI water as draw agent and feed solution); which was significantly greater than 7.5 LMH by using the PSf-supported membrane. [411] However, highly swollen hydrophilic coating materials may not be perfect for use, due to poor mechanical stability. Moreover, when the modified support is too hydrophilic, its different swelling characteristics would cause a poor adhesion to active layer.

[410] The strategy by covalently bonding the thin layer onto the support can improve stability. For example, use of acyl chlorides as linking molecules to react with hydroxyl groups on a hydrolysed CA support resulted in forming a high separation performance membrane with superior structure stability. [413, 414] However, the reverse salt flux of TFC membrane using TMC as a linking molecule could reach up to ~ 123 gMH against DI water by running 3.8 M NaCl draw solution under PRO mode. More systematic

Field Code Changed

Field Code Changed

Field Code Changed

Field Code Changed

Field Code Changed

Field Code Changed

Field Code Changed

Field Code Changed

Field Code Changed

Field Code Changed

Field Code Changed

Field Code Changed

Field Code Changed

Field Code Changed

Field Code Changed

Field Code Changed

Field Code Changed

Field Code Changed

Field Code Changed

Field Code Changed

Field Code Changed

Field Code Changed

Field Code Changed

Field Code Changed

Field Code Changed

Field Code Changed

Field Code Changed

Field Code Changed

Field Code Changed

Field Code Changed

Field Code Changed

Field Code Changed

Field Code Changed

Field Code Changed

investigation may be carried out to explore other potential linking molecules for optimizing performances of FO membranes and study their long-term physical stability.

In recent years, some research effort has also been contributed to the preparation of supports with inclusion of fillers. [406, 415-422] Ismail's group synthesized TFC membranes on top of TiO₂-incorporated PSf support; which exhibited favourable structures for improving mass transfer and reducing ICP, thus enhanced water flux was observed in FO. [415-418] In BSA fouling test (under PRO mode), the TFC membrane with TiO₂-embedded support could recover 92% flux after 30 min-rinsing under water flow; whereas the flux recovery for the PSf-supported counterpart was only 79%. [415] The TFC membrane with a support derived from blending of montmorillonite, potassium sulfonated polyether sulfone and PES outperformed the neat PES-based TFC membrane by a factor of over sixfold in terms of water flux with reduced reverse salt leakage flux in FO. [421] In addition to adjusting parameters during support preparation, introduction of porous materials is an alternative way altering pore structure, achieving small *S_t* and in turn minimizing ICP. For example, zeolites, which were incorporated in PSf, improved surface porosity, reduced contact angle, and decreased thickness of resultant support, thus providing effective water pathways and effectively controlling ICP in FO. [420] The TFC membrane using MWCNTs-PES support exhibited improved separation performance, due to the open and interconnecting pores within support as well as surface smoothness of separation membrane. Meanwhile, the incorporation of MWCNTs increased tensile strength of support, thus being favourable for fabricating fabric-free support. [419] Undoubtedly, in depth understanding should be promoted on the correlation among inorganic fillers, supports, and their supported TFC membranes. In addition to the fillers which have been reported in literature, the search may be broadened to other mesoporous or microporous inorganic materials.

3.1.2.2 Effect of active layer on membrane performances

Preparation of PA TFC FO membranes is similarly to that of TFC RO membranes; requiring optimization of IP, e.g. composition of monomers, reaction time, and air drying duration. Vankelecom and co-workers suggested both use of surfactant additive and drying time of excess amine solution on PAN support before reaction be two critical parameters for control. [396] Addition of SDS enhanced polymerization to form

Field Code Changed

Field Code Changed

Field Code Changed

Field Code Changed

Field Code Changed

Field Code Changed

Field Code Changed

Field Code Changed

Field Code Changed

Field Code Changed

Field Code Changed

Field Code Changed

Field Code Changed

Field Code Changed

Field Code Changed

uniform and highly crosslinked PA film, thus promoting membrane salt rejection from ~57% to over 95% without seriously compromising permeability. On the other side, removal of excessive amine solution before interacting with TMC led to the formation of less rough membranes with improved salt rejection.

[396] The presence of cetyltrimethylammonium chloride (CTAC) could alter reaction of monomers and molecular aggregation of polymer, because of ionic interaction between CTAC and MPD in aqueous solution. [423] By increasing CTAC content, linear PA structure of active layer increased followed by more microcrystalline structure appearing; as a result, the water flux of PES-supported PA TFC hollow fibre membrane decreased despite higher reverse salt selectivity. [423] The post-treatment on TFC FO membranes using SDS/glycerol followed by thermal annealing facilitated removal of unreacted monomers from active layer, increased free volume size/fractional free volume and reduced membrane overall thickness; thus it was an effective way to improve flux without loss of rejection. [408]

Another great challenge in FO is membrane fouling, nevertheless it was reported to be less severe and more reversible as compared to that in RO. Undoubtedly, the structures of supports significantly tailor characteristics of active layers and in turn fouling property of TFC FO membranes. The surface with high roughness and large leaf-like structures is more prone to accumulation of foulants, leading to a dramatic decline of flux and difficulty in flux restoration by physical cleaning. [402] As a commonly adopted strategy, modification of TFC FO membrane surface, e.g. by covalently linking with PEG, significantly reduced its propensity to various foulants due to existence of barrier sheltering surface from foulant adsorption. [424-426] On the other side, attachment of functionalized silica on TFC membrane *via* covalent amide bonds between amine groups of functionalized nanoparticles and carboxyl groups of TFC surface improved fouling resistance and reduced adhesion to BSA or alginate; [427] which could be explained by the tightly bound hydration layer and neutralization of carboxyl groups on the TFC membrane surface. [427, 428]

In general, AL-DS (PRO) orientation provides higher flux in relative to AL-FS (FO) mode, but might promote fouling if feed containing scalants/foulants due to their easy transport into porous supports of FO membranes. [388, 429] To alleviate scaling or fouling without losing water flux in AL-DS mode, a design of FO hollow fibre with double layers was recommended by Wang's group; in which two active layers were on

Field Code Changed

Field Code Changed

Field Code Changed

Field Code Changed

Field Code Changed

Field Code Changed

Field Code Changed

Field Code Changed

Field Code Changed

Field Code Changed

Field Code Changed

Field Code Changed

Field Code Changed

Field Code Changed

Field Code Changed

Field Code Changed

Field Code Changed

Field Code Changed

Field Code Changed

Field Code Changed

the top and bottom sides of a highly porous support. [429] The hollow fibre membrane with RO and NF-like skins (Fig. 15a and b) fabricated on a PAI support after IP reaction and PEI modification exhibited superior water flux and reverse solute flux (41.3 LMH and 5.2 gMH against DI water using 2.0 M NaCl draw solution in AL-DS mode), [429] to those commercial HTI FO membrane and CA double-skinned membranes. [364, 365] Furthermore, the presence of NF-like layer on the support could largely enhance scaling resistance in AL-DS mode. The 2 h backwash recovered up to 96% of water flux from the CaHPO₄-scaled double-skinned hollow fibre; however, the flux recovery of hollow fibre membrane comprising a single RO selective layer was only 78% (Fig. 15c). [429] Latest work improved the approach without chemical modification of support but using polyelectrolyte LbL to form NF-like skin whilst keeping formation of PA RO-like skin layer. [430] The formed NF-like skin effectively avoided the direct contact between feed and support, thus avoiding transport of foulants, e.g. humic acid, dextran and lysozyme, and subsequent pore clogging. A stable water flux with less than 10% decline over 4 h was recorded for resulting double-skinned hollow fibre, whereas that for RO-skinned hollow fibre was as high as ~30% – 40% using the feed of 200 ppm foulant. [430]

Field Code Changed

Field Code Changed

Field Code Changed

Field Code Changed

Field Code Changed

Field Code Changed

Field Code Changed

Field Code Changed

Field Code Changed

Field Code Changed

Field Code Changed

Field Code Changed

Field Code Changed

Fig. 15. SEM images of cross-section of a double-skinned FO hollow fibre with (a) inner RO skin and (b) outer NF skin; (c) effect of cleaning on scaled double-skinned FO hollow fibre membrane (denoted as FO-RO/NF_s) and FO hollow fibre membrane with only RO active layer (denoted as FO-RO_s) (scaling test was carried out by flowing mixture of CaCl₂ and K₂HPO₄ as feed and 0.5 M NaCl as draw solution) (modified from the reference [429]).

Field Code Changed

Field Code Changed

3.1.3 Polyelectrolytes

Despite a difficulty existing in large scale production of LbL assembled polyelectrolyte membranes, they may offer good water flux and rejection to divalent ions accompanied with good solvent resistance and thermal stability. [431, 432] This group of materials has been regarded as suitable candidates in fabricating FO membranes with NF-like separation performances. Most current studies of LbL assembled polyelectrolyte FO films demonstrated flat sheet module by successive soaking of cation and anion

Field Code Changed

Field Code Changed

Field Code Changed

polyelectrolyte onto single side of flat support; later research extended to hollow fibre module. [430, 433]

Field Code Changed

On the contrary to the commonly adopted single-skinned membranes, double-skinned LbL polyelectrolyte

Field Code Changed

FO membranes (Fig. 16a) showed much better antifouling performance as compared to the single-skinned

Field Code Changed

counterpart (Fig. 16b), by largely minimizing foulant clogging within porous support and then reduction of

mass transfer. [434] Incorporation of antimicrobial Ag nanoparticles in LbL PAH/PSS FO membrane

Field Code Changed

provided excellent antibacterial properties against both *Bacillus subtilis* and *E. coli*; and showed great

Field Code Changed

potential to reduce biofouling in desalination. [310]

Field Code Changed

Field Code Changed

The first study reported utilization of polyelectrolyte PAH/PSS multilayer FO membranes fabricated by LbL

assembly method in 2011. [431] In AL-FS mode, a remarkable flux of 28.7 LMH was achieved by flowing

Field Code Changed

1.0 M MgCl₂ and DI water as draw and feed solution. Unfortunately, the severe reverse solute flux was

Field Code Changed

more than 15 gMH under this condition. [431] Assembling greater bilayers of polyelectrolyte enhanced

Field Code Changed

solute retention of resultant films; however, a reduction in water permeability was encountered. [431, 435-

Field Code Changed

437] Chemical crosslinking method may also improve separation performance as well as their long-term

Field Code Changed

stability. [438] As compared to non-crosslinked membrane, the glutaraldehyde-crosslinked PAH/PSS FO

Field Code Changed

membrane showed better MgCl₂ rejection rate over a wide range of concentration. Especially, it could reach

Field Code Changed

Field Code Changed

water flux of approximately 100 LMH against DI feed water using 2 or 3 M MgCl₂ draw solution in AL-DS,

strongly revealing their applicability for high flux FO application. [437] A subsequent exposure of

Field Code Changed

Field Code Changed

glutaraldehyde-crosslinked PAH/PSS FO membrane to UV irradiation could future improve its rejection

capacity to monovalent ion. [436] A highly crosslinked PAH/PSS membrane exhibited reverse salt flux as

Field Code Changed

Field Code Changed

low as ~8 gMH flux and water flux of ~11 LMH in AL-DS mode by flowing relatively low concentration

draw solution (0.3 M NaCl). [436]

Field Code Changed

Field Code Changed

Just as important in CA asymmetric and PA TFC FO membranes, hydrophilicity and porosity of sublayers

are essential in generating LbL polyelectrolyte FO membranes with improved performances. PAN was

commonly selected as the substrate material; which was hydrolysed by NaOH to be negatively charged and

hydrophilic for subsequent LbL assembly. Addition of inorganic fillers could alter characteristics of supports.

For example, the presence of hydrophilic porous silica gel particles in PAN substrate layer significantly

increased water permeability of PAH/PSS LbL membrane; ascribed to porosity of silica gel and improved support porosity. [439] The LbL chitosan/PAA polyelectrolyte membrane on top of the support integrating PVA and functionalized montmorillonite clay was able to achieve 34 LMH water flux when using 2 M NaCl draw solution in synthetic wastewater treatment (AL-DS mode). [440] Careful control on the introduction of fillers into polymeric supports is highly required yielding desired performance, since high loading of inorganic particles caused agglomeration, decreased effective water transport through support, and deteriorated membrane separation performances. [439]

Field Code Changed

Field Code Changed

Field Code Changed

Field Code Changed

Field Code Changed

Field Code Changed

Fig. 16. (a) Conceptual illustrations of double-skinned LbL membrane fabrication; (b) normalized flux for double-skinned LbL membranes under different fouling conditions (300 ppm dextran, 20 ppm alginate, or 300 ppm alginate) (In the membrane symbols of “xLbL3-0”, “xLbL3-1”, “xLbL3-2”, and “xLbL3-3”, the two numbers are referred to the number of polyelectrolyte layers for the top and bottom rejection skins; “xLbL” represents crosslinked LbL membranes). [434]

Field Code Changed

Field Code Changed

3.1.4 Others

Since commercially developed by Celanese Corporation in 1983, polybenzimidazole (PBI), well known for its good chemical, mechanical, and thermal properties, has been employed as an attractive separation membrane material. [441, 442] Thanks to heterocycle imidazole ring, hydrogen bonding between PBI molecules and delocalization of proton of imidazole group make PBI self-charged in aqueous solution accompanied with high hydrophilicity. [443, 444] The first prepared PBI asymmetric FO hollow fibres *via* phase inversion yielded high rejection to divalent ions (*i.e.* $\text{MgSO}_4 > 99\%$) and slightly lower monovalent salt rejection ($\text{NaCl} \sim 97\%$) in FO against DI water using 2.0 M single salt draw solution. However, under that condition, the maximal permeation flux was merely 9 LMH. [442] In order to enhance both selectivity and permeation, modification would be carried out towards more hydrophilic PBI membrane with tunable pore sizes. The crosslinking of PBI hollow fibre with *p*-xylylene dichloride improved salt selectivity but it sacrificed water permeance. [443] Later studies further verified functionalization of PBI flat sheet membranes, e.g. activation by 4-(chloromethyl) benzoic acid and subsequent surface modification

Field Code Changed

Field Code Changed

Field Code Changed

Field Code Changed

Field Code Changed

Field Code Changed

Field Code Changed

Field Code Changed

Field Code Changed

Field Code Changed

with taurine, *p*-phenylene diamine (PD), ethylene diamine, and poly(acrylamide-*co*-acrylic acid) (P(Am-*co*-AA)), finely increased negative surface charge, improved hydrophilicity, and adjusted pore sizes of membranes; thus promotion in separation performance was seen. [445-447] Especially, in addition to higher degree of NaCl rejection, the membrane treated by P(Am-*co*-AA) and PD could induce water flux of 5.6 LMH, which was approximately twofold increase to the nascent membrane, against 0.1 M NaCl solution driven by using 2 M NH₄HCO₃ draw solution across the permeate side of membrane. [445] Further experiment is needed with additional investigation on the effect of parameters in FO conditions, e.g. type or concentration of feed or draw solution and membrane orientation, on the modified membranes.

Field Code Changed

Field Code Changed

Field Code Changed

Field Code Changed

Poly(amide-imide) (PAI), known as Torlon[®], exhibits an excellent mechanical, thermal, and chemical stability; which has been utilized for fabricating FO membranes in the modules of flat sheet and hollow fibre.

[28, 448-451] The first study exploring a simple chemical post-treatment by immersing PAI hollow fibre into polyethyleneimine (PEI) solution under moderate heating to initiate reaction between imides of PAI and amines of PEI; this formed positively charged hollow fibres with a NF-like thin layer. [448] When using

Field Code Changed

Field Code Changed

Field Code Changed

0.5 M MgCl₂ and DI water as draw and feed solution in AL-DS and AL-FS, the water fluxes of modified PAI membranes were around 13 LMH and 9 LMH, respectively, with a rejection of ~92%. [448] Using a

Field Code Changed

Field Code Changed

dual-layer hollow fibre with PEI-crosslinked PAI outer layer supported by PES inner layer could avoid formation of a denser substrate, which negatively affected permeation flux during FO. The resultant fibre exhibited water flux as high as 27.5 LMH coupled with reverse salt flux of 5.5 gMH against DI water using

Field Code Changed

Field Code Changed

0.5 M MgCl₂ draw solution in AL-FS. [450] However, this modification of PAI layer by PEI increased positively charges on surface and might easily attract negatively charged foulants in feed; [449] coating of

Field Code Changed

Field Code Changed

Field Code Changed

Field Code Changed

polyelectrolytes would be a versatile way to alter charges as well as tighten pores of active layer. Deposition of negatively charged PSS onto PEI-modified PAI hollow fibre decreased zeta potential and enhanced membrane resistance to protein foulant; stable flux of approximately 11 LMH against feed mixture of

1000 ppm BSA and 2000 ppm Na₂SO₄ was observed in 4 h FO separation using 0.5 M Na₂SO₄ draw solution. [449] Similarly, the double-layer hollow fibre, consisting of an outer PEI-crosslinked PAI layer and an inner PES layer, was treated by multilayer deposition in a sequence of PSS/PAH/PSS. Due to PSS as last layer, the zeta potential of resultant fibre was reduced; meanwhile remarkably high water flux of

Field Code Changed

Field Code Changed

39.3 LMH with 13.8 gMH reverse salt flux was recorded in AL-DS (0.5 M MgCl₂ and DI water as draw and feed solution). [451]

Field Code Changed

Field Code Changed

As aforementioned in Section 2.1.4, AQP biomimetic membranes have been seen as potentially new generation water treatment membranes; however, they suffer some challenges, especially poor mechanical property under pressure for RO/NF purpose. Some recent studies explored their use in FO process, which is in principle driven by osmotic differential without use of hydraulic pressure. In the design of biomimetic FO membranes, several issues were identified in prior works. For instance, the activity of AQP should be sustained for effective water transport. Even though less mechanical strength is required in FO, the biomimetic FO membranes should be stable by preventing vesicles being peeled off *via* water flow in FO; thereby supports and vesicles normally need proper functionalization. Chung's group applied proteopolymersomes consisting of AQP and ABA with methacrylate end group onto acrylate functionalized gold-coated polycarbonate tracked-etched (PCTE) support under pressure, followed by UV to initiate covalent bonding between functional groups of ABA and support. It created an ultrathin active layer on the support; which could facilitate water flux of ~18 LMH at AQP:ABA molar ratio of 1:400 when flowing 0.5 M NaCl draw solution and ultrapure water feed. [275] However, a small amount of defects might still exist in the resultant membranes and a part of AQP could have lost function during that preparation. Following the similar strategy, the UV-crosslinked proteopolymersomes with acrylate and disulphide groups were immobilized onto the gold-coated PCTE membrane and then encapsulated by PDA-histidine coating. [278] Any defect between vesicles and pores of substrate would be reduced by using PDA coating. As compared to the aforesaid work with the same AQP:ABA ratio of 1:400, [275] the water flux was enhanced by around 2-fold to 40 LMH (with 7.1 gMH salt reverse flux) when using 0.5 M NaCl and water as draw and feed solution (in PRO mode). However, the dramatic decrease (~25%) in NaCl rejection between its use under FO and NF conditions revealed the instability of membrane. To simplify complex preparation in creating stable biomimetic membranes, the LbL polyelectrolyte assembly method shows advantageous characteristics. After PAH-PSS/PAA assembly onto a hydrolysed PAN support, deposition of poly-L-lysine (PLL)-protected proteoliposomes, and finally coating of PSS/PAA, the resultant membrane demonstrated a

Field Code Changed

Field Code Changed

Field Code Changed

Field Code Changed

Field Code Changed

Field Code Changed

satisfactory stability along with >25% higher permeability as compared to the counterpart without embedment of liposomes under agitation at 4 bar. [279] To further enhance the deposition of AQP-embedded vesicles, magnetic nanoparticles were incorporated into them (Fig. 17a). [280] With the aid of a strong magnet during the deposition of PLL-encapsulated magnetic proteoliposomes, confocal laser scanning microscopy (CLSM) confirmed adsorption and coverage of liposomes on the membrane surface was greatly improved (Fig. 17b). The biomimetic membrane with 2% magnetic proteoliposomes exhibited 83.5 LMH flux against DI water feed when using 1.5 M MgCl₂ draw solution (in PRO mode), which was ~70% improvement compared with the nascent membrane (49 LMH). [280] These high performance biomimetic FO membranes offer chance for revolution in the research field of water treatment membranes. Some promising progress has been made towards commercialization for practical use by Aquaporin A/S and its Singaporean subsidiary Aquaporin Asia Pte. Ltd. [27, 452] Special efforts are still needed to simplify fabrication and in turn reduce manufacturing cost. Low-cost production of active proteins and scale-up fabrication of non-defect biomimetic membranes would be other challenges during commercialization. Meanwhile, their long-term stability and integrity in permeation tests is urged for investigation in the future studies.

Fig. 17. (a) Schematic representation of the fabrication process for the magnetic-aided LbL membrane; (b) representative CLSM images of liposome adsorbed LbL films as a function of deposition time, (i) with and (ii) without the magnetic driving force. Scale bar: 10 μm. [280]

3.2 Mixed matrix membranes

Differently from the significant development of inorganic-organic MMMs for RO desalination, it is a relatively early stage for their utilization in FO separation. Improvement in separation performances, including water permeation and salt retention, has been motivating research interest at inclusion of inorganic fillers in polymeric matrix. [453-459] Inspired by zeolite-PA TFN RO membrane, a similar approach was reported to fabricate zeolite-PA TFN membranes for FO purpose in 2012. [454] The water flux of PA TFN membrane with 0.1 wt/v% zeolite (in TMC/hexane) was overall around 50% higher than that of TFC membrane in either AL-DS or AL-FS mode; however, further increasing zeolite content in membrane

Field Code Changed

Field Code Changed

Field Code Changed

Field Code Changed

Field Code Changed

Field Code Changed

Field Code Changed

Field Code Changed

Field Code Changed

Field Code Changed

Field Code Changed

Field Code Changed

Field Code Changed

Field Code Changed

Field Code Changed

increased solute flux and in turn did not endow remarkably additional improvement in water permeation.

[454] Similarly to zeolites, CNTs have been theoretically suggested in early work for their enormous potential in fabricating high performance water treatment membrane. [460] For the first time, experimental results proved the MPD-TMC TFN membranes incorporated with 0.1 wt/v% (in MPD aqueous solution) amine-functionalized MWCNTs exhibited water flux of 95.7 LMH and solute flux of 4.8 gMH, which were approximately 160% higher and 30% lower than those of the TFC FO membrane, respectively (2 M and 10 mM NaCl draw and feed solution; in AL-DS); representing a dramatic improvement regarding to FO membranes. [455] This similar concept was further explored in the double-skinned configuration of TFN membrane to induce significantly lower ICP but higher water flux; additionally, much better antifouling property to humic acid was observed as compared with the single-skinned membrane. [457]

Until now, only limited work has been initiated on integration of multiple types of fillers into polymeric matrix for fabricating FO membranes; [461] this is believed to provide additional opportunity to improve membrane separation. Moreover, the progress in utilization of MMMs for FO separation is still at its initial stage. Fundamental studies are needed to explicate the transport mechanisms governing this group of membranes; and facilitate optimization between loading of inorganic fillers and membrane separation performances.

4. Conclusions and future perspectives

RO process has been widely used for desalination for decades as one of the main technologies to tackle water shortage and scarcity crisis worldwide. Due to its simplicity and relatively low cost, RO technology is believed to play a crucial role in the water desalination in the future. The demand to reduce energy consumption and subsequent cost continuously has motivated research into exploration of RO membrane materials with high permeability and salt rejection. Significant interest also remains in discovering fouling-resistant and chemical-stable RO membranes, as alternative strategy to reduce energy and cost in RO desalination. Meanwhile, the research on FO separation, as an osmotically driven process, has blossomed in the last few years. FO process has shown vast potential in various applications such as desalination, wastewater treatment, and food processing. Note that the water flux of FO membranes is still unsatisfactory

Field Code Changed

Field Code Changed

Field Code Changed

Field Code Changed

Field Code Changed

Field Code Changed

Field Code Changed

Field Code Changed

Field Code Changed

Field Code Changed

as compared with RO desalination process under the similar theoretical applied pressure. In the short run, FO is suggested as a potential pre-treatment integrated into conventional RO desalination process to remove soluble species and in turn help improve quality of water product, including enhanced removal of boron and trace organic compounds. [462] In recent years studies have been focused on the improvement in water permeability and salt retention of FO membranes. FO and RO membranes, made of cellulosic ester, polyamide, zeolite-polyamide or aquaporin (Table 4), are commercially available in market; each of them has its own advantages and disadvantages. Research will continue on exploring RO and FO membranes with superior properties.

Field Code Changed

Field Code Changed

Table 4. Summary of commercially available RO and FO membranes developed thus far.

In the case of RO polymeric membranes, the improvement of flux and rejection undoubtedly has been the focus of research, targeting at outperforming conventional RO membranes. Meanwhile, significant research has been conducted to address two main issues with current desalination membranes, e.g. chlorine stability and fouling resistance. More attention was paid to the development of high flux and high rejection PA or related TFC membranes although some membranes fabricated in other types of structures or materials were developed because of niche applications. With regards to those newly developed membranes, water permeability and rejection of monovalent and divalent ions have been investigated to some extent; but research is needed to look into their removal of other compounds such as boron or trace organic compounds, which are commonly present in the natural water environment. The performances of those novel RO membranes reported in the literature, in terms of salt rejection and water permeability, have not been far superior to those of currently commercial PA TFC membranes. [463] Moreover, because of lack of data from long term and large scale operation, their stability and performances in the real world are yet to be known.

Field Code Changed

Field Code Changed

Compared to the research into novel polymeric materials, surface modification of commercial membranes by either chemical grafting/crosslinking or physical coating seems more preferable, ascribed to its relatively low cost and ease of operation. Especially, it may be more feasible for commercial implementation based on currently available membrane manufacturing processes. Until now, a variety of potential coating materials

have been investigated. In particular, some of the selected materials such as hydrophilic and biocompatible polyelectrolytes or zwitterionic materials have been found to improve not only separation performances but also antifouling property and chlorine stability. Despite some progress, there are still some issues associated with surface modification. For instance, in addition to pore blockage on the active layer, some modifiers such as polyelectrolytes may uptake water and then mask membrane surface, thus increasing concentration polarization and reducing water flux. The layer formed after modification should be ultrathin, which can largely avoid increasing transport resistance and sacrificing water permeability. Good chemical and mechanical stability must be sustained for long-term operation when using those modified membranes; which have not been studied in depth in most cases. As compared with physical surface coating, chemical grafting would be a more favourable approach to achieve that. The surface coating of nanoparticles such as Ag and Cu could largely maximize the contact between antibacterial materials and foulants, showing advantageous aspects as opposed to the adoption of traditional MMMs or direct addition of nanoparticles into feed of water treatment processes. Importantly, the route using surface modification makes the recharge of those depleting antimicrobial materials feasible to operate. From a more practical perspective, the quest on the observation on the stability and efficiency of those modified membranes over long term should be continued. Moreover, there is an urgent need to simplify their preparation process and reduce related cost in large scale manufacturing.

Mixed matrix membranes (MMMs) with nanostructured fillers, taking advantages of distinct characteristics of each phase, have offered exceptional performances in terms of permeability, rejection, chlorine and fouling resistance for RO desalination. Until now, tremendous progress has been made as seen from the published laboratory work; some conclusive findings have driven their practical application and commercialization. For example, zeolites-PA TFN membranes have been successfully commercialized. It is believed that enormous market potential also exists in MMMs with other inorganic fillers. The class of carbon nanomaterials such as CNTs and GO stand out as interesting fillers and they have achieved some exciting results in the fabrication of MMMs despite some hurdles yet to be overcome. For example, if proper orientation of CNT pore opening to flow direction, such RO MMMs may have extremely high permeability, potentially several orders of magnitude greater than current membranes; however, this is difficult to achieve

at a reasonable cost for large scale fabrication. Additionally, the integrated use of multiple types of fillers is expected to further advance performances of MMMs. Some challenges line in the preparation of MMMs, including uniform dispersion of inorganic particles into polymeric matrix as well as improved interfacial correlation between polymer and fillers. To optimize the preparation process, a holistic understanding on the separation mechanisms of MMMs is necessary; on the other hand, the use of these membranes in treating real water will provide reliable data on their practical performances. The safety issue by using such nanostructured materials in separation membranes should also be well investigated in the future work. Last, but not least, it requires careful consideration on their suitability into current membrane modules and manufacturing process as well as cost of producing such nanostructured materials and membranes.

In recent decade, some breakthroughs have been reported in the development of FO membranes, such as using phase inversion (e.g. CA asymmetric membranes), IP (e.g. PA TFC membranes), and LbL assembly (e.g. polyelectrolyte multilayer membranes). For instance, double-skinned FO membranes, featuring two selective skin layers and a fully porous support, have been theoretically and experimentally shown to induce low fouling propensity and minimize ICP. Similarly to RO membranes, ideal FO membranes are expected to have the characteristics of high water permeability and salt retention, in addition to good antifouling property and chemical stability. The use of FO membranes with low reverse salt flux would also reduce the loss of draw solution during FO. It is known that FO membranes need small values of structural parameter (St) (e.g. $<200 \mu\text{m}$), which reflects the thickness, porosity and tortuosity of FO membrane supports, thus minimizing ICP. [33] Despite some debate, it is generally accepted that highly porous, hydrophilic and thin support helps achieve low St . Note that a small St value indicates low transport resistance within the structure, which may sacrifice mechanical strength of membrane. Suitable mechanical strength of membranes is essential to sustain their performances under shear forces induced by cross-flow over membrane surface. Some prior works initiated interest in use of nanofibers and incorporation of porous materials, which may further be explored in future research. In addition, the structures of supports strongly impact the formation of active layers with desirable transport properties. A much better understanding of correlation between supports and thin layers will promote optimization of materials selection, membrane structure, and fabrication process. Meanwhile, most of current studies focus on the testing of newly

Field Code Changed

Field Code Changed

developed FO membranes (in FO or PRO mode) using DI water or low concentration of salt solution (e.g. NaCl) as feed even though they are intended for practical applications in water treatment or desalination. Thus it is necessary to verify their performances using actual feed water for a specific application. Especially, when using the feed contaminated with foulants or scalants, the fouling on FO membranes requires detailed investigation.

Since 1970s, the concept of osmotic power has attracted research attention. PRO membranes used for that purpose share some similarity to FO membranes, but they require greater mechanical strength due to hydraulic pressure involved. [49] Seen from the current development of membranes [464-474], little information has been available on mechanical stability or durability in relation to PRO application. The continuing research may provide more insight into PRO operation and PRO membrane design.

Biomimetic membranes have shown remarkable performances for potential application in both FO and RO/NF and thus captured a great deal of research interest. They are believed to have opened an avenue for fabricating high-performance water treatment membranes. Albeit some existing results have been achieved, the widespread application of biomimetic membranes still faces a number of challenges. It is crucial to further improve membrane mechanical strength and integrity for practical applications, including FO and RO. Moreover, more work should look into how to maximize the function of AQP during membrane fabrication and practical operation. Other issues remain in manufacturing cost and simplicity, and the difficulty in large-scale fabrication of defect-free biomimetic membranes also needs to be addressed.

Acknowledgement

This work was in part supported by the Australian Research Council (Discovery Project no. DP140101591). D. Li would like to acknowledge the support from Murdoch University Small Grant Scheme (2015).

Field Code Changed

Field Code Changed

Field Code Changed

Field Code Changed

References

- [1] Greenlee LF, Lawler DF, B.D. F, B. M, Moulin P. Reverse osmosis desalination: Water sources, technology, and today's challenges. *Water Res* 2009;43:2317-48.
- [2] Lee KP, Arnot TC, Mattia D. A review of reverse osmosis membrane materials for desalination—Development to date and future potential. *J Membr Sci* 2011;370:1-22.
- [3] Shannon MA, Bohn PW, Elimelech M, Georgiadis JG, Marinas BJ, Mayes AM. Science and technology for water purification in the coming decades. *Nature* 2008;452:301-10.
- [4] Humplik T, Lee J, O'Hern S, Fellman B, Baig M, Hassan S, Atieh M, Rahman F, Laoui T, Karnik RW, EN. Nanostructured materials for water desalination. *Nanotechnology* 2011;22:292001/1-19.
- [5] Burn S, Hoang M, Zarzo D, Olewniak F, Campos E, Bolto B, Barron O. Desalination techniques — A review of the opportunities for desalination in agriculture. *Desalination* 2015;364:2-16.
- [6] Malaeb L, Ayoub GM. Reverse osmosis technology for water treatment: State of the art review. *Desalination* 2011;267:1-8.
- [7] Reid CE, Breton EJ. Water and ion flow across cellulosic membranes. *J Appl Polym Sci* 1959;1:133-43.
- [8] Loeb S. The Loeb-Sourirajan membrane: How it came about. In: Turbak AF, editor. *Synthetic Membranes*. Washington DC: American Chemical Society; 1981. p. 1-9.
- [9] Loeb S, Sourirajan S. Sea water demineralization by means of an osmotic membrane. *Adv Chem* 1963;38:117-32.
- [10] Geise GM, Lee H-S, Miller DJ, Freeman BD, McGrath JE, Paul DR. Water purification by membranes: The role of polymer science. *J Polym Sci B* 2010;48:1685-718.
- [11] Shenvi SS, Isloor AM, Ismail AF. A review on RO membrane technology: Developments and challenges. *Desalination* 2015;368:10-26.
- [12] Zhao S, Zou L, Tang CY, Mulcahy D. Recent developments in forward osmosis: Opportunities and challenges. *J Membr Sci* 2012;396:1-21.
- [13] Baker RW. *Membrane Technology and Applications*. 3rd Edition ed. New York: Wiley; 2012:97-247.
- [14] Cadotte JE. Interfacially synthesized reverse osmosis membrane. *US* 4,277,3441981.
- [15] Petersen RJ. Composite reverse osmosis and nanofiltration membranes. *J Membr Sci* 1993;83:81-150.
- [16] Liyanaarachchi S, Shu L, Muthukumar S, Jegatheesan V, Baskaran K. Problems in seawater industrial desalination processes and potential sustainable solutions: a review. *Rev Environ Sci Biotechnol* 2014;13:203-14.
- [17] Subramani A, Jacangelo JG. Emerging desalination technologies for water treatment: A critical review. *Water Res* 2015;75:164-87.
- [18] Semiat R. Energy Issues in Desalination Processes. *Envir Sci Tech* 2008;42:8193-201.
- [19] Cohen-Tanugi D, McGovern RK, Dave SH, Lienhard JH, Grossman JC. Quantifying the potential of ultra-permeable membranes for water desalination. *Energy Environ Sci* 2014;7:1134-41.
- [20] Cath T, Childress AE, Elimelech M. Forward osmosis: Principles, applications, and recent developments. *J Membr Sci* 2006;281:70-87.
- [21] Chung T-S. Emerging forward osmosis (FO) technologies and challenges ahead for clean water and clean energy applications. *Curr Opin Chem Eng* 2012;1:246-57.
- [22] Hoover LA. Forward with osmosis: Emerging applications for greater sustainability. *Envir Sci Tech* 2011;45:9824-30.
- [23] Su J, Zhang S, Ling MM, Chung TS. Forward osmosis: an emerging technology for sustainable supply of clean water. *Clean Technol Envir* 2012;14:507-11.
- [24] Qin J-J, Lay WCL, Kekre KA. Recent developments and future challenges of forward osmosis for desalination: a review. *Desalin Water Treat* 2012;39:123-36.
- [25] Chung T-S, Zhang S, Wang KY, Su J, Ling MM. Forward osmosis processes: Yesterday, today and tomorrow. *Desalination* 2012;287:78-81.
- [26] Ge Q, Ling M, Chung T-S. Draw solutions for forward osmosis processes: Developments, challenges, and prospects for the future. *J Membr Sci* 2013;442:225-37.
- [27] Tang C, Wang Z, Petričić I, Fane AG, Hélix-Nielsen C. Biomimetic aquaporin membranes coming of age. *Desalination* 2015;368:89-105.
- [28] Qiu C, Setiawan L, Wang R, Tang CY, Fane AG. High performance flat sheet forward osmosis membrane with an NF-like selective layer on a woven fabric embedded substrate. *Desalination* 2012;287:266-70.
- [29] Wei J, Qiu C, Tang CY, Wang R, Fane AG. Synthesis and characterization of flat-sheet thin film composite forward osmosis membranes. *J Membr Sci* 2011;372:292-302.

Field Code Changed

- [30] McCutcheon JR, McGinnis RL, Elimelech M. A novel ammonia—carbon dioxide forward (direct) osmosis desalination process. *Desalination* 2005;174:1-11.
- [31] Herron J. Asymmetric forward osmosis membranes. US 7,445,712 B2: Hydration Technologies Ltd; 2008.
- [32] Ren J, McCutcheon JR. A new commercial thin film composite membrane for forward osmosis. *Desalination* 2014;343:187-93.
- [33] Fane AG, Wang R, Hu MX. Synthetic membranes for water purification: Status and future. *Angew Chem Int Edit* 2015;54:3368-86.
- [34] Das R, Ali ME, Hamid SBA, Ramakrishna S, Chowdhury ZZ. Carbon nanotube membranes for water purification: A bright future in water desalination. *Desalination* 2014;336:97-109.
- [35] Goh PS, Ismail AF, Ng BC. Carbon nanotubes for desalination: Performance evaluation and current hurdles. *Desalination* 2013;308:2-14.
- [36] Lau WJ, Ismail AF, Misdan N, Kassim MA. A recent progress in thin film composite membrane: A review. *Desalination* 2012;287:190-9.
- [37] Peñate B, García-Rodríguez L. Current trends and future prospects in the design of seawater reverse osmosis desalination technology. *Desalination* 2012;284:1-8.
- [38] Mezher T, Fath H, Abbas Z, Khaled A. Techno-economic assessment and environmental impacts of desalination technologies. *Desalination* 2011;266:263-73.
- [39] Kang G-d, Cao Y-m. Development of antifouling reverse osmosis membranes for water treatment: A review. *Water Res* 2012;46:584-600.
- [40] Buonomenna MG. Nano-enhanced reverse osmosis membranes. *Desalination* 2013;314:73-88.
- [41] Misdan N, Lau WJ, Ismail AF. Seawater Reverse Osmosis (SWRO) desalination by thin-film composite membrane—Current development, challenges and future prospects. *Desalination* 2012;287:228-37.
- [42] Xu G-R, Wang J-N, Li C-J. Strategies for improving the performance of the polyamide thin film composite (PA-TFC) reverse osmosis (RO) membranes: Surface modifications and nanoparticles incorporations. *Desalination* 2013;328:83-100.
- [43] Mohammad AW, Teow YH, Ang WL, Chung YT, Oatley-Radcliffe DL, Hilal N. Nanofiltration membranes review: Recent advances and future prospects. *Desalination* 2015;356:226-54.
- [44] Goh PS, Ismail AF. Review: is interplay between nanomaterial and membrane technology the way forward for desalination? *J Chem Technol Biot* 2015;90:971-80.
- [45] Chekli L, Phuntsho S, Shon HK, Vigneswaran S, Kandasamy J, Chanan A. A review of draw solutes in forward osmosis process and their use in modern applications. *Desalin Water Treat* 2012;43:167-84.
- [46] Lutchmiah K, Verliefe ARD, Roest K, Rietveld LC, Cornelissen ER. Forward osmosis for application in wastewater treatment: A review. *Water Res* 2014;58:179-97.
- [47] Akther N, Sodiq A, Giwa A, Daer S, Arafat HA, Hasan SW. Recent advancements in forward osmosis desalination: A review. *Chem Eng J* 2015;281:502-22.
- [48] Alsvik IL, Hägg MB. Pressure retarded osmosis and forward osmosis membranes: Materials and methods. *Polymers* 2013;5:303-27.
- [49] Klaysom C, Cath TY, Depuydt T, Vankelecom IFJ. Forward and pressure retarded osmosis: Potential solutions for global challenges in energy and water supply. *Chem Soc Rev* 2013;42:6959-89.
- [50] Wang J, Dlamini DS, Mishra AK, Pendergast MTM, Wong MCY, Mamba BB, Freger V, Verliefe ARD, Hoek EMV. A critical review of transport through osmotic membranes. *J Membr Sci* 2014;454:516-37.
- [51] Li D, Wang H. Recent developments in reverse osmosis desalination membranes. *J Mater Chem* 2010;20:4551-66.
- [52] McCutcheon JR, Elimelech M. Influence of membrane support layer hydrophobicity on water flux in osmotically driven membrane processes. *J Membr Sci* 2008;318:458-66.
- [53] Peng F, Jiang Z, Hoek EMV. Tuning the molecular structure, separation performance and interfacial properties of poly(vinyl alcohol)—polysulfone interfacial composite membranes. *J Membr Sci* 2011;368:26-33.
- [54] Gohil JM, Ray P. Polyvinyl alcohol as the barrier layer in thin film composite nanofiltration membranes: Preparation, characterization, and performance evaluation. *J Colloid Interf Sci* 2009;338:121-7.
- [55] Jahanshahi M, Rahimpour A, Peyravi M. Developing thin film composite poly(piperazine-amide) and poly(vinyl-alcohol) nanofiltration membranes. *Desalination* 2010;257:129-36.
- [56] Lau W-J, Ismail AF. Effect of SPEEK content on the morphological and electrical properties of PES/SPEEK blend nanofiltration membranes. *Desalination* 2009;249:996-1005.
- [57] Wang K, Zeng Y, He L, Yao J, Suresh AK, Bellare J, Sridhar T, Wang H. Evaluation of quaternary phosphonium-based polymer membranes for desalination application. *Desalination* 2012;292:119-23.

- [58] Lee CH, McCloskey BD, Cook J, Lane O, Xie W, Freeman BD, Lee YM, McGrath JE. Disulfonated poly(arylene ether sulfone) random copolymer thin film composite membrane fabricated using a benign solvent for reverse osmosis applications. *J Membr Sci* 2012;389:363-71.
- [59] He L, Li D, Zhang G, Webley PA, Zhao D, Wang H. Synthesis of carbonaceous poly(furfuryl alcohol) membrane for water desalination. *Ind Eng Chem Res* 2010;49:4175-80.
- [60] Zhang Y, Zhao C, Yan H, Pan G, Guo M, Na H, Liu Y. Highly chlorine-resistant multilayer reverse osmosis membranes based on sulfonated poly(arylene ether sulfone) and poly(vinyl alcohol). *Desalination* 2014;336:58-63.
- [61] Huang R, Chen G, Sun M, Gao C. Preparation and characterization of quaternized chitosan/poly(acrylonitrile) composite nanofiltration membrane from anhydride mixture cross-linking. *Sep Purif Technol* 2008;8:393-9.
- [62] Miao J, Chen G-h, Gao C-j. A novel kind of amphoteric composite nanofiltration membrane prepared from sulfated chitosan (SCS). *Desalination* 2005;181:173-83.
- [63] Miao J, Zhang L-C, Lin H. A novel kind of thin film composite nanofiltration membrane with sulfated chitosan as the active layer material. *Chem Eng Sci* 2013;87:152-9.
- [64] Zhou C, Gao X-l, Li S-s, Gao C-j. Fabrication and characterization of novel composite nanofiltration membranes based on zwitterionic O-carboxymethyl chitosan. *Desalination* 2013;317:67-76.
- [65] Paul M, Park HB, Freeman BD, Roy A, McGrath JE, Riffle JS. Synthesis and crosslinking of partially disulfonated poly(arylene ether sulfone) random copolymers as candidates for chlorine resistant reverse osmosis membranes. *Polymer* 2008;49:2243-52.
- [66] Park HB, Freeman BD, Zhang Z-B, Sankir M, McGrath JE. Highly chlorine-tolerant polymers for desalination. *Angew Chem Int Edit* 2008;47:6019-24.
- [67] Zhang Q, Wang H, Zhang S, Dai L. Positively charged nanofiltration membrane based on cardo poly(arylene ether sulfone) with pendant tertiary amine groups. *J Membr Sci* 2011;375:191-7.
- [68] Kim SG, Park SY, Chun JH, Chun B-H, Kim SH. Novel thin-film composite membrane for seawater desalination with sulfonated poly(arylene ether sulfone) containing amino groups. *Desalin Water Treat* 2012;43:230-7.
- [69] Kim Y-J, Lee K-S, Jeong M-H, Lee J-S. Highly chlorine-resistant end-group crosslinked sulfonated-fluorinated poly(arylene ether) for reverse osmosis membrane. *J Membr Sci* 2011;378:512-9.
- [70] Bano S, Mahmood A, Kim SJ, Lee K-H. Chlorine resistant binary complexed NaAlg/PVA composite membrane for nanofiltration. *Sep Purif Technol* 2014;137:21-7.
- [71] Perera DHN, Nataraj SK, Thomson NM, Sepe A, Hüttner S, Steiner U, Qiblawey H, Sivaniah E. Room-temperature development of thin film composite reverse osmosis membranes from cellulose acetate with antibacterial properties. *J Membr Sci* 2014;453:212-20.
- [72] Han J, Cho YH, Kong H, Han S, Park HB. Preparation and characterization of novel acetylated cellulose ether (ACE) membranes for desalination applications. *J Membr Sci* 2013;428:533-45.
- [73] Saljoughi E, Mohammadi T. Cellulose acetate (CA)/polyvinylpyrrolidone (PVP) blend asymmetric membranes: Preparation, morphology and performance. *Desalination* 2009;249:850-4.
- [74] Waheed S, Ahmad A, Khan SM, Gul S-e, Jamil T, Islam A, Hussain T. Synthesis, characterization, permeation and antibacterial properties of cellulose acetate/polyethylene glycol membranes modified with chitosan. *Desalination* 2014;351:59-69.
- [75] Choi H-g, Yoon SH, Son M, Celik E, Park H, Choi H. Efficacy of synthesis conditions on functionalized carbon nanotube blended cellulose acetate membrane for desalination. *Desalin Water Treat* 2015:1-10.
- [76] El Badawi N, Ramadan AR, Esawi AMK, El-Morsi M. Novel carbon nanotube–cellulose acetate nanocomposite membranes for water filtration applications. *Desalination* 2014;344:79-85.
- [77] Abedini R, Mousavi SM, Aminzadeh R. A novel cellulose acetate (CA) membrane using TiO₂ nanoparticles: Preparation, characterization and permeation study. *Desalination* 2011;277:40-5.
- [78] Sabad e G, Waheed S, Ahmad A, Khan SM, Hussain M, Jamil T, Zuber M. Synthesis, characterization and permeation performance of cellulose acetate/polyethylene glycol-600 membranes loaded with silver particles for ultra low pressure reverse osmosis. *J Taiwan Inst Chem E* 2015;57:129-38.
- [79] Khan SB, Alamry KA, Bifari EN, Asiri AM, Yasir M, Gzara L, Ahmad RZ. Assessment of antibacterial cellulose nanocomposites for water permeability and salt rejection. *J Ind Eng Chem* 2015;24:266-75.
- [80] Guezguez I, Mrabet B, Ferjani E. XPS and contact angle characterization of surface modified cellulose acetate membranes by mixtures of PMHS/PDMS. *Desalination* 2013;313:208-11.
- [81] Yu S, Cheng Q, Huang C, Liu J, Peng X, Liu M, Gao C. Cellulose acetate hollow fiber nanofiltration membrane with improved permselectivity prepared through hydrolysis followed by carboxymethylation. *J Membr Sci* 2013;434:44-54.
- [82] Hadj Lajimi R, Ferjani E, Roudesli MS, Deratani A. Effect of LbL surface modification on characteristics and performances of cellulose acetate nanofiltration membranes. *Desalination* 2011;266:78-86.

- [83] Worthley CH, Constantopoulos KT, Ginic-Markovic M, Pillar RJ, Matisons JG, Clarke S. Surface modification of commercial cellulose acetate membranes using surface-initiated polymerization of 2-hydroxyethyl methacrylate to improve membrane surface biofouling resistance. *J Membr Sci* 2011;385–386:30-9.
- [84] Ismail AF, Padaki M, Hilal N, Matsuura T, Lau WJ. Thin film composite membrane — Recent development and future potential. *Desalination* 2015;356:140-8.
- [85] Ghosh AK, Hoek EMV. Impacts of support membrane structure and chemistry on polyamide–polysulfone interfacial composite membranes. *J Membr Sci* 2009;336:140-8.
- [86] Fathizadeh M, Aroujalian A, Raisi A. Effect of lag time in interfacial polymerization on polyamide composite membrane with different hydrophilic sub layers. *Desalination* 2012;284:32-41.
- [87] Ramon GZ, Wong MCY, Hoek EMV. Transport through composite membrane, part 1: Is there an optimal support membrane? *J Membr Sci* 2012;415–416:298-305.
- [88] Singh PS, Joshi SV, Trivedi JJ, Devmurari CV, Rao AP, Ghosh PK. Probing the structural variations of thin film composite RO membranes obtained by coating polyamide over polysulfone membranes of different pore dimensions. *J Membr Sci* 2006;278:19-25.
- [89] Jimenez-Solomon MF, Gorgojo P, Munoz-Ibanez M, Livingston AG. Beneath the surface: Influence of supports on thin film composite membranes by interfacial polymerization for organic solvent nanofiltration. *J Membr Sci* 2013;15:102-13.
- [90] Hermans S, Bernstein R, Volodin A, Vankelecom IFJ. Study of synthesis parameters and active layer morphology of interfacially polymerized polyamide–polysulfone membranes. *React and Funct Polym* 2015;86:199-208.
- [91] Peng J, Su Y, Chen W, Zhao X, Jiang Z, Dong Y, Zhang Y, Liu J, Cao X. Polyamide nanofiltration membrane with high separation performance prepared by EDC/NHS mediated interfacial polymerization. *J Membr Sci* 2013;427:92-100.
- [92] Sotto A, Rashed A, Zhang R-X, Martínez A, Braken L, Luis P, Van der Bruggen B. Improved membrane structures for seawater desalination by studying the influence of sublayers. *Desalination* 2012;287:317-25.
- [93] Zhang R-X, Vanneste J, Poelmans L, Sotto A, Wang X-L, Van der Bruggen B. Effect of the manufacturing conditions on the structure and performance of thin-film composite membranes. *J Appl Polym Sci* 2012;125:3755-69.
- [94] Maruf SH, Greenberg AR, Pellegrino J, Ding Y. Fabrication and characterization of a surface-patterned thin film composite membrane. *J Membr Sci* 2014;452:11-9.
- [95] Gorgojo P, Jimenez-Solomon MF, Livingston AG. Polyamide thin film composite membranes on cross-linked polyimide supports: Improvement of RO performance via activating solvent. *Desalination* 2014;344:181-8.
- [96] Kim E-S, Kim YJ, Yu Q, Deng B. Preparation and characterization of polyamide thin-film composite (TFC) membranes on plasma-modified polyvinylidene fluoride (PVDF). *J Membr Sci* 2009;344:71-81.
- [97] Wu C, Zhang S, Yang D, Wei J, Yan C, Jian X. Preparation, characterization and application in wastewater treatment of a novel thermal stable composite membrane. *J Membr Sci* 2006;279:238-45.
- [98] Ba C, Economy J. Preparation of PMDA/ODA polyimide membrane for use as substrate in a thermally stable composite reverse osmosis membrane. *J Membr Sci* 2010;363:140-8.
- [99] Hu L, Zhang S, Han R, Jian X. Preparation and performance of novel thermally stable polyamide/PPENK composite nanofiltration membranes. *Appl Surf Sci* 2012;258:9047-53.
- [100] Chao W-C, Huang Y-H, Hung W-S, An Q, Hu C-C, Lee K-R, Lai J-Y. Effect of the surface property of poly(tetrafluoroethylene) support on the mechanism of polyamide active layer formation by interfacial polymerization. *Soft Matter* 2012;8:8998-9004.
- [101] Kang G-d, Cao Y-m. Application and modification of poly(vinylidene fluoride) (PVDF) membranes – A review. *J Membr Sci* 2014;463:145-65.
- [102] Pendergast MTM, Nygaard JM, Ghosh AK, Hoek EMV. Using nanocomposite materials technology to understand and control reverse osmosis membrane compaction. *Desalination* 2010;261:255-63.
- [103] Pendergast MM, Ghosh AK, Hoek EMV. Separation performance and interfacial properties of nanocomposite reverse osmosis membranes. *Desalination* 2013;308:180-5.
- [104] Kim E-S, Hwang G, Gamal El-Din M, Liu Y. Development of nanosilver and multi-walled carbon nanotubes thin-film nanocomposite membrane for enhanced water treatment. *J Membr Sci* 2012;394–395:37-48.
- [105] Li Q, Pan X, Hou C, Jin Y, Dai H, Wang H, Zhao X, Liu X. Exploring the dependence of bulk properties on surface chemistries and microstructures of commercially composite RO membranes by novel characterization approaches. *Desalination* 2012;292:9-18.
- [106] Tang CY, Kwon Y-N, Leckie JO. Effect of membrane chemistry and coating layer on physicochemical properties of thin film composite polyamide RO and NF membranes: II. Membrane physicochemical properties and their dependence on polyamide and coating layers. *Desalination* 2009;242:168-82.

- [107] Tang CY, Kwon Y-N, Leckie JO. Effect of membrane chemistry and coating layer on physiochemical properties of thin film composite polyamide RO and NF membranes: I. FTIR and XPS characterization of polyamide and coating layer chemistry. *Desalination* 2009;242:149-67.
- [108] Tang CY, Kwon YN, Leckie JO. Probing the nano- and micro-scales of reverse osmosis membranes-A comprehensive characterization of physiochemical properties of uncoated and coated membranes by XPS, TEM, ATR-FTIR, and streaming potential measurements. *J Membr Sci* 2007;287:146-56.
- [109] Roh IJ, Khare VP. Investigation of the specific role of chemical structure on the material and permeation properties of ultrathin aromatic polyamides. *J Mater Chem* 2002;12:2334-8.
- [110] Ghosh AK, Jeong B-H, Huang X, Hoek EMV. Impacts of reaction and curing conditions on polyamide composite reverse osmosis membrane properties. *J Membr Sci* 2008;311:34-45.
- [111] Soroush A, Barzin J, Barikani M, Fathizadeh M. Interfacially polymerized polyamide thin film composite membranes: Preparation, characterization and performance evaluation. *Desalination* 2012;287:310-6.
- [112] Jin Y, Su Z. Effects of polymerization conditions on hydrophilic groups in aromatic polyamide thin films. *J Membr Sci* 2009;330:175-9.
- [113] Saha NK, Joshi SV. Performance evaluation of thin film composite polyamide nanofiltration membrane with variation in monomer type. *J Membr Sci* 2009;342:60-9.
- [114] Wang T, Dai L, Zhang Q, Li A, Zhang S. Effects of acyl chloride monomer functionality on the properties of polyamide reverse osmosis (RO) membrane. *J Membr Sci* 2013;440:48-57.
- [115] Kamada T, Ohara T, Shintani T, Tsuru T. Optimizing the preparation of multi-layered polyamide membrane via the addition of a co-solvent. *J Membr Sci* 2014;453:489-97.
- [116] Zou H, Jin Y, Yang J, Dai H, Yu X, Xu J. Synthesis and characterization of thin film composite reverse osmosis membranes via novel interfacial polymerization approach. *Sep Purif Technol* 2010;72:256-62.
- [117] Khorshidi B, Thundat T, Fleck BA, Sadrzadeh M. Thin film composite polyamide membranes: parametric study on the influence of synthesis conditions. *RSC Adv* 2015;5:54985-97.
- [118] Kong C, Kanezashi M, Yamamoto T, Shintani T, Tsuru T. Controlled synthesis of high performance polyamide membrane with thin dense layer for water desalination. *J Membr Sci* 2010;362:76-80.
- [119] Kim I-C, Jeong B-R, Kim S-J, Lee K-H. Preparation of high flux thin film composite polyamide membrane: The effect of alkyl phosphate additives during interfacial polymerization. *Desalination* 2013;308:111-4.
- [120] Xiang J, Xie Z, Hoang M, Zhang K. Effect of amine salt surfactants on the performance of thin film composite poly(piperazine-amide) nanofiltration membranes. *Desalination* 2013;315:156-63.
- [121] Xiang J, Xie Z, Hoang M, Ng D, Zhang K. Effect of ammonium salts on the properties of poly(piperazineamide) thin film composite nanofiltration membrane. *J Membr Sci* 2014;465:34-40.
- [122] Tang B, Zou C, Wu P. Study on a novel polyester composite nanofiltration membrane by interfacial polymerization. II. The role of lithium bromide in the performance and formation of composite membrane. *J Membr Sci* 2010;365:276-85.
- [123] Tang B, Huo Z, Wu P. Study on a novel polyester composite nanofiltration membrane by interfacial polymerization of triethanolamine (TEOA) and trimesoyl chloride (TMC): I. Preparation, characterization and nanofiltration properties test of membrane. *J Membr Sci* 2008;320:198-205.
- [124] Wang H, Li L, Zhang X, Zhang S. Polyamide thin-film composite membranes prepared from a novel triamine 3,5-diamino-N-(4-aminophenyl)-benzamide monomer and m-phenylenediamine. *J Membr Sci* 2010;353:78-84.
- [125] Chiang Y-C, Hsub Y-Z, Ruaan R-C, Chuang C-J, Tung K-L. Nanofiltration membranes synthesized from hyperbranched polyethyleneimine. *J Membr Sci* 2009;326:19-26.
- [126] Perera DHN, Song Q, Qiblawey H, Sivaniah E. Regulating the aqueous phase monomer balance for flux improvement in polyamide thin film composite membranes. *J Membr Sci* 2015;487:74-82.
- [127] Zhao L, Chang PCY, Yen C, Ho WSW. High-flux and fouling-resistant membranes for brackish water desalination. *J Membr Sci* 2013;425-426:1-10.
- [128] Zhao L, Chang PCY, Ho WSW. High-flux reverse osmosis membranes incorporated with hydrophilic additives for brackish water desalination. *Desalination* 2013;308:225-32.
- [129] Yu S, Liu M, Liu X, Gao C. Performance enhancement in interfacially synthesized thin-film composite polyamide-urethane reverse osmosis membrane for seawater desalination. *J Membr Sci* 2009;342:313-20.
- [130] Liu M, Yu S, Tao J, Gao C. Preparation, structure characteristics and separation properties of thin-film composite polyamide-urethane seawater reverse osmosis membrane. *J Membr Sci* 2008;325:947-56.
- [131] Zhou Y, Yu S, Liu M, Gao C. Preparation and characterization of polyamide-urethane thin-film composite membranes. *Desalination* 2005;180:189-96.

- [132] Liu M, Wu D, Yu S, Gao C. Influence of the polyacyl chloride structure on the reverse osmosis performance, surface properties and chlorine stability of the thin-film composite polyamide membranes. *J Membr Sci* 2009;326:205-14.
- [133] Liu M, Yu S, Qi M, Pan Q, Gao C. Impact of manufacture technique on seawater desalination performance of thin-film composite polyamide-urethane reverse osmosis membranes and their spiral wound elements. *J Membr Sci* 2010;348:268-76.
- [134] Liu L-F, Cai Z-B, Shen J-N, Wu L-X, Hoek EMV, Gao C-J. Fabrication and characterization of a novel poly(amide-urethane@imide) TFC reverse osmosis membrane with chlorine-tolerant property. *J Membr Sci* 2014;469:397-409.
- [135] An Q-F, Sun W-D, Zhao Q, Ji Y-L, Gao C-J. Study on a novel nanofiltration membrane prepared by interfacial polymerization with zwitterionic amine monomers. *J Membr Sci* 2013;431:171-9.
- [136] Louie JS, Pinnau I, Reinhard M. Effects of surface coating process conditions on the water permeation and salt rejection properties of composite polyamide reverse osmosis membranes. *J Membr Sci* 2011;367:249-55.
- [137] Wu D, Liu X, Yu S, Liu M, Gao C. Modification of aromatic polyamide thin-film composite reverse osmosis membranes by surface coating of thermo-responsive copolymers P(NIPAM-co-Am). I: Preparation and characterization. *J Membr Sci* 2010;352:76-85.
- [138] Ishigami T, Amano K, Fujii A, Ohmukai Y, Kamio E, Maruyama T, Matsuyama H. Fouling reduction of reverse osmosis membrane by surface modification via layer-by-layer assembly. *Sep Purif Technol* 2012;99:1-7.
- [139] Ba C, Ladner DA, Economy J. Using polyelectrolyte coatings to improve fouling resistance of a positively charged nanofiltration membrane. *J Membr Sci* 2010;347:250-9.
- [140] Mitrouli ST, Karabelas AJ, Isaías NP, Al Rammah AS. Application of hydrophilic macromolecules on thin film composite polyamide membranes for performance restoration. *Desalination* 2011;278:105-16.
- [141] Malaisamy R, Talla-Nwafo A, Jones KL. Polyelectrolyte modification of nanofiltration membrane for selective removal of monovalent anions. *Sep Purif Technol* 2011;77:367-74.
- [142] Yu S, Liu X, Liu J, Wu D, Liu M, Gao C. Surface modification of thin-film composite polyamide reverse osmosis membranes with thermo-responsive polymer (TRP) for improved fouling resistance and cleaning efficiency. *Sep Purif Technol* 2011;76:283-91.
- [143] Liu M, Chen Z, Yu S, Wu D, Gao C. Thin-film composite polyamide reverse osmosis membranes with improved acid stability and chlorine resistance by coating N-isopropylacrylamide-co-acrylamide copolymers. *Desalination* 2011;270:248-57.
- [144] Yu S, Lü Z, Chen Z, Liu X, Liu M, Gao C. Surface modification of thin-film composite polyamide reverse osmosis membranes by coating N-isopropylacrylamide-co-acrylic acid copolymers for improved membrane properties. *J Membr Sci* 2011;371:293-306.
- [145] Bernstein R, Belfer S, Freger V. Surface modification of dense membranes using radical graft polymerization enhanced by monomer filtration. *Langmuir* 2010;26:12358-65.
- [146] Bernstein R, Belfer S, Freger V. Toward improved boron removal in RO by membrane modification: Feasibility and challenges. *Envir Sci Tech* 2011;45:3613-20.
- [147] Ben-David A, Bernstein R, Oren Y, Belfer S, Dosoretz C, Freger V. Facile surface modification of nanofiltration membranes to target the removal of endocrine-disrupting compounds. *J Membr Sci* 2010;357:152-9.
- [148] Potts DE, Ahlert RC, Wang SS. A critical review of fouling of reverse osmosis membranes. *Desalination* 1981;36:235-64.
- [149] Fritzmann C, Löwenberg J, Wintgens T, Melin T. State-of-the-art of reverse osmosis desalination. *Desalination* 2007;216:1-76.
- [150] Mansouri J, Harrisson S, Chen V. Strategies for controlling biofouling in membrane filtration systems: challenges and opportunities. *J Mater Chem* 2010;20:4567-86.
- [151] Rana D, Matsuura T. Surface modifications for antifouling membranes. *Chem Rev* 2010;110:2448-71.
- [152] Kochkodan V, Johnson DJ, Hilal N. Polymeric membranes: Surface modification for minimizing (bio)colloidal fouling. *Adv Colloid Interfac* 2014;206:116-40.
- [153] Kochkodan V, Hilal N. A comprehensive review on surface modified polymer membranes for biofouling mitigation. *Desalination* 2015;356:187-207.
- [154] Zhao D, Yu S. A review of recent advance in fouling mitigation of NF/RO membranes in water treatment: pretreatment, membrane modification, and chemical cleaning. *Desalin Water Treat* 2014;55:870-91.
- [155] Low D, Hamood A, Reid T, Mosley T, Tran P, Song L, Morse A. Attachment of selenium to a reverse osmosis membrane to inhibit biofilm formation of *S. aureus*. *J Membr Sci* 2011;378:171-8.
- [156] Baek Y, Yu J, Kim S-H, Lee S, Yoon J. Effect of surface properties of reverse osmosis membranes on biofouling occurrence under filtration conditions. *J Membr Sci* 2011;382:91-9.

- [157] Vrijenhoek EM, Hong S, Elimelech M. Influence of membrane surface properties on initial rate of colloidal fouling of reverse osmosis and nanofiltration membranes. *J Membr Sci* 2001;188:115-28.
- [158] Bousso K, Belpaire A, Volodin A, Van Haesendonck C, Van der Meeren P, Vandecasteele C, Van der Bruggen B. Influence of membrane and colloid characteristics on fouling of nanofiltration membranes. *J Membr Sci* 2007;289:220-30.
- [159] Nikkola J, Liu X, Li Y, Raulio M, Alakomi H-L, Wei J, Tang CY. Surface modification of thin film composite RO membrane for enhanced anti-biofouling performance. *J Membr Sci* 2013;444:192-200.
- [160] Zhao L, Ho WSW. Novel reverse osmosis membranes incorporated with a hydrophilic additive for seawater desalination. *J Membr Sci* 2014;455:44-54.
- [161] An Q, Li F, Ji Y, Chen H. Influence of polyvinyl alcohol on the surface morphology, separation and anti-fouling performance of the composite polyamide nanofiltration membranes. *J Membr Sci* 2011;367:158-65.
- [162] Gol RM, Jewrajka SK. Facile in situ PEGylation of polyamide thin film composite membranes for improving fouling resistance. *J Membr Sci* 2014;455:271-82.
- [163] Liu M, Zheng Y, Shuai S, Zhou Q, Yu S, Gao C. Thin-film composite membrane formed by interfacial polymerization of polyvinylamine (PVAm) and trimesoyl chloride (TMC) for nanofiltration. *Desalination* 2012;288:98-107.
- [164] Mo Y, Tiraferri A, Yip NY, Adout A, Huang X, Elimelech M. Improved antifouling properties of polyamide nanofiltration membranes by reducing the density of surface carboxyl groups. *Envir Sci Tech* 2012;46:13253-61.
- [165] Rana D, Kim Y, Matsuura T, Arafat HA. Development of antifouling thin-film-composite membranes for seawater desalination. *J Membr Sci* 2011;367:110-8.
- [166] Matin A, Khan Z, Gleason KK, Khaled M, Zaidi SMJ, Khalil A, Moni P, Yang R. Surface-modified reverse osmosis membranes applying a copolymer film to reduce adhesion of bacteria as a strategy for biofouling control. *Sep Purif Technol* 2014;124:117-23.
- [167] Ng LY, Mohammad AW, Ng CY, Rohani R. Development of nanofiltration membrane with high salt selectivity and performance stability using polyelectrolyte multilayers. *Desalination* 2014;351:19-26.
- [168] Rahaman MS, Therien-Aubin H, Ben-Sasson M, Ober CK, Nielsen M, Elimelech M. Control of biofouling on reverse osmosis polyamide membranes modified with biocidal nanoparticles and antifouling polymer brushes. *J Mater Chem B* 2014;2:1724-32.
- [169] Ji Y-L, An Q-F, Zhao Q, Sun W-D, Lee K-R, Chen H-L, Gao C-J. Novel composite nanofiltration membranes containing zwitterions with high permeate flux and improved anti-fouling performance. *J Membr Sci* 2012;390-391:243-53.
- [170] Azari S, Zou L. Using zwitterionic amino acid l-DOPA to modify the surface of thin film composite polyamide reverse osmosis membranes to increase their fouling resistance. *J Membr Sci* 2012;401-402:68-75.
- [171] Nguyen A, Azari S, Zou L. Coating zwitterionic amino acid l-DOPA to increase fouling resistance of forward osmosis membrane. *Desalination* 2013;312:82-7.
- [172] Azari S, Zou L, Cornelissen E. Assessing the effect of surface modification of polyamide RO membrane by l-DOPA on the short range physicochemical interactions with biopolymer fouling on the membrane. *Colloid Surface B* 2014;120:222-8.
- [173] Chen S, Li L, Zhao C, Zheng J. Surface hydration: Principles and applications toward low-fouling/nonfouling biomaterials. *Polymer* 2010;51:5283-93.
- [174] Choi H, Jung Y, Han S, Tak T, Kwon Y-N. Surface modification of SWRO membranes using hydroxyl poly(oxyethylene) methacrylate and zwitterionic carboxylated polyethyleneimine. *J Membr Sci* 2015;486:97-105.
- [175] Li X, Cao Y, Kang G, Yu H, Jie X, Yuan Q. Surface modification of polyamide nanofiltration membrane by grafting zwitterionic polymers to improve the antifouling property. *J Appl Polym Sci* 2014;131:41144-53.
- [176] Karkhanechi H, Razi F, Sawada I, Takagi R, Ohmukai Y, Matsuyama H. Improvement of antibiofouling performance of a reverse osmosis membrane through biocide release and adhesion resistance. *Sep Purif Technol* 2013;105:106-13.
- [177] Kim E-S, Yu Q, Deng B. Plasma surface modification of nanofiltration (NF) thin-film composite (TFC) membranes to improve anti organic fouling. *Appl Surf Sci* 2011;257:9863-71.
- [178] Sarkar A, Carver PI, Zhang T, Merrington A, Bruza KJ, Rousseau JL, Keinath SE, Dvornic PR. Dendrimer-based coatings for surface modification of polyamide reverse osmosis membranes. *J Membr Sci* 2010;349:421-8.
- [179] Van Wagner EM, Sagle AC, Sharma MM, La Y-H, Freeman BD. Surface modification of commercial polyamide desalination membranes using poly(ethylene glycol) diglycidyl ether to enhance membrane fouling resistance. *J Membr Sci* 2011;367:273-87.

- [180] Saeki D, Nagao S, Sawada I, Ohmukai Y, Maruyama T, Matsuyama H. Development of antibacterial polyamide reverse osmosis membrane modified with a covalently immobilized enzyme. *J Membr Sci* 2013;428:403-9.
- [181] Zhang T, Zhu C, Ma H, Li R, Dong B, Liu Y, Li S. Surface modification of APA-TFC membrane with quaternary ammonium cation and salicylaldehyde to improve performance. *J Membr Sci* 2014;457:88-94.
- [182] Zhang Y, Wang Z, Lin W, Sun H, Wu L, Chen S. A facile method for polyamide membrane modification by poly(sulfobetaine methacrylate) to improve fouling resistance. *J Membr Sci* 2013;446:164-70.
- [183] Saeki D, Tanimoto T, Matsuyama H. Anti-biofouling of polyamide reverse osmosis membranes using phosphorylcholine polymer grafted by surface-initiated atom transfer radical polymerization. *Desalination* 2014;350:21-7.
- [184] Ginic-Markovic M, Barclay TG, Constantopoulos KT, Markovic E, Clarke SR, Matison JG. Biofouling resistance of polysulfobetaine coated reverse osmosis membranes. *Desalination* 2015;369:37-45.
- [185] Akbari A, Derikvandi Z, Mojallali Rostami SM. Influence of chitosan coating on the separation performance, morphology and anti-fouling properties of the polyamide nanofiltration membranes. *J Ind Eng Chem* 2015;28:268-76.
- [186] Xu J, Wang Z, Wang J, Wang S. Positively charged aromatic polyamide reverse osmosis membrane with high anti-fouling property prepared by polyethylenimine grafting. *Desalination* 2015;365:398-406.
- [187] Abuhabib AA, Mohammad AW, Hilal N, Rahman RA, Shafie AH. Nanofiltration membrane modification by UV grafting for salt rejection and fouling resistance improvement for brackish water desalination. *Desalination* 2012;295:16-25.
- [188] Kang G, Yu H, Liu Z, Cao Y. Surface modification of a commercial thin film composite polyamide reverse osmosis membrane by carbodiimide-induced grafting with poly(ethylene glycol) derivatives. *Desalination* 2011;275:252-9.
- [189] Vercellino T, Morse A, Tran P, Song L, Hamood A, Reid T, Moseley T. Attachment of organo-selenium to polyamide composite reverse osmosis membranes to inhibit biofilm formation of *S. aureus* and *E. coli*. *Desalination* 2013;309:291-5.
- [190] Vercellino T, Morse A, Tran P, Hamood A, Reid T, Song L, Moseley T. The use of covalently attached organo-selenium to inhibit *S. aureus* and *E. coli* biofilms on RO membranes and feed spacers. *Desalination* 2013;317:142-51.
- [191] Cheng Q, Zheng Y, Yu S, Zhu H, Peng X, Liu J, Liu J, Liu M, Gao C. Surface modification of a commercial thin-film composite polyamide reverse osmosis membrane through graft polymerization of N-isopropylacrylamide followed by acrylic acid. *J Membr Sci* 2013;447:236-45.
- [192] Mi Y-F, Zhao Q, Ji Y-L, An Q-F, Gao C-J. A novel route for surface zwitterionic functionalization of polyamide nanofiltration membranes with improved performance. *J Membr Sci* 2015;490:311-20.
- [193] Meng J, Cao Z, Ni L, Zhang Y, Wang X, Zhang X, Liu E. A novel salt-responsive TFC RO membrane having superior antifouling and easy-cleaning properties. *J Membr Sci* 2014;461:123-9.
- [194] Mondal S, Wickramasinghe SR. Photo-induced graft polymerization of N-isopropyl acrylamide on thin film composite membrane: Produced water treatment and antifouling properties. *Sep Purif Technol* 2012;90:231-8.
- [195] Mansourpanah Y, Momeni Habili E. Preparation and modification of thin film PA membranes with improved antifouling property using acrylic acid and UV irradiation. *J Membr Sci* 2013;430:158-66.
- [196] Varin KJ, Lin NH, Cohen Y. Biofouling and cleaning effectiveness of surface nanostructured reverse osmosis membranes. *J Membr Sci* 2013;446:472-81.
- [197] Lin NH, Kim M-m, Lewis GT, Cohen Y. Polymer surface nano-structuring of reverse osmosis membranes for fouling resistance and improved flux performance. *J Mater Chem* 2010;20:4642-52.
- [198] Zou L, Vidalis I, Steele D, Michelmore A, Low SP, Verberk JQJC. Surface hydrophilic modification of RO membranes by plasma polymerization for low organic fouling. *J Membr Sci* 2011;369:420-8.
- [199] Ozaydin-Ince G, Matin A, Khan Z, Zaidi SMJ, Gleason KK. Surface modification of reverse osmosis desalination membranes by thin-film coatings deposited by initiated chemical vapor deposition. *Thin Solid Films* 2013;539:181-7.
- [200] Yang R, Gleason KK. Ultrathin antifouling coatings with stable surface zwitterionic functionality by initiated chemical vapor deposition (iCVD). *Langmuir* 2012;28:12266-74.
- [201] Yang R, Jang H, Stocker R, Gleason KK. Synergistic prevention of biofouling in seawater desalination by zwitterionic surfaces and low-level chlorination. *Adv Mater* 2014;26:1711-8.
- [202] Yang R, Xu J, Ozaydin-Ince G, Wong SY, Gleason KK. Surface-tethered zwitterionic ultrathin antifouling coatings on reverse osmosis membranes by initiated chemical vapor deposition. *Chem Mater* 2011;23:1263-72.
- [203] Matin A, Shafi HZ, Khan Z, Khaled M, Yang R, Gleason K, Rehman F. Surface modification of seawater desalination reverse osmosis membranes: Characterization studies & performance evaluation. *Desalination* 2014;343:128-39.

- [204] Shafi HZ, Khan Z, Yang R, Gleason KK. Surface modification of reverse osmosis membranes with zwitterionic coating for improved resistance to fouling. *Desalination* 2015;362:93-103.
- [205] Hilal N, Ogunbiyi OO, Miles NJ, Nigmatullin R. Methods employed for control of fouling in MF and UF membranes: A comprehensive review. *Separ Sci Technol* 2005;40:1957-2005.
- [206] Sagle AC, Van Wagner EM, Ju H, McCloskey BD, Freeman BD, Sharma MM. PEG-coated reverse osmosis membranes: Desalination properties and fouling resistance. *J Membr Sci* 2009;340:92-108.
- [207] Ben-Sasson M, Lu X, Bar-Zeev E, Zdrov KR, Nejati S, Qi G, Giannelis EP, Elimelech M. In situ formation of silver nanoparticles on thin-film composite reverse osmosis membranes for biofouling mitigation. *Water Res* 2014;62:260-70.
- [208] Yin J, Yang Y, Hu Z, Deng B. Attachment of silver nanoparticles (AgNPs) onto thin-film composite (TFC) membranes through covalent bonding to reduce membrane biofouling. *J Membr Sci* 2013;441:73-82.
- [209] Nikkola J, Sievänen J, Raulio M, Wei J, Vuorinen J, Tang CY. Surface modification of thin film composite polyamide membrane using atomic layer deposition method. *J Membr Sci* 2014;450:174-80.
- [210] Choi W, Choi J, Bang J, Lee J-H. Layer-by-layer assembly of graphene oxide nanosheets on polyamide membranes for durable reverse-osmosis applications. *ACS Appl Mater Inter* 2013;5:12510-9.
- [211] Ray JR, Tadepalli S, Nergiz SZ, Liu K-K, You L, Tang Y, Singamaneni S, Jun Y-S. Hydrophilic, bactericidal nanoheater-enabled reverse osmosis membranes to improve fouling resistance. *ACS Appl Mater Inter* 2015;7:11117-26.
- [212] Tiraferri A, Vecitis CD, Elimelech M. Covalent binding of single-walled carbon nanotubes to polyamide membranes for antimicrobial surface properties. *ACS Appl Mater Inter* 2011;3:2869-77.
- [213] Ben-Sasson M, Zdrov KR, Genggeng Q, Kang Y, Giannelis EP, Elimelech M. Surface functionalization of thin-film composite membranes with copper nanoparticles for antimicrobial surface properties. *Envir Sci Tech* 2013;48:384-93.
- [214] Avlonitis S. Chlorine degradation of aromatic polyamides. *Desalination* 1992;85:321-34.
- [215] Glater J. The search for a chlorine-resistant reverse osmosis membrane. *Desalination* 1994;95:325-45.
- [216] Kawaguchi T. Chlorine-resistant membrane for reverse osmosis. I. Correlation between chemical structures and chlorine resistance of polyamides. *J Appl Polym Sci* 1984;29:3359-67.
- [217] Kim M, Kim M, Park B, Kim S. Changes in characteristics of polyamide reverse osmosis membrane due to chlorine attack. *Desalin Water Treat* 2014;54:923-8.
- [218] Raval HD, Trivedi JJ, Joshi SV, Devmurari CV. Flux enhancement of thin film composite RO membrane by controlled chlorine treatment. *Desalination* 2010;250:945-9.
- [219] Do VT, Tang CY, Reinhard M, Leckie JO. Effects of hypochlorous acid exposure on the rejection of salt, polyethylene glycols, boron and arsenic(V) by nanofiltration and reverse osmosis membranes. *Water Res* 2012;46:5217-23.
- [220] Kwon Y-N, Tang CY, Leckie JO. Change of membrane performance due to chlorination of crosslinked polyamide membranes. *J Appl Polym Sci* 2006;102:5895-902.
- [221] Kang G-D, Gao C-J, Chen W-D, Jie X-M, Cao Y-M, Yuan Q. Study on hypochlorite degradation of aromatic polyamide reverse osmosis membrane. *J Membr Sci* 2007;300:165-71.
- [222] Do VT, Tang CY, Reinhard M, Leckie JO. Degradation of polyamide nanofiltration and reverse osmosis membranes by hypochlorite. *Envir Sci Tech* 2012;46:852-9.
- [223] Ettori A, Gaudichet-Maurin E, Schrotter J-C, Aimar P, Causserand C. Permeability and chemical analysis of aromatic polyamide based membranes exposed to sodium hypochlorite. *J Membr Sci* 2011;375:220-30.
- [224] Kwon Y-N, Leckie JO. Hypochlorite degradation of crosslinked polyamide membranes: II. Changes in hydrogen bonding behavior and performance. *J Membr Sci* 2006;282:456-64.
- [225] Do VT, Tang CY, Reinhard M, Leckie JO. Effects of chlorine exposure conditions on physicochemical properties and performance of a polyamide membrane—mechanisms and implications. *Envir Sci Tech* 2012;46:13184-92.
- [226] Xu J, Wang Z, Wei X, Yang S, Wang J, Wang S. The chlorination process of crosslinked aromatic polyamide reverse osmosis membrane: New insights from the study of self-made membrane. *Desalination* 2013;313:145-55.
- [227] Xu J, Feng X, Gao C. Surface modification of thin-film-composite polyamide membranes for improved reverse osmosis performance. *J Membr Sci* 2011;370:116-23.
- [228] Raval HD, Rana PS, Maiti S. A novel high-flux, thin-film composite reverse osmosis membrane modified by chitosan for advanced water treatment. *RSC Adv* 2015;5:6687-94.
- [229] Hong S, Kim I-C, Tak T, Kwon Y-N. Interfacially synthesized chlorine-resistant polyimide thin film composite (TFC) reverse osmosis (RO) membranes. *Desalination* 2013;309:18-26.

- [230] Son SH, Jegal J. Preparation and characterization of polyamide reverse-osmosis membranes with good chlorine tolerance. *J Appl Polym Sci* 2011;120:1245-52.
- [231] Shintani T. Development of a chlorine-resistant polyamide reverse osmosis membrane. *Desalination* 2007;207:340-8.
- [232] Konagaya S, Kuzumoto H, Watanabe O. New reverse osmosis membrane materials with higher resistance to chlorine. *J Appl Polym Sci* 2000;75:1357-64.
- [233] La Y-H, Sooriyakumaran R, Miller DC, Fujiwara M, Terui Y, Yamanaka K, McCloskey BD, Freeman BD, Allen RD. Novel thin film composite membrane containing ionizable hydrophobes: pH-dependent reverse osmosis behavior and improved chlorine resistance. *J Mater Chem* 2010;20:4615-20.
- [234] Han R. Formation and characterization of (melamine-TMC) based thin film composite NF membranes for improved thermal and chlorine resistances. *J Membr Sci* 2013;425-426:176-81.
- [235] Ni L, Meng J, Li X, Zhang Y. Surface coating on the polyamide TFC RO membrane for chlorine resistance and antifouling performance improvement. *J Membr Sci* 2014;451:205-15.
- [236] Kim YK, Lee SY, Kim DH, Lee BS, Nam SY, Rhim JW. Preparation and characterization of thermally crosslinked chlorine resistant thin film composite polyamide membranes for reverse osmosis. *Desalination* 2010;250:865-7.
- [237] Kwon Y-N, Hong S, Choi H, Tak T. Surface modification of a polyamide reverse osmosis membrane for chlorine resistance improvement. *J Membr Sci* 2012;415-416:192-8.
- [238] Shin DH, Kim N, Lee YT. Modification to the polyamide TFC RO membranes for improvement of chlorine-resistance. *J Membr Sci* 2011;376:302-11.
- [239] Zhang Z, Wang Z, Wang J, Wang S. Enhancing chlorine resistances and anti-biofouling properties of commercial aromatic polyamide reverse osmosis membranes by grafting 3-allyl-5,5-dimethylhydantoin and N,N'-Methylenebis(acrylamide). *Desalination* 2013;309:187-96.
- [240] Rana HH, Saha NK, Jewrajka SK, Reddy AVR. Low fouling and improved chlorine resistant thin film composite reverse osmosis membranes by cerium(IV)/polyvinyl alcohol mediated surface modification. *Desalination* 2015;357:93-103.
- [241] Wei X, Wang Z, Chen J, Wang J, Wang S. A novel method of surface modification on thin-film-composite reverse osmosis membrane by grafting hydantoin derivative. *J Membr Sci* 2010;346:152-62.
- [242] Wei X, Wang Z, Zhang Z, Wang J, Wang S. Surface modification of commercial aromatic polyamide reverse osmosis membranes by graft polymerization of 3-allyl-5,5-dimethylhydantoin. *J Membr Sci* 2010;351:222-33.
- [243] Xu J, Wang Z, Yu L, Wang J, Wang S. A novel reverse osmosis membrane with regenerable anti-biofouling and chlorine resistant properties. *J Membr Sci* 2013;435:80-91.
- [244] Stanton BW, Harris JJ, Miller MD, Bruening ML. Ultrathin, multilayered polyelectrolyte films as nanofiltration membranes. *Langmuir* 2003;19:7038-42.
- [245] Tieké B. Selective transport of ions and molecules across layer-by-layer assembled membranes of polyelectrolytes, p-sulfonato-calix[n]arenes and Prussian Blue-type complex salts. *Adv Colloid Interfac* 2005;116:121-31.
- [246] Toutianoush A. Selective ion transport and complexation in layer-by-layer assemblies of p-sulfonato-calix[n]arenes and cationic polyelectrolytes. *Adv Funct Mater* 2005;15:700-8.
- [247] El-Hashani A. Electrostatic layer-by-layer assembly of ultrathin films containing hexacyclen and p-sulfonatocalix[n]arene macrocycles. *J Nanosci Nanotechnol* 2006;6:1710-7.
- [248] El-Hashani A, Toutianoush A, Tieké B. Use of layer-by-layer assembled ultrathin membranes of dicopper-[18]azacrown-N6 complex and polyvinylsulfate for water desalination under nanofiltration conditions. *J Membr Sci* 2008;318:65-70.
- [249] Jin W, Toutianoush A, Tieké B. Size- and charge-selective transport of aromatic compounds across polyelectrolyte multilayer membranes. *Appl Surf Sci* 2005;246:444-50.
- [250] Toutianoush A, Tieké B. Selective transport and incorporation of highly charged metal and metal complex ions in self-assembled polyelectrolyte multilayer membranes. *Mat Sci Eng C* 2002;22:135-9.
- [251] Jin W, Toutianoush A, Tieké B. Use of polyelectrolyte layer-by-layer assemblies as nanofiltration and reverse osmosis membranes. *Langmuir* 2003;19:2550-3.
- [252] Fadhillah F, Zaidi SMJ, Khan Z, Khaled MM, Rahman F, Hammond PT. Development of polyelectrolyte multilayer thin film composite membrane for water desalination application. *Desalination* 2013;318:19-24.
- [253] Joseph N, Ahmadiannamini P, Hoogenboom R, Vankelecom IFJ. Layer-by-layer preparation of polyelectrolyte multilayer membranes for separation. *Polym Chem* 2014;5:1817-31.

- [254] Ng LY, Mohammad AW, Ng CY. A review on nanofiltration membrane fabrication and modification using polyelectrolytes: Effective ways to develop membrane selective barriers and rejection capability. *Adv Colloid Interfac Sci* 2013;197–198:85-107.
- [255] Toutianoush A, El-Hashani A, Schnepf J, Tieke B. Multilayer membranes of p-sulfonato-calix[8]arene and polyvinylamine and their use for selective enrichment of rare earth metal ions. *Appl Surf Sci* 2005;246:430-6.
- [256] Toutianoush A. Polyelectrolyte multilayer membranes for desalination of aqueous salt solutions and seawater under reverse osmosis conditions. *Appl Surf Sci* 2005;246:437-43.
- [257] Park J, Park J, Kim SH, Cho J, Bang J. Desalination membranes from pH-controlled and thermally-crosslinked layer-by-layer assembled multilayers. *J Mater Chem* 2010;20:2085-91.
- [258] Deng H-Y, Xu Y-Y, Zhu B-K, Wei X-Z, Liu F, Cui Z-Y. Polyelectrolyte membranes prepared by dynamic self-assembly of poly (4-styrenesulfonic acid-co-maleic acid) sodium salt (PSSMA) for nanofiltration (I). *J Membr Sci* 2008;323:125-33.
- [259] Su B, Wang T, Wang Z, Gao X, Gao C. Preparation and performance of dynamic layer-by-layer PDADMAC/PSS nanofiltration membrane. *J Membr Sci* 2012;423–424:324-31.
- [260] Fadhillah F, Javaid Zaidi SM, Khan Z, Khaled M, Hammond PT. Reverse osmosis desalination membrane formed from weak polyelectrolytes by spin assisted layer by layer technique. *Desalin Water Treat* 2011;34:44-9.
- [261] Shan W, Bacchin P, Aimar P, Bruening ML, Tarabara VV. Polyelectrolyte multilayer films as backflushable nanofiltration membranes with tunable hydrophilicity and surface charge. *J Membr Sci* 2010;349:268-78.
- [262] Hoffmann K, Friedrich T, Tieke B. Layer-by-layer assembled polyelectrolyte blend membranes and their use for ion separation and rejection. *Polym Eng Sci* 2011;51:1497-506.
- [263] Tieke B, El-Hashani A, Toutianoush A, Fendt A. Multilayered films based on macrocyclic polyamines, calixarenes and cyclodextrins and transport properties of the corresponding membranes. *Thin Solid Films* 2008;516:8814-20.
- [264] El-Hashani A, Toutianoush A, Tieke B. Layer-by-layer assembled membranes of protonated 18-azacrown-6 and polyvinylsulfate and their application for highly efficient anion separation. *The J Phys Chem B* 2007;111:8582-8.
- [265] de Grooth J, Reurink DM, Ploegmakers J, de Vos WM, Nijmeijer K. Charged micropollutant removal with hollow fiber nanofiltration membranes based on polycation/polyzwitterion/polyanion multilayers. *ACS Appl Mater Inter* 2014;6:17009-17.
- [266] Ouyang L, Malaisamy R, Bruening ML. Multilayer polyelectrolyte films as nanofiltration membranes for separating monovalent and divalent cations. *J Membr Sci* 2008;310:76-84.
- [267] Hong SU, Malaisamy R, Bruening ML. Optimization of flux and selectivity in $\text{Cl}^-/\text{SO}_4^{2-}$ separations with multilayer polyelectrolyte membranes. *J Membr Sci* 2006;283:366-72.
- [268] Park M-K. pH-sensitive bipolar ion-permselective ultrathin films. *Journal of the American Chemical Society* 2004;126:13723-31.
- [269] Stair JL, Harris JJ, Bruening ML. Enhancement of the ion-transport selectivity of Layered polyelectrolyte membranes through cross-linking and hybridization. *Chem Mater* 2001;13:2641-8.
- [270] Kumar M, Grzelakowski M, Zilles J, Clark M, Meier W. Highly permeable polymeric membranes based on the incorporation of the functional water channel protein Aquaporin Z. *Proceedings of the National Academy of Sciences* 2007;104:20719-24.
- [271] Tang CY, Zhao Y, Wang R, Hélix-Nielsen C, Fane AG. Desalination by biomimetic aquaporin membranes: Review of status and prospects. *Desalination* 2013;308:34-40.
- [272] Pendergast MM, Hoek EMV. A review of water treatment membrane nanotechnologies. *Energy Environ Sci* 2011;4:1946-71.
- [273] Shen Y-x, Saboe PO, Sines IT, Erbakan M, Kumar M. Biomimetic membranes: A review. *J Membr Sci* 2014;454:359-81.
- [274] Sun G, Chung T-S, Jeyaseelan K, Armugam A. Stabilization and immobilization of aquaporin reconstituted lipid vesicles for water purification. *Colloids Surf B* 2013;102:466-71.
- [275] Wang H, Chung T-S, Tong YW, Jeyaseelan K, Armugam A, Chen Z, Hong M, Meier W. Highly permeable and selective pore-spanning biomimetic membrane embedded with Aquaporin Z. *Small* 2012;8:1185-90.
- [276] Sun G, Zhou H, Li Y, Jeyaseelan K, Armugam A, Chung T-S. A novel method of AquaporinZ incorporation via binary-lipid Langmuir monolayers. *Colloid Surface B* 2012;89:283-8.
- [277] Li X, Wang R, Tang C, Vararattanavech A, Zhao Y, Torres J, Fane T. Preparation of supported lipid membranes for aquaporin Z incorporation. *Colloids Surf B* 2012;94:333-40.
- [278] Wang HL, Chung T-S, Tong YW, Jeyaseelan K, Armugam A, Duong HHP, Fu F, Seah H, Yang J, Hong M. Mechanically robust and highly permeable AquaporinZ biomimetic membranes. *J Membr Sci* 2013;434:130-6.

- [279] Sun G, Chung T-S, Jeyaseelan K, Armugam A. A layer-by-layer self-assembly approach to developing an aquaporin-embedded mixed matrix membrane. *RSC Adv* 2013;3:473-81.
- [280] Sun G, Chung T-S, Chen N, Lu X, Zhao Q. Highly permeable aquaporin-embedded biomimetic membranes featuring a magnetic-aided approach. *RSC Adv* 2013;3:9178-84.
- [281] Zhong PS, Chung T-S, Jeyaseelan K, Armugam A. Aquaporin-embedded biomimetic membranes for nanofiltration. *J Membr Sci* 2012;407-408:27-33.
- [282] Duong PHH, Chung T-S, Jeyaseelan K, Armugam A, Chen Z, Yang J, Hong M. Planar biomimetic aquaporin-incorporated triblock copolymer membranes on porous alumina supports for nanofiltration. *J Membr Sci* 2012;409-410:34-43.
- [283] Li X, Wang R, Wicaksana F, Tang C, Torres J, Fane AG. Preparation of high performance nanofiltration (NF) membranes incorporated with aquaporin Z. *J Membr Sci* 2014;450:181-8.
- [284] Xie W, He F, Wang B, Chung T-S, Jeyaseelan K, Armugam A, Tong YW. An aquaporin-based vesicle-embedded polymeric membrane for low energy water filtration. *J Mater Chem A* 2013;1:7592-600.
- [285] Wang H, Chung T-S, Tong YW, Meier W, Chen Z, Hong M, Jeyaseelan K, Armugam A. Preparation and characterization of pore-suspending biomimetic membranes embedded with Aquaporin Z on carboxylated polyethylene glycol polymer cushion. *Soft Matter* 2011;7:7274-80.
- [286] Wang M, Wang Z, Wang X, Wang S, Ding W, Gao C. Layer-by-layer assembly of aquaporin Z-incorporated biomimetic membranes for water purification. *Envir Sci Tech* 2015;49:3761-8.
- [287] Zhao Y, Qiu C, Li X, Vararattanavech A, Shen W, Torres J, Hélix-Nielsen C, Wang R, Hu X, Fane AG, Tang CY. Synthesis of robust and high-performance aquaporin-based biomimetic membranes by interfacial polymerization-membrane preparation and RO performance characterization. *J Membr Sci* 2012;423-424:422-8.
- [288] Hoek EMV, Ghosh AK. Nanotechnology-based membranes for water purification. In: Savage J, Diallo M, Duncan J, Street A, Sustich R, editors. *Nanotechnology Applications for Clean Water*. Boston: William Andrew Publishing; 2009. p. 47-58.
- [289] Daer S, Kharraz J, Giwa A, Hasan SW. Recent applications of nanomaterials in water desalination: A critical review and future opportunities. *Desalination* 2015;367:37-48.
- [290] Lau WJ, Gray S, Matsuura T, Emadzadeh D, Paul Chen J, Ismail AF. A review on polyamide thin film nanocomposite (TFN) membranes: History, applications, challenges and approaches. *Water Res* 2015;80:306-24.
- [291] Kim HJ, Lim M-Y, Jung KH, Kim D-G, Lee J-C. High-performance reverse osmosis nanocomposite membranes containing the mixture of carbon nanotubes and graphene oxides. *J Mater Chem A* 2015;3:6798-809.
- [292] Moon JH, Katha AR, Pandian S, Kolake SM, Han S. Polyamide-POSS hybrid membranes for seawater desalination: Effect of POSS inclusion on membrane properties. *J Membr Sci* 2014;461:89-95.
- [293] Duan J, Litwiller E, Pinnau I. Preparation and water desalination properties of POSS-polyamide nanocomposite reverse osmosis membranes. *J Membr Sci* 2015;473:157-64.
- [294] Dalwani M, Zheng J, Hempenius M, Raaijmakers MJT, Doherty CM, Hill AJ, Wessling M, Benes NE. Ultra-thin hybrid polyhedral silsesquioxane-polyamide films with potentially unlimited 2D dimensions. *J Mater Chem* 2012;22:14835-8.
- [295] Rajaeian B, Rahimpour A, Tade MO, Liu S. Fabrication and characterization of polyamide thin film nanocomposite (TFN) nanofiltration membrane impregnated with TiO₂ nanoparticles. *Desalination* 2013;313:176-88.
- [296] Zhang L, Shi G-Z, Qiu S, Cheng L-H, Chen H-L. Preparation of high-flux thin film nanocomposite reverse osmosis membranes by incorporating functionalized multi-walled carbon nanotubes. *Desalin Water Treat* 2011;34:19-24.
- [297] Park J, Choi W, Kim SH, Chun BH, Bang J, Lee KB. Enhancement of chlorine resistance in carbon nanotube based nanocomposite reverse osmosis membranes. *Desalin Water Treat* 2010;15:198-204.
- [298] Kim E-S, Deng B. Fabrication of polyamide thin-film nano-composite (PA-TFN) membrane with hydrophilized ordered mesoporous carbon (H-OMC) for water purifications. *J Membr Sci* 2011;375:46-54.
- [299] Jadav GL, Singh PS. Synthesis of novel silica-polyamide nanocomposite membrane with enhanced properties. *J Membr Sci* 2009;328:257-67.
- [300] Yin J, Kim E-S, Yang J, Deng B. Fabrication of a novel thin-film nanocomposite (TFN) membrane containing MCM-41 silica nanoparticles (NPs) for water purification. *J Membr Sci* 2012;423-424:238-46.
- [301] Bao M, Zhu G, Wang L, Wang M, Gao C. Preparation of monodispersed spherical mesoporous nanosilica-polyamide thin film composite reverse osmosis membranes via interfacial polymerization. *Desalination* 2013;309:261-6.
- [302] Dong H, Qu X-Y, Zhang L, Cheng L-H, Chen H-L, Gao C-J. Preparation and characterization of surface-modified zeolite-polyamide thin film nanocomposite membranes for desalination. *Desalin Water Treat* 2011;34:6-12.

- [303] Li D, He L, Dong D, Forsyth M, Wang H. Preparation of silicalite–polyamide composite membranes for desalination. *Asian Pac J Chem Eng* 2012;7:434-41.
- [304] Lind ML, Ghosh AK, Jawor A, Huang X, Hou W, Yang Y, Hoek EMV. Influence of zeolite crystal size on zeolite-polyamide thin film nanocomposite membranes. *Langmuir* 2009;25:10139-45.
- [305] Lind ML, Eumine Suk D, Nguyen T-V, Hoek EMV. Tailoring the structure of thin film nanocomposite membranes to achieve seawater RO membrane performance. *Envir Sci Tech* 2010;44:8230-5.
- [306] Fathizadeh M, Aroujalian A, Raisi A. Effect of added NaX nano-zeolite into polyamide as a top thin layer of membrane on water flux and salt rejection in a reverse osmosis process. *J Membr Sci* 2011;375:88-95.
- [307] Huang H, Qu X, Dong H, Zhang L, Chen H. Role of NaA zeolites in the interfacial polymerization process towards a polyamide nanocomposite reverse osmosis membrane. *RSC Adv* 2013;3:8203-7.
- [308] Kong C, Shintani T, Tsuru T. "Pre-seeding"-assisted synthesis of a high performance polyamide-zeolite nanocomposite membrane for water purification. *New J Chem* 2010;34:2101-4.
- [309] Jeong B-H, Hoek EMV, Yan Y, Subramani A, Huang X, Hurwitz G, Ghosh AK, Jawor A. Interfacial polymerization of thin film nanocomposites: A new concept for reverse osmosis membranes. *J Membr Sci* 2007;294:1-7.
- [310] Liu X, Qi S, Li Y, Yang L, Cao B, Tang CY. Synthesis and characterization of novel antibacterial silver nanocomposite nanofiltration and forward osmosis membranes based on layer-by-layer assembly. *Water Res* 2013;47:3081-92.
- [311] Rajesh S, Fauzi Ismail A, Mohan DR. Structure-property interplay of poly(amide-imide) and TiO₂ nanoparticles impregnated poly(ether-sulfone) asymmetric nanofiltration membranes. *RSC Adv* 2012;2:6854-70.
- [312] Vatanpour V, Madaeni SS, Moradian R, Zinadini S, Astinchap B. Novel antibifouling nanofiltration polyethersulfone membrane fabricated from embedding TiO₂ coated multiwalled carbon nanotubes. *Sep Purif Technol* 2012;90:69-82.
- [313] Pourjafar S, Rahimpour A, Jahanshahi M. Synthesis and characterization of PVA/PES thin film composite nanofiltration membrane modified with TiO₂ nanoparticles for better performance and surface properties. *J Ind Eng Chem* 2012;18:1398-405.
- [314] Park J, Choi W, Cho J, Chun BH, Kim SH, Lee KB, Bang J. Carbon nanotube-based nanocomposite desalination membranes from layer-by-layer assembly. *Desalin Water Treat* 2010;15:76-83.
- [315] Wu H, Tang B, Wu P. MWNTs/polyester thin film nanocomposite membrane: An approach to overcome the trade-off Effect between permeability and selectivity. *The J Phys Chem C* 2010;114:16395-400.
- [316] Wu H, Tang B, Wu P. Optimization, characterization and nanofiltration properties test of MWNTs/polyester thin film nanocomposite membrane. *J Membr Sci* 2013;428:425-33.
- [317] Vatanpour V, Madaeni SS, Moradian R, Zinadini S, Astinchap B. Fabrication and characterization of novel antifouling nanofiltration membrane prepared from oxidized multiwalled carbon nanotube/polyethersulfone nanocomposite. *J Membr Sci* 2011;375:284-94.
- [318] Park KT, Kim SG, Chun B-H, Bang J, Kim SH. Sulfonated poly(arylene ether sulfone) thin-film composite reverse osmosis membrane containing SiO₂ nano-particles. *Desalin Water Treat* 2010;15:69-75.
- [319] Worthley CH, Constantopoulos KT, Ginic-Markovic M, Markovic E, Clarke S. A study into the effect of POSS nanoparticles on cellulose acetate membranes. *J Membr Sci* 2013;431:62-71.
- [320] Park SY, Kim SG, Chun JH, Chun B-H, Kim SH. Fabrication and characterization of the chlorine-tolerant disulfonated poly(arylene ether sulfone)/hyperbranched aromatic polyamide-grafted silica composite reverse osmosis membrane. *Desalin Water Treat* 2012;43:221-9.
- [321] Kovacs JR, Liu C, Hammond PT. Spray layer-by-layer assembled clay composite thin films as selective layers in reverse osmosis membranes. *ACS Appl Mater Inter* 2015;7:13375-83.
- [322] Klaine SJ, Alvarez PJJ, Batley GE, Fernandes TF, Handy RD, Lyon DY, Mahendra S, McLaughlin MJ, Lead JR. Nanomaterials in the environment: Behavior, fate, bioavailability, and effects. *Environ Toxicol Chem* 2008;27:1825-51.
- [323] Marambio-Jones C, Hoek EV. A review of the antibacterial effects of silver nanomaterials and potential implications for human health and the environment. *J Nanopart Res* 2010;12:1531-51.
- [324] Li Q, Mahendra S, Lyon DY, Brunet L, Liga MV, Li D, Alvarez PJJ. Antimicrobial nanomaterials for water disinfection and microbial control: Potential applications and implications. *Water Res* 2008;42:4591-602.
- [325] Choi O, Yu C-P, Esteban Fernández G, Hu Z. Interactions of nanosilver with *Escherichia coli* cells in planktonic and biofilm cultures. *Water Res* 2010;44:6095-103.
- [326] Lee HS, Im SJ, Kim JH, Kim HJ, Kim JP, Min BR. Polyamide thin-film nanofiltration membranes containing TiO₂ nanoparticles. *Desalination* 2008;219:48-56.

- [327] Liu Y, Rosenfield E, Hu M, Mi B. Direct observation of bacterial deposition on and detachment from nanocomposite membranes embedded with silver nanoparticles. *Water Res* 2013;47:2949-58.
- [328] Lee SY, Kim HJ, Patel R, Im SJ, Kim JH, Min BR. Silver nanoparticles immobilized on thin film composite polyamide membrane: characterization, nanofiltration, antifouling properties. *Polym Advan Technol* 2007;18:562-8.
- [329] Rajaeian B, Heitz A, Tade MO, Liu S. Improved separation and antifouling performance of PVA thin film nanocomposite membranes incorporated with carboxylated TiO₂ nanoparticles. *J Membr Sci* 2015;485:48-59.
- [330] Cong H, Radosz M, Towler BF, Shen Y. Polymer-inorganic nanocomposite membranes for gas separation. *Sep Purif Technol* 2007;55:281-91.
- [331] Peyravi M, Jahanshahi M, Rahimpour A, Javadi A, Hajavi S. Novel thin film nanocomposite membranes incorporated with functionalized TiO₂ nanoparticles for organic solvent nanofiltration. *Chem Eng J* 2014;241:155-66.
- [332] Yang HL, Lin JCT, Huang C. Application of nanosilver surface modification to RO membrane and spacer for mitigating biofouling in seawater desalination. *Water Res* 2009;43:3777-86.
- [333] Lind ML, Jeong B-H, Subramani A, Huang X, Hoek EMV. Effect of mobile cation on zeolite-polyamide thin film nanocomposite membranes. *J Mater Res* 2009;24:1624-31.
- [334] Subramani A, Voutchkov N, Jacangelo JG. Desalination energy minimization using thin film nanocomposite membranes. *Desalination* 2014;350:35-43.
- [335] Chem. AL. LG NanoH₂O Inc., <http://www.lgwatersolutions.com/2015>, Accessed Nov 2015.
- [336] Hofs B, Schurer R, Harmsen DJH, Ceccarelli C, Beerendonk EF, Cornelissen ER. Characterization and performance of a commercial thin film nanocomposite seawater reverse osmosis membrane and comparison with a thin film composite. *J Membr Sci* 2013;446:68-78.
- [337] Dong H, Zhao L, Zhang L, Chen H, Gao C, Winston Ho WS. High-flux reverse osmosis membranes incorporated with NaY zeolite nanoparticles for brackish water desalination. *J Membr Sci* 2015;476:373-83.
- [338] Huang H, Qu X, Ji X, Gao X, Zhang L, Chen H, Hou L. Acid and multivalent ion resistance of thin film nanocomposite RO membranes loaded with silicalite-1 nanozeolites. *J Mater Chem A* 2013;1:11343-9.
- [339] Kim SG, Hyeon DH, Chun JH, Chun B-H, Kim SH. Nanocomposite poly(arylene ether sulfone) reverse osmosis membrane containing functional zeolite nanoparticles for seawater desalination. *J Membr Sci* 2013;443:10-8.
- [340] Duan J, Pan Y, Pacheco F, Litwiller E, Lai Z, Pinnau I. High-performance polyamide thin-film-nanocomposite reverse osmosis membranes containing hydrophobic zeolitic imidazolate framework-8. *J Membr Sci* 2015;476:303-10.
- [341] Basu S, Maes M, Cano-Odena A, Alaerts L, De Vos DE, Vankelecom IFJ. Solvent resistant nanofiltration (SRNF) membranes based on metal-organic frameworks. *J Membr Sci* 2009;344:190-8.
- [342] Hu Z, Chen Y, Jiang J. Zeolitic imidazolate framework-8 as a reverse osmosis membrane for water desalination: Insight from molecular simulation. *J Chem Phys* 2011;134:134705/1-6.
- [343] Lee J-Y, Tang CY, Huo F. Fabrication of porous matrix membrane (PMM) using metal-organic framework as green template for water treatment. *Scientific Reports* 2014;4:3740.
- [344] Jadav GL, Aswal VK, Singh PS. SANS study to probe nanoparticle dispersion in nanocomposite membranes of aromatic polyamide and functionalized silica nanoparticles. *J Colloid Interf Sci* 2010;351:304-14.
- [345] Wu H, Tang B, Wu P. Optimizing polyamide thin film composite membrane covalently bonded with modified mesoporous silica nanoparticles. *J Membr Sci* 2013;428:341-8.
- [346] Hu D, Xu Z-L, Chen C. Polypiperazine-amide nanofiltration membrane containing silica nanoparticles prepared by interfacial polymerization. *Desalination* 2012;301:75-81.
- [347] de Lannoy C-F, Jassby D, Gloe K, Gordon AD, Wiesner MR. Aquatic biofouling prevention by electrically charged nanocomposite polymer thin film membranes. *Envir Sci Tech* 2013;47:2760-8.
- [348] Zhao H, Qiu S, Wu L, Zhang L, Chen H, Gao C. Improving the performance of polyamide reverse osmosis membrane by incorporation of modified multi-walled carbon nanotubes. *J Membr Sci* 2014;450:249-56.
- [349] Kim HJ, Choi K, Baek Y, Kim D-G, Shim J, Yoon J, Lee J-C. High-performance reverse osmosis CNT/polyamide nanocomposite membrane by controlled interfacial interactions. *ACS Appl Mater Inter* 2014;6:2819-29.
- [350] Holt JK, Park HG, Wang Y, Stadermann M, Artyukhin AB, Grigoropoulos CP, Noy A, Bakajin O. Fast Mass Transport Through Sub-2-Nanometer Carbon Nanotubes. *Science* 2006;312:1034-7.
- [351] Hinds BJ, Chopra N, Rantell T, Andrews R, Gavalas V, Bachas LG. Aligned Multiwalled Carbon Nanotube Membranes. *Science* 2004;303:62-5.
- [352] Chan W-F, Chen H-y, Surapathi A, Taylor MG, Shao X, Marand E, Johnson JK. Zwitterion functionalized carbon nanotube/polyamide nanocomposite membranes for water desalination. *ACS Nano* 2013;7:5308-19.
- [353] Hegab HM, Zou L. Graphene oxide-assisted membranes: Fabrication and potential applications in desalination and water purification. *J Membr Sci* 2015;484:95-106.

Formatted: Font color: Auto

- [354] Cohen-Tanugi D, Grossman JC. Nanoporous graphene as a reverse osmosis membrane: Recent insights from theory and simulation. *Desalination* 2015;366:59-70.
- [355] Mahmoud KA, Mansoor B, Mansour A, Khraisheh M. Functional graphene nanosheets: The next generation membranes for water desalination. *Desalination* 2015;356:208-25.
- [356] Hu M, Mi B. Enabling Graphene Oxide Nanosheets as Water Separation Membranes. *Envir Sci Tech* 2013;47:3715-23.
- [357] Kim SG, Hyeon DH, Chun JH, Chun BH, Kim SH. Novel thin nanocomposite RO membranes for chlorine resistance. *Desalin Water Treat* 2013;51:6338-45.
- [358] Chae H-R, Lee J, Lee C-H, Kim I-C, Park P-K. Graphene oxide-embedded thin-film composite reverse osmosis membrane with high flux, anti-biofouling, and chlorine resistance. *J Membr Sci* 2015;483:128-35.
- [359] Safarpour M, Khataee A, Vatanpour V. Thin film nanocomposite reverse osmosis membrane modified by reduced graphene oxide/TiO₂ with improved desalination performance. *J Membr Sci* 2015;489:43-54.
- [360] McCutcheon JR, McGinnis RL, Elimelech M. Desalination by ammonia-carbon dioxide forward osmosis: Influence of draw and feed solution concentrations on process performance. *J Membr Sci* 2006;278:114-23.
- [361] McCutcheon JR, Elimelech M. Modeling water flux in forward osmosis: Implications for improved membrane design. *AIChE J* 2007;53:1736-44.
- [362] Nguyen TPN, Yun E-T, Kim I-C, Kwon Y-N. Preparation of cellulose triacetate/cellulose acetate (CTA/CA)-based membranes for forward osmosis. *J Membr Sci* 2013;433:49-59.
- [363] Su J, Ong RC, Wang P, Chung T-S, Helmer BJ, de Wit JS. Advanced FO membranes from newly synthesized CAP polymer for wastewater reclamation through an integrated FO-MD hybrid system. *AIChE J* 2013;59:1245-54.
- [364] Wang KY, Ong RC, Chung T-S. Double-skinned forward osmosis membranes for reducing internal concentration polarization within the porous sublayer. *Ind Eng Chem Res* 2010;49:4824-31.
- [365] Zhang S, Wang KY, Chung T-S, Chen H, Jean YC, Amy G. Well-constructed cellulose acetate membranes for forward osmosis: Minimized internal concentration polarization with an ultra-thin selective layer. *J Membr Sci* 2010;360:522-35.
- [366] Ong RC, Chung T-S. Fabrication and positron annihilation spectroscopy (PAS) characterization of cellulose triacetate membranes for forward osmosis. *J Membr Sci* 2012;394-395:230-40.
- [367] Su J, Yang Q, Teo JF, Chung T-S. Cellulose acetate nanofiltration hollow fiber membranes for forward osmosis processes. *J Membr Sci* 2010;355:36-44.
- [368] Zhang S, Wang KY, Chung TS, Jean YC, Chen H. Molecular design of the cellulose ester-based forward osmosis membranes for desalination. *Chem Eng Sci* 2011;66:2008-18.
- [369] Su J, Zhang S, Chen H, Chen H, Jean YC, Chung T-S. Effects of annealing on the microstructure and performance of cellulose acetate membranes for pressure-retarded osmosis processes. *J Membr Sci* 2010;364:344-53.
- [370] Su J, Chung T-S, Helmer BJ, de Wit JS. Enhanced double-skinned FO membranes with inner dense layer for wastewater treatment and macromolecule recycle using Sucrose as draw solute. *J Membr Sci* 2012;396:92-100.
- [371] Su J, Chung T-S. Sublayer structure and reflection coefficient and their effects on concentration polarization and membrane performance in FO processes. *J Membr Sci* 2011;376:214-24.
- [372] Tang CY, She Q, Lay WCL, Wang R, Field R, Fane AG. Modeling double-skinned FO membranes. *Desalination* 2011;283:178-86.
- [373] Li G, Li X-M, He T, Jiang B, Gao C. Cellulose triacetate forward osmosis membranes: preparation and characterization. *Desalin Water Treat* 2013;51:2656-65.
- [374] Sairam M, Sereewatthanawut E, Li K, Bismarck A, Livingston AG. Method for the preparation of cellulose acetate flat sheet composite membranes for forward osmosis—Desalination using MgSO₄ draw solution. *Desalination* 2011;273:299-307.
- [375] Ong RC, Chung T-S, Helmer BJ, de Wit JS. Novel cellulose esters for forward osmosis membranes. *Ind Eng Chem Res* 2012;51:16135-45.
- [376] Zhang S, Zhang R, Jean YC, Paul DR, Chung T-S. Cellulose esters for forward osmosis: Characterization of water and salt transport properties and free volume. *Polymer* 2012;53:2664-72.
- [377] Nguyen A, Zou L, Priest C. Evaluating the antifouling effects of silver nanoparticles regenerated by TiO₂ on forward osmosis membrane. *J Membr Sci* 2014;454:264-71.
- [378] Yip NY, Tiraferri A, Phillip WA, Schiffman JD, Elimelech M. High performance thin-film composite forward osmosis membrane. *Envir Sci Tech* 2010;44:3812-8.
- [379] Tian EL, Zhou H, Ren YW, mirza Za, Wang XZ, Xiong SW. Novel design of hydrophobic/hydrophilic interpenetrating network composite nanofibers for the support layer of forward osmosis membrane. *Desalination* 2014;347:207-14.

- [380] Bui N-N, McCutcheon JR. Hydrophilic nanofibers as new supports for thin film composite membranes for engineered osmosis. *Envir Sci Tech* 2012;47:1761-9.
- [381] Hoover LA, Schiffman JD, Elimelech M. Nanofibers in thin-film composite membrane support layers: Enabling expanded application of forward and pressure retarded osmosis. *Desalination* 2013;308:73-81.
- [382] Song X, Liu Z, Sun DD. Nano gives the answer: Breaking the bottleneck of internal concentration polarization with a nanofiber composite forward osmosis membrane for a high water production rate. *Adv Mater* 2011;23:3256-60.
- [383] Bui NN, Lind ML, Hoek EMV, McCutcheon JR. Electrospun nanofiber supported thin film composite membranes for engineered osmosis. *J Membr Sci* 2011;385-386:10-9.
- [384] Tian M, Qiu C, Liao Y, Chou S, Wang R. Preparation of polyamide thin film composite forward osmosis membranes using electrospun polyvinylidene fluoride (PVDF) nanofibers as substrates. *Sep Purif Technol* 2013;118:727-36.
- [385] Dumée L, Lee J, Sears K, Tardy B, Duke M, Gray S. Fabrication of thin film composite poly(amide)-carbon-nanotube supported membranes for enhanced performance in osmotically driven desalination systems. *J Membr Sci* 2013;427:422-30.
- [386] Wang R, Shi L, Tang CY, Chou S, Qiu C, Fane AG. Characterization of novel forward osmosis hollow fiber membranes. *J Membr Sci* 2010;355:158-67.
- [387] Luo L, Wang P, Zhang S, Han G, Chung T-S. Novel thin-film composite tri-bore hollow fiber membrane fabrication for forward osmosis. *J Membr Sci* 2014;461:28-38.
- [388] Arkhangelsky E, Wicaksana F, Chou S, Al-Rabiah AA, Al-Zahrani SM, Wang R. Effects of scaling and cleaning on the performance of forward osmosis hollow fiber membranes. *J Membr Sci* 2012;415-416:101-8.
- [389] Sukitpaneent P, Chung T-S. High performance thin-film composite forward osmosis hollow fiber membranes with macrovoid-free and highly porous structure for sustainable water production. *Envir Sci Tech* 2012;46:7358-65.
- [390] Chou S, Shi L, Wang R, Tang CY, Qiu C, Fane AG. Characteristics and potential applications of a novel forward osmosis hollow fiber membrane. *Desalination* 2010;261:365-72.
- [391] Shi L, Chou SR, Wang R, Fang WX, Tang CY, Fane AG. Effect of substrate structure on the performance of thin-film composite forward osmosis hollow fiber membranes. *J Membr Sci* 2011;382:116-23.
- [392] Peng N, Widjojo N, Sukitpaneent P, Teoh MM, Lipscomb GG, Chung T-S, Lai J-Y. Evolution of polymeric hollow fibers as sustainable technologies: Past, present, and future. *Progress Polym Sci* 2012;37:1401-24.
- [393] Han G, Chung T-S, Toriida M, Tamai S. Thin-film composite forward osmosis membranes with novel hydrophilic supports for desalination. *J Membr Sci* 2012;423-424:543-55.
- [394] Duong PHH, Chisca S, Hong P-Y, Cheng H, Nunes SP, Chung T-S. Hydroxyl functionalized polytriazole-co-polyoxadiazole as substrates for forward osmosis membranes. *ACS Appl Mater Inter* 2015;7:3960-73.
- [395] Yasukawa M, Mishima S, Shibuya M, Saeki D, Takahashi T, Miyoshi T, Matsuyama H. Preparation of a forward osmosis membrane using a highly porous polyketone microfiltration membrane as a novel support. *J Membr Sci* 2015;487:51-9.
- [396] Klaysom C, Hermans S, Gahlaut A, Van Craenenbroeck S, Vankelecom IFJ. Polyamide/polyacrylonitrile (PA/PAN) thin film composite osmosis membranes: Film optimization, characterization and performance evaluation. *J Membr Sci* 2013;445:25-33.
- [397] Tiraferri A, Yip NY, Phillip WA, Schiffman JD, Elimelech M. Relating performance of thin-film composite forward osmosis membranes to support layer formation and structure. *J Membr Sci* 2011;367:340-52.
- [398] Wang KY, Chung T-S, Amy G. Developing thin-film-composite forward osmosis membranes on the PES/SPSf substrate through interfacial polymerization. *AIChE J* 2012;58:770-81.
- [399] Widjojo N, Chung T-S, Weber M, Maletzko C, Warzelhan V. The role of sulphonated polymer and macrovoid-free structure in the support layer for thin-film composite (TFC) forward osmosis (FO) membranes. *J Membr Sci* 2011;383:214-23.
- [400] Li X, Wang KY, Helmer B, Chung T-S. Thin-film composite membranes and formation mechanism of thin-film layers on hydrophilic cellulose acetate propionate substrates for forward osmosis processes. *Ind Eng Chem Res* 2012;51:10039-50.
- [401] Huang L, McCutcheon JR. Impact of support layer pore size on performance of thin film composite membranes for forward osmosis. *J Membr Sci* 2015;483:25-33.
- [402] Lu X, Arias Chavez LH, Romero-Vargas Castrillón S, Ma J, Elimelech M. Influence of active layer and support layer surface structures on organic fouling propensity of thin-film composite forward osmosis membranes. *Envir Sci Tech* 2015;49:1436-44.

- [403] Cho YH, Han J, Han S, Guiver MD, Park HB. Polyamide thin-film composite membranes based on carboxylated polysulfone microporous support membranes for forward osmosis. *J Membr Sci* 2013;445:220-7.
- [404] Liu X, Ng HY. Double-blade casting technique for optimizing substrate membrane in thin-film composite forward osmosis membrane fabrication. *J Membr Sci* 2014;469:112-26.
- [405] Xiao P, Nghiem LD, Yin Y, Li X-M, Zhang M, Chen G, Song J, He T. A sacrificial-layer approach to fabricate polysulfone support for forward osmosis thin-film composite membranes with reduced internal concentration polarisation. *J Membr Sci* 2015;481:106-14.
- [406] Liu X, Ng HY. Fabrication of layered silica-polysulfone mixed matrix substrate membrane for enhancing performance of thin-film composite forward osmosis membrane. *J Membr Sci* 2015;481:148-63.
- [407] Vilakati GD, Wong MCY, Hoek EMV, Mamba BB. Relating thin film composite membrane performance to support membrane morphology fabricated using lignin additive. *J Membr Sci* 2014;469:216-24.
- [408] Ong RC, Chung T-S, de Wit JS, Helmer BJ. Novel cellulose ester substrates for high performance flat-sheet thin-film composite (TFC) forward osmosis (FO) membranes. *J Membr Sci* 2015;473:63-71.
- [409] Saraf A, Johnson K, Lind ML. Poly(vinyl) alcohol coating of the support layer of reverse osmosis membranes to enhance performance in forward osmosis. *Desalination* 2014;333:1-9.
- [410] Arena JT, McCloskey B, Freeman BD, McCutcheon JR. Surface modification of thin film composite membrane support layers with polydopamine: Enabling use of reverse osmosis membranes in pressure retarded osmosis. *J Membr Sci* 2011;375:55-62.
- [411] Han G, Zhang S, Li X, Widjojo N, Chung T-S. Thin film composite forward osmosis membranes based on polydopamine modified polysulfone substrates with enhancements in both water flux and salt rejection. *Chem Eng Sci* 2012;80:219-31.
- [412] Huang L, Bui N-N, Meyering MT, Hamlin TJ, McCutcheon JR. Novel hydrophilic nylon 6,6 microfiltration membrane supported thin film composite membranes for engineered osmosis. *J Membr Sci* 2013;437:141-9.
- [413] Alsvik IL, Zodrow KR, Elimelech M, Hägg M-B. Polyamide formation on a cellulose triacetate support for osmotic membranes: Effect of linking molecules on membrane performance. *Desalination* 2013;312:2-9.
- [414] Alsvik IL, Hägg M-B. Preparation of thin film composite membranes with polyamide film on hydrophilic supports. *J Membr Sci* 2013;428:225-31.
- [415] Emadzadeh D, Lau WJ, Matsuura T, Hilal N, Ismail AF. The potential of thin film nanocomposite membrane in reducing organic fouling in forward osmosis process. *Desalination* 2014;348:82-8.
- [416] Emadzadeh D, Lau WJ, Matsuura T, Rahbari-Sisakht M, Ismail AF. A novel thin film composite forward osmosis membrane prepared from PSf-TiO₂ nanocomposite substrate for water desalination. *Chem Eng J* 2014;237:70-80.
- [417] Emadzadeh D, Lau WJ, Matsuura T, Ismail AF, Rahbari-Sisakht M. Synthesis and characterization of thin film nanocomposite forward osmosis membrane with hydrophilic nanocomposite support to reduce internal concentration polarization. *J Membr Sci* 2014;449:74-85.
- [418] Emadzadeh D, Lau WJ, Ismail AF. Synthesis of thin film nanocomposite forward osmosis membrane with enhancement in water flux without sacrificing salt rejection. *Desalination* 2013;330:90-9.
- [419] Wang Y, Ou R, Ge Q, Wang H, Xu T. Preparation of polyethersulfone/carbon nanotube substrate for high-performance forward osmosis membrane. *Desalination* 2013;330:70-8.
- [420] Ma N, Wei J, Qi S, Zhao Y, Gao Y, Tang CY. Nanocomposite substrates for controlling internal concentration polarization in forward osmosis membranes. *J Membr Sci* 2013;441:54-62.
- [421] Wang Y, Xu T. Anchoring hydrophilic polymer in substrate: An easy approach for improving the performance of TFC FO membrane. *J Membr Sci* 2015;476:330-9.
- [422] Wang Y, Ou R, Wang H, Xu T. Graphene oxide modified graphitic carbon nitride as a modifier for thin film composite forward osmosis membrane. *J Membr Sci* 2015;475:281-9.
- [423] Jia Q, Han H, Wang L, Liu B, Yang H, Shen J. Effects of CTAC micelles on the molecular structures and separation performance of thin-film composite (TFC) membranes in forward osmosis processes. *Desalination* 2014;340:30-41.
- [424] Shaffer DL, Jaramillo H, Romero-Vargas Castrillón S, Lu X, Elimelech M. Post-fabrication modification of forward osmosis membranes with a poly(ethylene glycol) block copolymer for improved organic fouling resistance. *J Membr Sci* 2015;490:209-19.
- [425] Romero-Vargas Castrillón S, Lu X, Shaffer DL, Elimelech M. Amine enrichment and poly(ethylene glycol) (PEG) surface modification of thin-film composite forward osmosis membranes for organic fouling control. *J Membr Sci* 2014;450:331-9.
- [426] Lu X, Romero-Vargas Castrillón S, Shaffer DL, Ma J, Elimelech M. In situ surface chemical modification of thin-film composite forward osmosis membranes for enhanced organic fouling resistance. *Envir Sci Tech* 2013;47:12219-28.

- [427] Tiraferri A, Kang Y, Giannelis EP, Elimelech M. Highly hydrophilic thin-film composite forward osmosis membranes functionalized with surface-tailored nanoparticles. *ACS Appl Mater Inter* 2012;4:5044-53.
- [428] Tiraferri A, Kang Y, Giannelis EP, Elimelech M. Superhydrophilic thin-film composite forward osmosis membranes for organic fouling control: Fouling behavior and antifouling mechanisms. *Envir Sci Tech* 2012;46:11135-44.
- [429] Fang W, Wang R, Chou S, Setiawan L, Fane AG. Composite forward osmosis hollow fiber membranes: Integration of RO- and NF-like selective layers to enhance membrane properties of anti-scaling and anti-internal concentration polarization. *J Membr Sci* 2012;394–395:140-50.
- [430] Fang W, Liu C, Shi L, Wang R. Composite forward osmosis hollow fiber membranes: Integration of RO- and NF-like selective layers for enhanced organic fouling resistance. *J Membr Sci* 2015;492:147-55.
- [431] Saren Q, Qiu CQ, Tang CY. Synthesis and characterization of novel forward osmosis membranes based on layer-by-layer assembly. *Envir Sci Tech* 2011;45:5201-8.
- [432] Bruening ML, Dotzauer DM, Jain P, Ouyang L, Baker GL. Creation of functional membranes using polyelectrolyte multilayers and polymer brushes. *Langmuir* 2008;24:7663-73.
- [433] Liu C, Fang W, Chou S, Shi L, Fane AG, Wang R. Fabrication of layer-by-layer assembled FO hollow fiber membranes and their performances using low concentration draw solutions. *Desalination* 2013;308:147-53.
- [434] Qi S, Qiu CQ, Zhao Y, Tang CY. Double-skinned forward osmosis membranes based on layer-by-layer assembly—FO performance and fouling behavior. *J Membr Sci* 2012;405–406:20-9.
- [435] Qi S, Li W, Zhao Y, Ma N, Wei J, Chin TW, Tang CY. Influence of the properties of layer-by-layer active layers on forward osmosis performance. *J Membr Sci* 2012;423–424:536-42.
- [436] Duong PHH, Zuo J, Chung T-S. Highly crosslinked layer-by-layer polyelectrolyte FO membranes: Understanding effects of salt concentration and deposition time on FO performance. *J Membr Sci* 2013;427:411-21.
- [437] Qiu C, Qi S, Tang CY. Synthesis of high flux forward osmosis membranes by chemically crosslinked layer-by-layer polyelectrolytes. *J Membr Sci* 2011;381:74-80.
- [438] Wang F, Feng J, Gao C. Manipulating the properties of coacervated polyelectrolyte microcapsules by chemical crosslinking. *Colloid Polym Sci* 2008;286:951-7.
- [439] Lee J-Y, Qi S, Liu X, Li Y, Huo F, Tang CY. Synthesis and characterization of silica gel–polyacrylonitrile mixed matrix forward osmosis membranes based on layer-by-layer assembly. *Sep Purif Technol* 2014;124:207-16.
- [440] Pardeshi P, Mungray AA. Synthesis, characterization and application of novel high flux FO membrane by layer-by-layer self-assembled polyelectrolyte. *J Membr Sci* 2014;453:202-11.
- [441] Choe EW, Choe DD. Polybenzimidazoles (overview). In: Salamone JC, editor. *Polymeric Materials Encyclopedia*. New York CRC Press; 1996. p. 1113-4.
- [442] Wang KY, Chung T-S, Qin J-J. Polybenzimidazole (PBI) nanofiltration hollow fiber membranes applied in forward osmosis process. *J Membr Sci* 2007;300:6-12.
- [443] Wang KY, Yang Q, Chung T-S, Rajagopalan R. Enhanced forward osmosis from chemically modified polybenzimidazole (PBI) nanofiltration hollow fiber membranes with a thin wall. *Chem Eng Sci* 2009;64:1577-84.
- [444] Yang Q, Wang KY, Chung T-S. Dual-layer hollow fibers with enhanced flux as novel forward osmosis membranes for water production. *Envir Sci Tech* 2009;43:2800-5.
- [445] Flanagan MF, Escobar IC. Novel charged and hydrophilized polybenzimidazole (PBI) membranes for forward osmosis. *J Membr Sci* 2013;434:85-92.
- [446] Michael F, Richard H, Brett D, Isabel CE, Maria C, Tai-Shung C. Surface functionalization of polybenzimidazole membranes to increase hydrophilicity and charge. In: Escobar I, van der Bruggen B, editors. *Modern Applications in Membrane Science and Technology*, ACS Symp Ser 1078. Washington DC: American Chemical Society; 2011. p. 303-21.
- [447] Hausman R, Digman B, Escobar IC, Coleman M, Chung T-S. Functionalization of polybenzimidazole membranes to impart negative charge and hydrophilicity. *J Membr Sci* 2010;363:195-203.
- [448] Setiawan L, Wang R, Li K, Fane AG. Fabrication of novel poly(amide–imide) forward osmosis hollow fiber membranes with a positively charged nanofiltration-like selective layer. *J Membr Sci* 2011;369:196-205.
- [449] Setiawan L, Wang R, Li K, Fane AG. Fabrication and characterization of forward osmosis hollow fiber membranes with antifouling NF-like selective layer. *J Membr Sci* 2012;394–395:80-8.
- [450] Setiawan L, Wang R, Shi L, Li K, Fane AG. Novel dual-layer hollow fiber membranes applied for forward osmosis process. *J Membr Sci* 2012;421–422:238-46.
- [451] Setiawan L, Wang R, Tan S, Shi L, Fane AG. Fabrication of poly(amide-imide)-polyethersulfone dual layer hollow fiber membranes applied in forward osmosis by combined polyelectrolyte cross-linking and depositions. *Desalination* 2013;312:99-106.

- [452] Madsen HT, Bajraktari N, Hélix-Nielsen C, Van der Bruggen B, Søgaaard EG. Use of biomimetic forward osmosis membrane for trace organics removal. *J Membr Sci* 2015;476:469-74.
- [453] Niksefat N, Jahanshahi M, Rahimpour A. The effect of SiO₂ nanoparticles on morphology and performance of thin film composite membranes for forward osmosis application. *Desalination* 2014;343:140-6.
- [454] Ma N, Wei J, Liao R, Tang CY. Zeolite-polyamide thin film nanocomposite membranes: Towards enhanced performance for forward osmosis. *J Membr Sci* 2012;405-406:149-57.
- [455] Amini M, Jahanshahi M, Rahimpour A. Synthesis of novel thin film nanocomposite (TFN) forward osmosis membranes using functionalized multi-walled carbon nanotubes. *J Membr Sci* 2013;435:233-41.
- [456] Goh K, Setiawan L, Wei L, Jiang W, Wang R, Chen Y. Fabrication of novel functionalized multi-walled carbon nanotube immobilized hollow fiber membranes for enhanced performance in forward osmosis process. *J Membr Sci* 2013;446:244-54.
- [457] Song X, Wang L, Tang CY, Wang Z, Gao C. Fabrication of carbon nanotubes incorporated double-skinned thin film nanocomposite membranes for enhanced separation performance and antifouling capability in forward osmosis process. *Desalination* 2015;369:1-9.
- [458] Ghanbari M, Emadzadeh D, Lau WJ, Lai SO, Matsuura T, Ismail AF. Synthesis and characterization of novel thin film nanocomposite (TFN) membranes embedded with halloysite nanotubes (HNTs) for water desalination. *Desalination* 2015;358:33-41.
- [459] Zirehpour A, Rahimpour A, Seyedpour F, Jahanshahi M. Developing new CTA/CA-based membrane containing hydrophilic nanoparticles to enhance the forward osmosis desalination. *Desalination* 2015;371:46-57.
- [460] Jia Y-x, Li H-l, Wang M, Wu L-y, Hu Y-d. Carbon nanotube: Possible candidate for forward osmosis. *Sep Purif Technol* 2010;75:55-60.
- [461] Ghanbari M, Emadzadeh D, Lau WJ, Matsuura T, Davoody M, Ismail AF. Super hydrophilic TiO₂/HNT nanocomposites as a new approach for fabrication of high performance thin film nanocomposite membranes for FO application. *Desalination* 2015;371:104-14.
- [462] Shaffer DL, Werber JR, Jaramillo H, Lin S, Elimelech M. Forward osmosis: Where are we now? *Desalination* 2015;356:271-84.
- [463] Geise GM, Park HB, Sagle AC, Freeman BD, McGrath JE. Water permeability and water/salt selectivity tradeoff in polymers for desalination. *J Membr Sci* 2011;369:130-8.
- [464] Ingole PG, Choi W, Kim KH, Park CH, Choi WK, Lee HK. Synthesis, characterization and surface modification of PES hollow fiber membrane support with polydopamine and thin film composite for energy generation. *Chem Eng J* 2014;243:137-46.
- [465] Han G, Chung T-S. Robust and high performance pressure retarded osmosis hollow fiber membranes for osmotic power generation. *AIChE J* 2014;60:1107-19.
- [466] Han G, Zhang S, Li X, Chung T-S. High performance thin film composite pressure retarded osmosis (PRO) membranes for renewable salinity-gradient energy generation. *J Membr Sci* 2013;440:108-21.
- [467] Zhang S, Fu F, Chung T-S. Substrate modifications and alcohol treatment on thin film composite membranes for osmotic power. *Chem Eng Sci* 2013;87:40-50.
- [468] Fu F-J, Sun S-P, Zhang S, Chung T-S. Pressure retarded osmosis dual-layer hollow fiber membranes developed by co-casting method and ammonium persulfate (APS) treatment. *J Membr Sci* 2014;469:488-98.
- [469] Ingole PG, Kim KH, Park CH, Choi WK, Lee HK. Preparation, modification and characterization of polymeric hollow fiber membranes for pressure-retarded osmosis. *RSC Adv* 2014;4:51430-9.
- [470] Han G, Wang P, Chung T-S. Highly Robust Thin-Film Composite Pressure Retarded Osmosis (PRO) Hollow Fiber Membranes with High Power Densities for Renewable Salinity-Gradient Energy Generation. *Envir Sci Tech* 2013;47:8070-7.
- [471] Bui N-N, McCutcheon JR. Nanofiber Supported Thin-Film Composite Membrane for Pressure-Retarded Osmosis. *Envir Sci Tech* 2014;48:4129-36.
- [472] Song X, Liu Z, Sun DD. Energy recovery from concentrated seawater brine by thin-film nanofiber composite pressure retarded osmosis membranes with high power density. *Energy Environ Sci* 2013;6:1199-210.
- [473] Chou S, Wang R, Fane AG. Robust and High performance hollow fiber membranes for energy harvesting from salinity gradients by pressure retarded osmosis. *J Membr Sci* 2013;448:44-54.
- [474] Li X, Zhang S, Fu F, Chung T-S. Deformation and reinforcement of thin-film composite (TFC) polyamide-imide (PAI) membranes for osmotic power generation. *J Membr Sci* 2013;434:204-17.
- [475] Zhao J, Su Y, He X, Zhao X, Li Y, Zhang R, Jiang Z. Dopamine composite nanofiltration membranes prepared by self-polymerization and interfacial polymerization. *J Membr Sci* 2014;465:41-8.

- [476] Liu Y, He B, Li J, Sanderson RD, Li L, Zhang S. Formation and structural evolution of biphenyl polyamide thin film on hollow fiber membrane during interfacial polymerization. *J Membr Sci* 2011;373:98-106.
- [477] Wang H, Zhang Q, Zhang S. Positively charged nanofiltration membrane formed by interfacial polymerization of 3,3',5,5'-biphenyl tetraacyl chloride and piperazine on a poly(acrylonitrile) (PAN) support. *J Membr Sci* 2011;378:243-9.
- [478] Wang T, Yang Y, Zheng J, Zhang Q, Zhang S. A novel highly permeable positively charged nanofiltration membrane based on a nanoporous hyper-crosslinked polyamide barrier layer. *J Membr Sci* 2013;448:180-9.
- [479] Xie W, Geise GM, Freeman BD, Lee H-S, Byun G, McGrath JE. Polyamide interfacial composite membranes prepared from m-phenylene diamine, trimesoyl chloride and a new disulfonated diamine. *J Membr Sci* 2012;403-404:152-61.
- [480] Yu S, Liu M, Lü Z, Zhou Y, Gao C. Aromatic-cycloaliphatic polyamide thin-film composite membrane with improved chlorine resistance prepared from m-phenylenediamine-4-methyl and cyclohexane-1,3,5-tricarbonyl chloride. *J Membr Sci* 2009;344:155-64.
- [481] Seman MNA, Khayet M, Hilal N. Nanofiltration thin-film composite polyester polyethersulfone-based membranes prepared by interfacial polymerization. *J Membr Sci* 2010;348:109-16.
- [482] Wang L, Li D, Cheng L, Zhang L, Chen H. Synthesis of 4-Aminobenzoylpiperazine for Preparing the Thin Film Composite Nanofiltration Membrane by Interfacial Polymerization with TMC. *Separ Sci Technol* 2012;48:466-72.
- [483] Baroña GNB, Lim J, Jung B. High performance thin film composite polyamide reverse osmosis membrane prepared via m-phenylenediamine and 2,2'-benzidinedisulfonic acid. *Desalination* 2012;291:69-77.
- [484] Yu S, Ma M, Liu J, Tao J, Liu M, Gao C. Study on polyamide thin-film composite nanofiltration membrane by interfacial polymerization of polyvinylamine (PVAm) and isophthaloyl chloride (IPC). *J Membr Sci* 2011;379:164-73.
- [485] Fang W, Shi L, Wang R. Interfacially polymerized composite nanofiltration hollow fiber membranes for low-pressure water softening. *J Membr Sci* 2013;430:129-39.
- [486] Jewrajka SK, Reddy AVR, Rana HH, Mandal S, Khullar S, Haldar S, Joshi N, Ghosh PK. Use of 2,4,6-pyridinetricarboxylic acid chloride as a novel co-monomer for the preparation of thin film composite polyamide membrane with improved bacterial resistance. *J Membr Sci* 2013;439:87-95.
- [487] Zhang Z, Wang S, Chen H, Liu Q, Wang J, Wang T. Preparation of polyamide membranes with improved chlorine resistance by bis-2,6-N,N-(2-hydroxyethyl) diaminotoluene and trimesoyl chloride. *Desalination* 2013;331:16-25.
- [488] Bera A, Gol RM, Chatterjee S, Jewrajka SK. PEGylation and incorporation of triazine ring into thin film composite reverse osmosis membranes for enhancement of anti-organic and anti-biofouling properties. *Desalination* 2015;360:108-17.
- [489] Jin J-b, Liu D-q, Zhang D-d, Yin Y-h, Zhao X-y, Zhang Y-f. Preparation of thin-film composite nanofiltration membranes with improved antifouling property and flux using 2,2'-oxybis-ethylamine. *Desalination* 2015;355:141-6.
- [490] Mollahosseini A, Rahimpour A. Interfacially polymerized thin film nanofiltration membranes on TiO₂ coated polysulfone substrate. *J Ind Eng Chem* 2014;20:1261-8.
- [491] Pal A, Dey TK, Singhal A, Bindal RC, Tewari PK. Nano-ZnO impregnated inorganic-polymer hybrid thinfilm nanocomposite nanofiltration membranes: an investigation of variation in structure, morphology and transport properties. *RSC Adv* 2015;5:34134-51.
- [492] Peyki A, Rahimpour A, Jahanshahi M. Preparation and characterization of thin film composite reverse osmosis membranes incorporated with hydrophilic SiO₂ nanoparticles. *Desalination* 2015;368:152-8.
- [493] Kim SG, Chun JH, Chun B-H, Kim SH. Preparation, characterization and performance of poly(arylene ether sulfone)/modified silica nanocomposite reverse osmosis membrane for seawater desalination. *Desalination* 2013;325:76-83.
- [494] Ahmad A, Waheed S, Khan SM, e-Gul S, Shafiq M, Farooq M, Sanaullah K, Jamil T. Effect of silica on the properties of cellulose acetate/polyethylene glycol membranes for reverse osmosis. *Desalination* 2015;355:1-10.
- [495] Shen Jn, Yu Cc, Ruan Hm, Gao Cj, Van der Bruggen B. Preparation and characterization of thin-film nanocomposite membranes embedded with poly(methyl methacrylate) hydrophobic modified multiwalled carbon nanotubes by interfacial polymerization. *J Membr Sci* 2013;442:18-26.
- [496] Baroña GNB, Lim J, Choi M, Jung B. Interfacial polymerization of polyamide-aluminosilicate SWNT nanocomposite membranes for reverse osmosis. *Desalination* 2013;325:138-47.
- [497] Ghanbari M, Emadzadeh D, Lau WJ, Matsuura T, Ismail AF. Synthesis and characterization of novel thin film nanocomposite reverse osmosis membranes with improved organic fouling properties for water desalination. *RSC Adv* 2015;5:21268-76.

- [498] Emadzadeh D, Lau WJ, Rahbari-Sisakht M, Daneshfar A, Ghanbari M, Mayahi A, Matsuura T, Ismail AF. A novel thin film nanocomposite reverse osmosis membrane with superior anti-organic fouling affinity for water desalination. *Desalination* 2015;368:106-13.
- [499] Bano S, Mahmood A, Kim S-J, Lee K-H. Graphene oxide modified polyamide nanofiltration membrane with improved flux and antifouling properties. *J Mater Chem A* 2015;3:2065-71.
- [500] He L, Dumée LF, Feng C, Velleman L, Reis R, She F, Gao W, Kong L. Promoted water transport across graphene oxide-poly(amide) thin film composite membranes and their antibacterial activity. *Desalination* 2015;365:126-35.
- [501] Widjojo N, Chung T-S, Weber M, Maletzko C, Warzelhan V. A sulfonated polyphenylenesulfone (sPPSU) as the supporting substrate in thin film composite (TFC) membranes with enhanced performance for forward osmosis (FO). *Chem Eng J* 2013;220:15-23.
- [502] Sun Y, Xue L, Zhang Y, Zhao X, Huang Y, Du X. High flux polyamide thin film composite forward osmosis membranes prepared from porous substrates made of polysulfone and polyethersulfone blends. *Desalination* 2014;336:72-9.
- [503] Kwon S-B, Lee JS, Kwon SJ, Yun S-T, Lee S, Lee J-H. Molecular layer-by-layer assembled forward osmosis membranes. *J Membr Sci* 2015;488:111-20.

Figure Captions

Fig. 1. Schematic diagram illustrating the working principles of (a) reverse osmosis (RO) and (b) forward osmosis (FO) processes. Water flows in different directions in RO and FO (indicated by blue arrows); green arrow shows reverse salt diffusion from draw solution to feed in FO. Hydraulic pressure is used as driving force in RO, whilst osmotic pressure differential between feed and draw solution serves as driving force in FO. [20]

Field Code Changed

Field Code Changed

Fig. 2. Cross-sectional SEM images of CA RO membrane (a; GE Osmonics CE), PA TFC RO membrane (b; Dow Filmtec SW30 XLE), and CTA FO membrane (c; HTI). [52]

Field Code Changed

Field Code Changed

Fig. 3. Comparison of the membranes in terms of flux and rejection at the feed of 2000, 3000 and 5000 ppm NaCl, corresponding to 0, 30 and 60% recovery for a feed concentration of 2000 ppm NaCl at 15.5 bar (a) and 31.0 bar (b). “High-flux” and “Commercial” are denoted to the PA TFC membrane, which was prepared with 2.85 wt% *o*-aminobenzoic acid-triethylamine salt (*o*-ABA-TEA) and optimal post-treatment, and a commercial membrane, respectively (modified from the Reference [128]).

Field Code Changed

Field Code Changed

Fig. 4. (a) Oxidative polymerization of amino acid 3-(3,4-dihydroxyphenyl)-L-alanine (L-DOPA) and surface adsorption resistance to organic matter imparted by the hydrated zwitterionic coated surface; (b) normalised flux of the original and modified SW30XLE RO membranes (“12 hr SW30XLE” and “24 hr SW30XLE” are referred to the SW30XLE RO membranes with a 12-hr and 24-hr coating) as a function of time during BSA/sodium alginate (100 ppm of each; 18 bar) fouling (the dashed part shows the treatment of water cleaning) (modified from the reference [170]).

Field Code Changed

Field Code Changed

Fig. 5. (a) Schematic representation of temperature responsive properties of poly(*N*-isopropylacrylamide) (PNIPAM) brushes grafted on TFC membrane surface; (b) repeated produced water flux results of grafted membrane as a function of applied pressure: after each cycle, the membrane was placed in flushed with lukewarm water (40 °C) for cleaning (modified from [194]).

Field Code Changed

Field Code Changed

Fig. 6. Antifouling zwitterionic coating applied onto commercial RO membranes *via* iCVD. (a-b) Cross-sectional SEM image of (a) bare and (b) iCVD coated RO membrane; (c) salt rejection and (d) water flux of bare and coated membranes; (e) surface coverage by *V. cyclitrophicus* on bare glass (black) and iCVD zwitterionic surface (orange) and relative fouling index F_1 (blue). The relative fouling index F_1 (blue) is defined as the fraction of surface coverage for the coated surface compared to the bare glass control (modified from the reference [201]).

Field Code Changed

Field Code Changed

Fig. 7. (a) Effect of chlorine concentration (Cl_T) and solution pH on membrane properties by two competing mechanisms of chlorination-promoted hydrolysis and *N*-chlorination; (b) performance of NF90 membranes, both virgin and chlorinated for 100 h at different Cl_T and pH (at 584.4 ppm NaCl feed and 6.89 bar). Salt rejection (%) shown by the numbers in white and water flux (LMH) shown by the numbers in parentheses; NP: membrane failed to perform (modified from the reference [225]).

Field Code Changed

Field Code Changed

Fig. 8. (a) Schematic of antifouling and chlorine resistant properties of imidazolidinyl urea (IU)-modified membrane; (b) water fluxes and salt rejections of both virgin membrane and IU-modified membrane during the three operation cycles (at 2000 ppm NaCl and 15.5 bar). [243]

Field Code Changed

Field Code Changed

Fig. 9. Water molecules in the feed solution penetrate the membrane in 3 steps: (1) passing from the feed solution to the vesicles through the aquaporin (AQP) water channel located at the polymer bilayer facing the feed solution, (2) passing from the vesicles to the support through the AQP located at the polymer bilayer facing the support membrane, and (3) penetrating the porous support into the permeate solution. Other solutes in the feed solution will be rejected. [284]

Field Code Changed

Field Code Changed

Fig. 10. Schematic for PA TFN membrane fabricated by dispersing *N*-[3-(trimethoxysilyl) propyl] ethylenediamine (AAPTS)-modified TiO₂ nanoparticles in MPD aqueous solution (modified from the reference [295]).

Field Code Changed

Field Code Changed

Fig. 11. SEM (left) and TEM images (right) of TFN membrane with 0.1 w/v% zeolites added in MPD aqueous phase (a); and TFN membrane with 0.1 w/v% zeolites added in TMC hexane organic phase (b) (modified from the reference [307])

Field Code Changed

Field Code Changed

Fig. 12. (a) Schematic illustration of hypothesized mechanism of MCM-41-incorporated TFN membrane (1 shows the feed solution containing NaCl; 2 shows the PA active layer with MCM-41 or nonporous silica; 3 denotes the porous support); (b) water flux and salt rejection of TFN membranes with MCM-41 nanoparticles at 20.7 bar and 2000 ppm NaCl or Na₂SO₄ feed. [300]

Field Code Changed

Field Code Changed

Fig. 13. Schematic illustration of fast water transport in CNTs-incorporated nanocomposite membrane. [349]

Field Code Changed

Field Code Changed

Fig. 14. A schematic diagram and FESEM images of double-skinned CA membrane cast on glass plate and phase transition in water; which is consisting of double selective skins, transition sublayers, and a porous bulk support (CS is denoted as cross-section of membrane). [365]

Field Code Changed

Field Code Changed

Fig. 15. SEM images of cross-section of a double-skinned FO hollow fibre with (a) inner RO skin and (b) outer NF skin; (c) effect of cleaning on scaled double-skinned FO hollow fibre membrane (denoted as FO-RO/NF_s) and FO hollow fibre membrane with only RO active layer (denoted as FO-RO_s) (scaling test was carried out by flowing mixture of CaCl₂ and K₂HPO₄ as feed and 0.5 M NaCl as draw solution) (modified from the reference [429])

Field Code Changed

Field Code Changed

Fig. 16. (a) Conceptual illustrations of double-skinned LbL membrane fabrication; (b) normalized flux for double-skinned LbL membranes under different fouling conditions (300 ppm dextran, 20 ppm alginate, or 300 ppm alginate) (In the membrane symbols of “xLbL3-0”, “xLbL3-1”, “xLbL3-2”, and “xLbL3-3”, the

two numbers are referred to the number of polyelectrolyte layers for the top and bottom rejection skins;

“xLbL” represents crosslinked LbL membranes). [434]

Field Code Changed

Field Code Changed

Fig. 17. (a) Schematic representation of the fabrication process for the magnetic-aided LbL membrane; (b) representative CLSM images of liposome adsorbed LbL films as a function of deposition time, (i) with and (ii) without the magnetic driving force. Scale bar: 10 μm . [280]

Field Code Changed

Field Code Changed

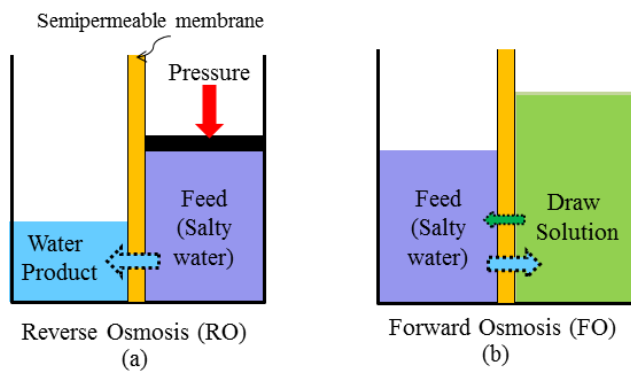


Fig. 1

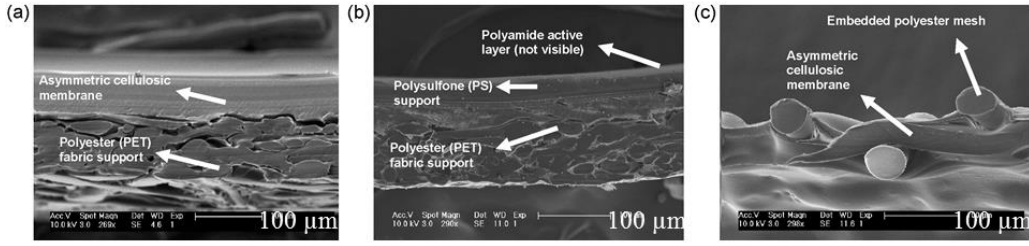


Fig. 2.

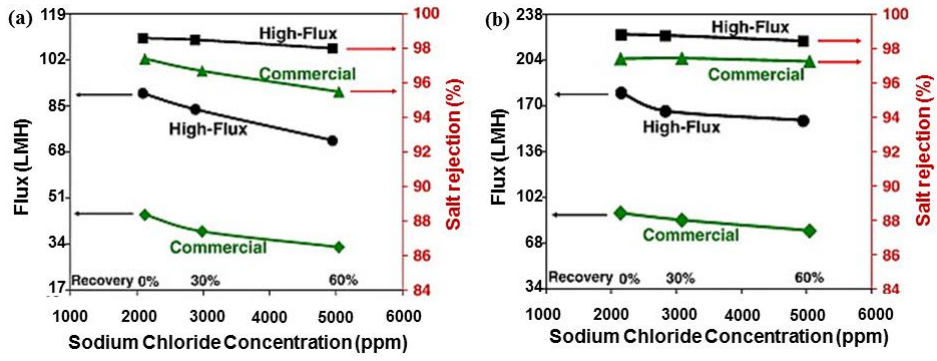


Fig. 3.

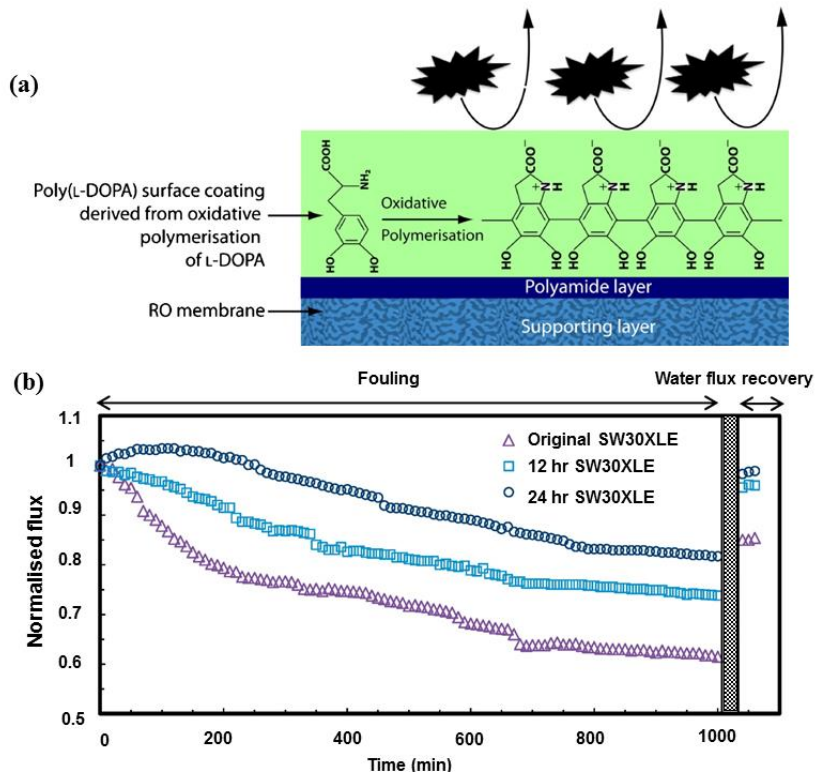


Fig. 4.

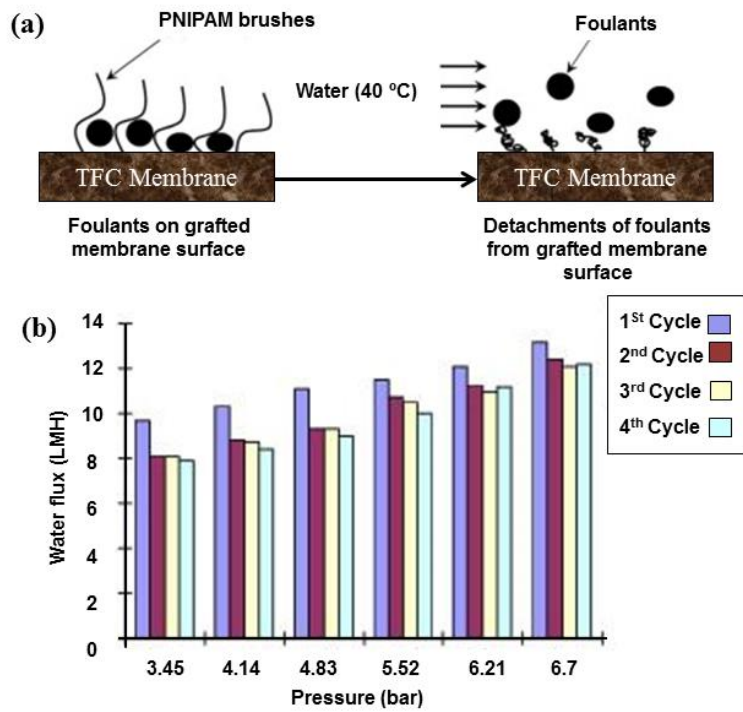


Fig. 5.

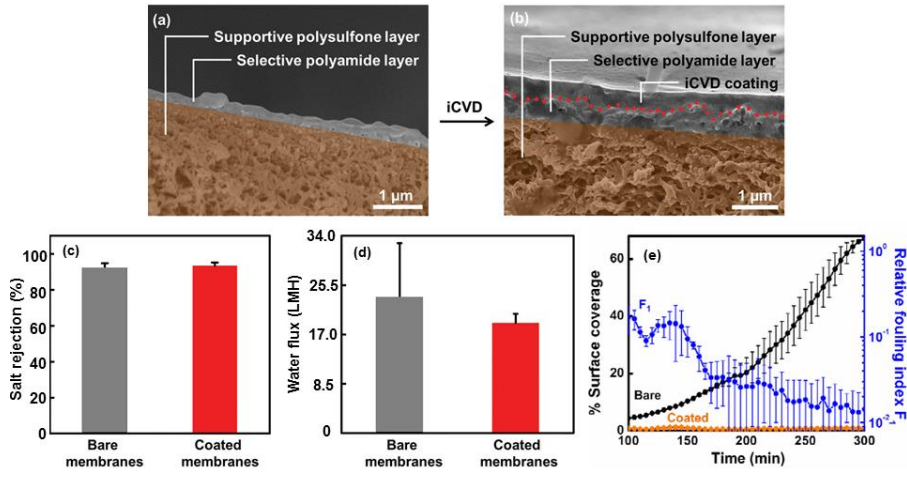


Fig. 6.

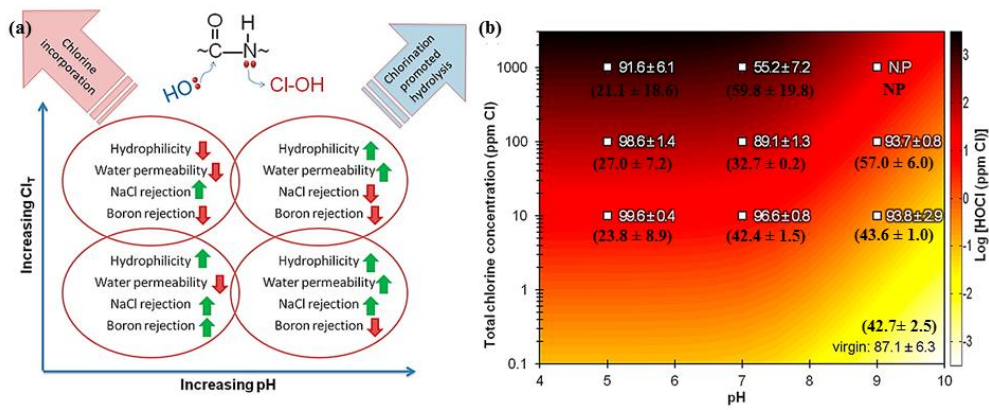


Fig. 7.

▲ Water molecule
● solute

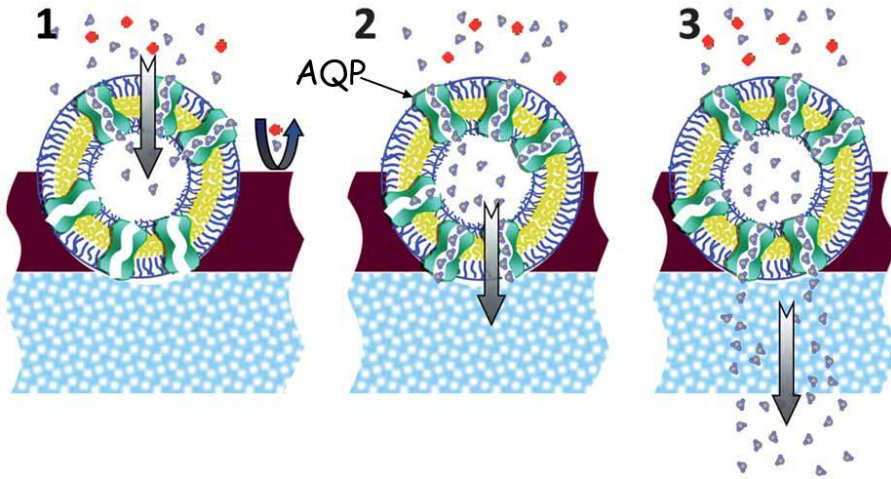


Fig. 9.

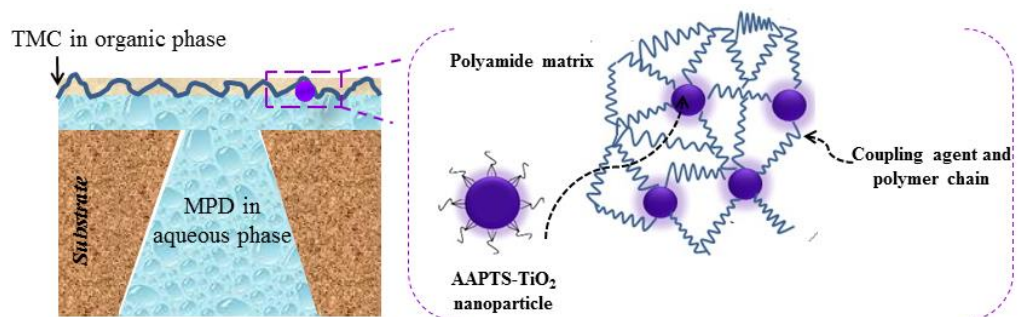
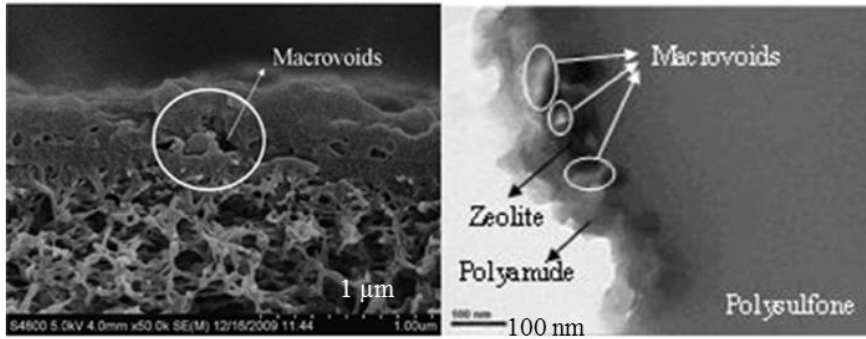
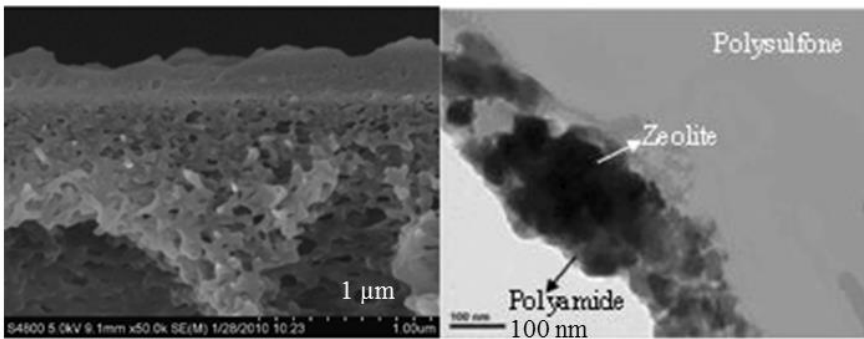


Fig.10.



(a)



(b)

Fig. 11.

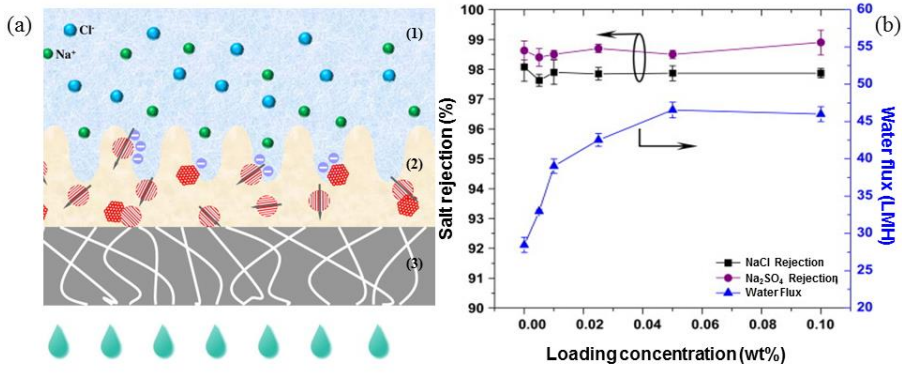


Fig. 12.

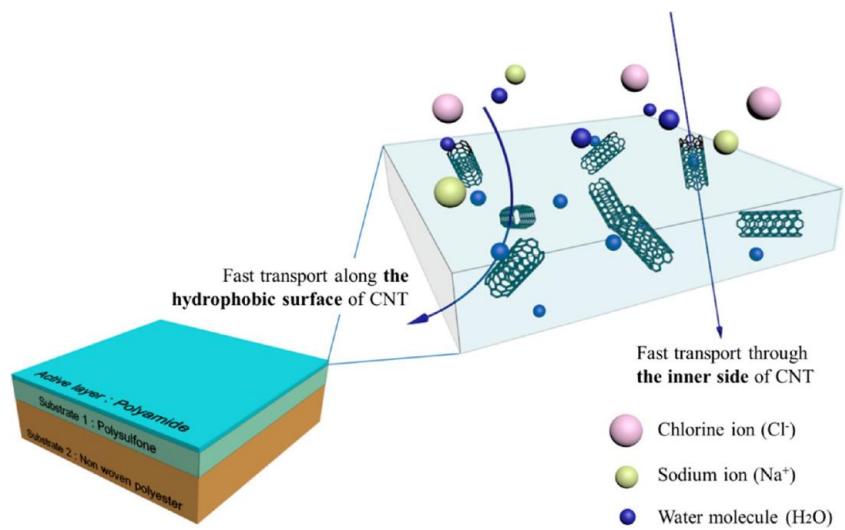


Fig. 13.

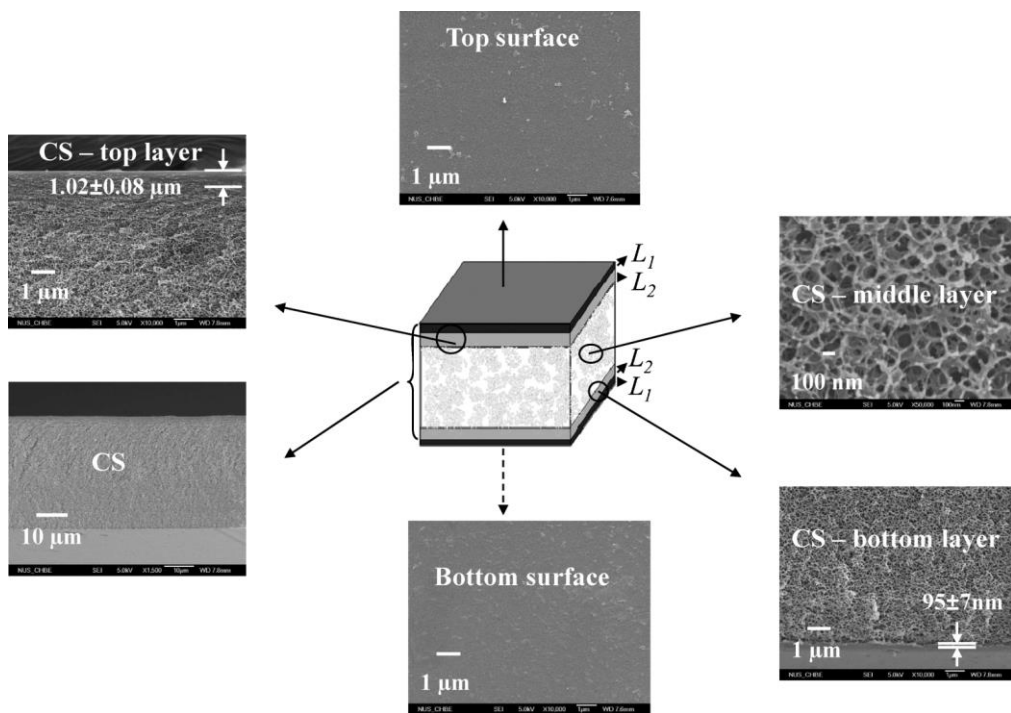


Fig. 14.

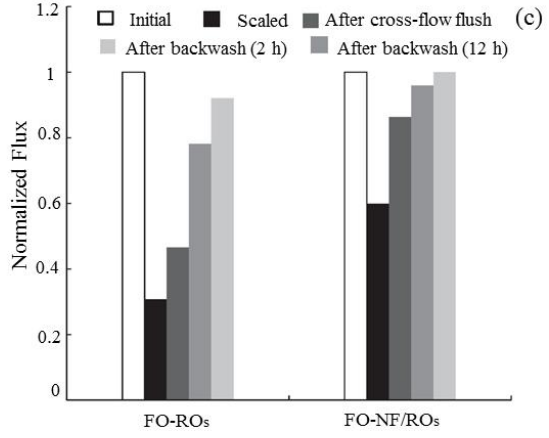
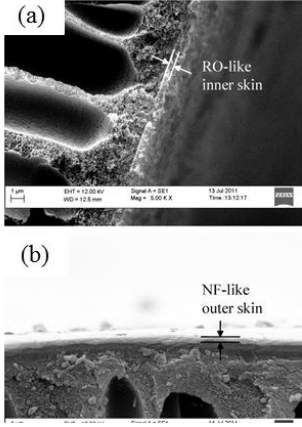


Fig. 15.

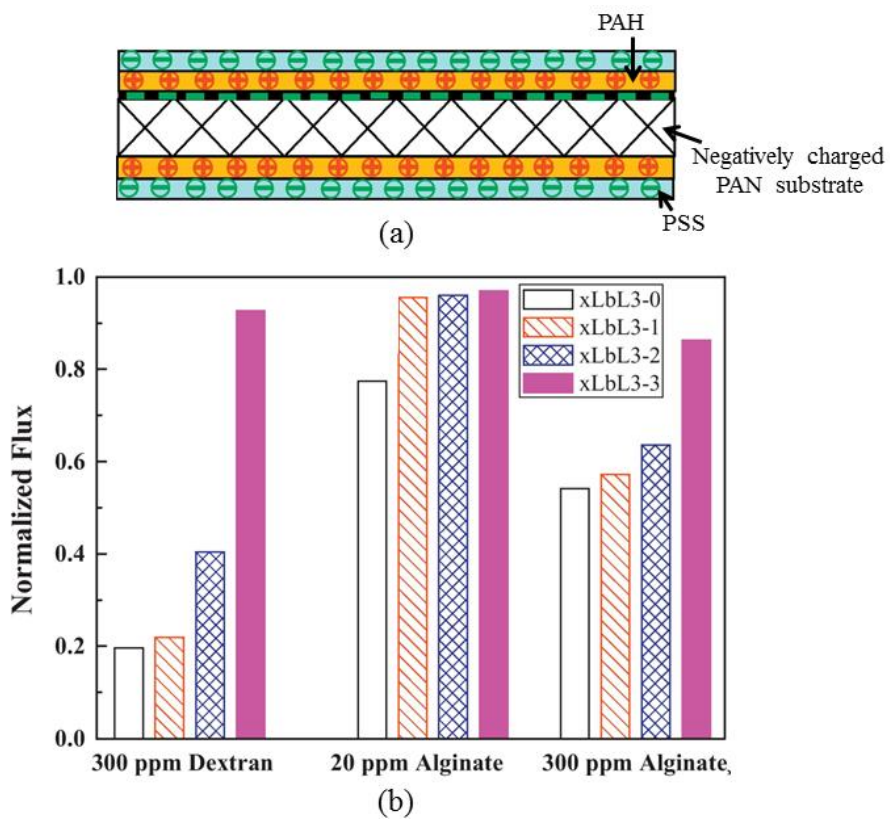


Fig. 16.

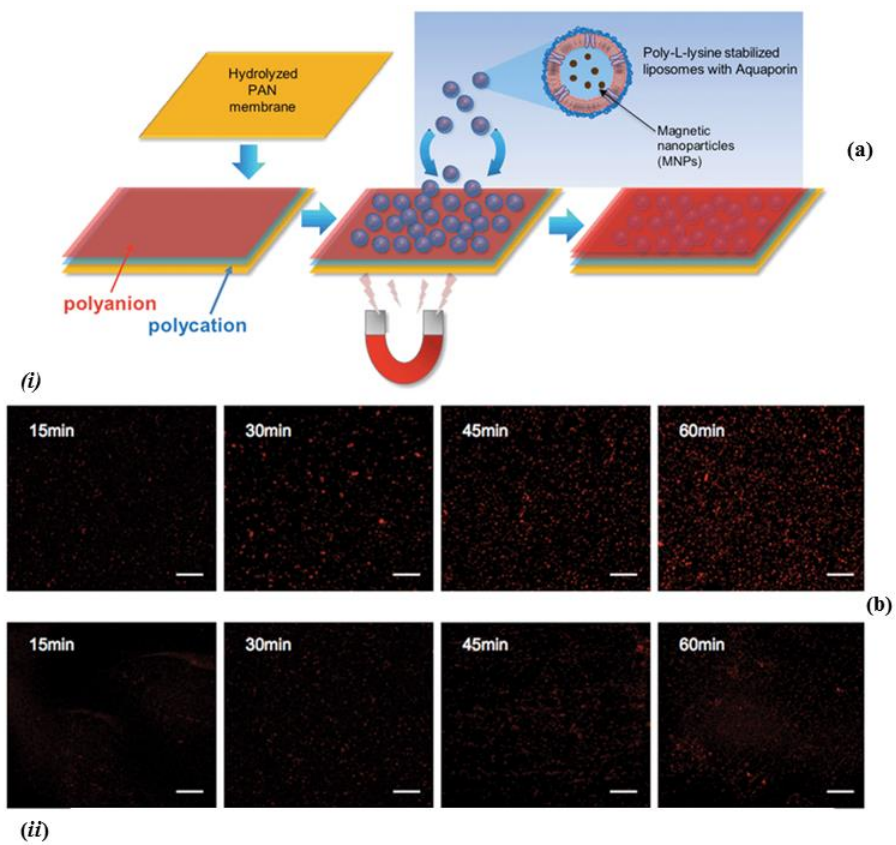


Fig. 17.

Table Captions

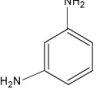
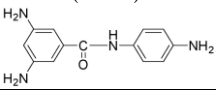
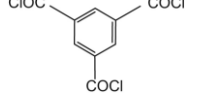
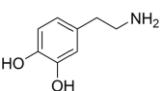
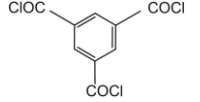
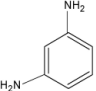
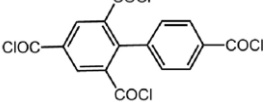
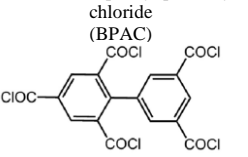
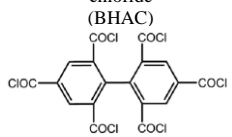
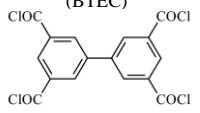
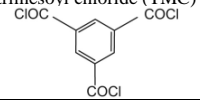
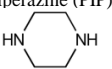
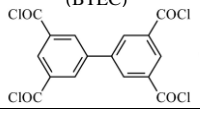
Table 1. Summary of selection of monomers or reactants for fabricating active layers of TFC membranes and their properties reported in recent literature.

Table 2. Fabrication and properties of recently reported MMMs for water desalination.

Table 3. Overview of the separation performances and testing conditions of TFC FO membranes fabricated on different support materials.

Table 4. Summary of commercially available RO and FO membranes developed thus far.

Table 1.

Aqueous phase monomers	Organic phase monomers	Properties	Ref.
<p><i>m</i>-phenylenediamine (MPD);</p>  <p>3,5-diamino-<i>N</i>-(4-aminophenyl) benzamide (DABA)</p> 	<p>trimesoyl chloride (TMC)</p> 	<p>More flexible, more hydrophilic, smoother and thinner as increasing DABA concentration; improved flux from 37.5 LMH (0 w/v% DABA) to 55.4 LMH (0.25 w/v% DABA) with salt rejection of 98.4% - 98.1% (20 bar and 2,000 ppm NaCl solution).</p>	<p>[124]</p>
<p>dopamine</p> 	<p>trimesoyl chloride (TMC)</p> 	<p>Hydrophilic surface; lower flux and higher rejection at pH >6, by increasing reaction time and temperature, or monomer concentration; good chemical stability.</p>	<p>[475]</p>
<p><i>m</i>-phenylenediamine (MPD)</p> 	<p>2,4,4',6'-biphenyl tetraacyl chloride (BTAC)</p>  <p>2,3',4,5',6-biphenyl pentaacyl chloride (BPAC)</p>  <p>2,2',4,4',6,6'-biphenyl hexaacyl chloride (BHAC)</p>  <p>3,3',5,5'-biphenyl tetraacyl chloride (BTEC)</p>  <p>trimesoyl chloride (TMC)</p> 	<p>Decreasing film thickness and roughness in the order of MPD-TMC, MPD-BTAC, MPD-BPAC, and MPD-BHAC; surface hydrophilicity in the order of MPD-BTAC ≈ MPD-BPAC > MPD-TMC > MPD-BHAC; 43.3 LMH, 31.2 LMH, and 22.1 LMH for MPD-BTAC, MPD-BPAC, MPD-BHAC compared with 54.1 LMH for MPD-TMC with similar rejection of ~99.0% at 15.5 bar and 2000 ppm NaCl feed. Hollow MPD-BTEC fibre membrane featuring three-layer structure: a loose low crosslinked initial layer, a high cross-linked dense middle layer and a loose low cross-linked surface layer; lower flux and higher rejection by longer immersion time in MPD or higher concentration of MPD or BTEC; increased rejection from ~47% to 98% and reduced flux from ~17 LMH to 4.5 LMH by increasing reaction time (7 bar and 1,000 ppm NaCl).</p>	<p>[114, 476]</p>
<p>piperazine (PIP)</p> 	<p>3,3',5,5'-biphenyl tetraacyl chloride (BTEC)</p> 	<p>Positively charged surface; higher rejection with reduced flux at greater monomer concentration; PIP-BTEC: 56.6 LMH and 58% NaCl rejection; PIP-BHAC: 49.7 LMH and 59.6% (500 ppm NaCl and 4</p>	<p>[477, 478]</p>

Field Code Changed

Field Code Changed

Field Code Changed

Field Code Changed

Field Code Changed

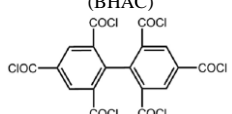
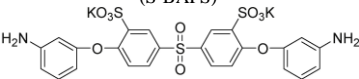
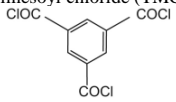
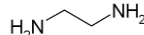
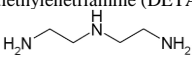
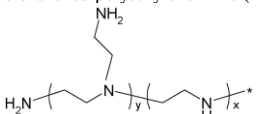
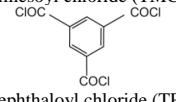
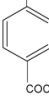
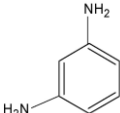
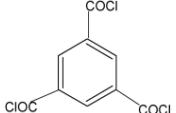
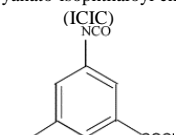
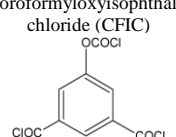
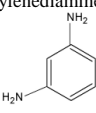
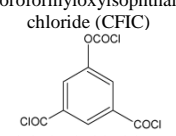
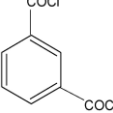
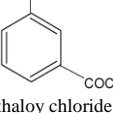
Field Code Changed

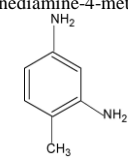
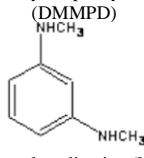
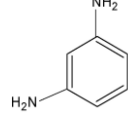
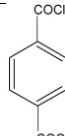
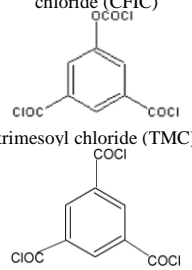
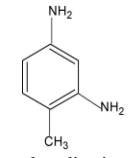
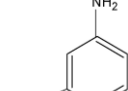
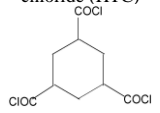
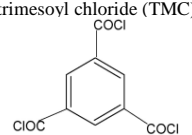
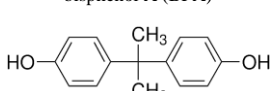
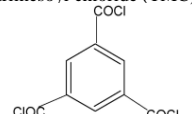
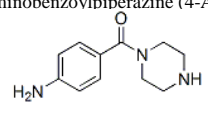
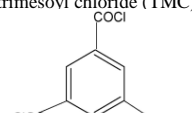
Field Code Changed

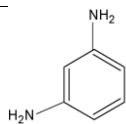
Field Code Changed

Field Code Changed

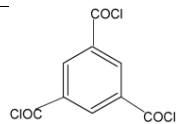
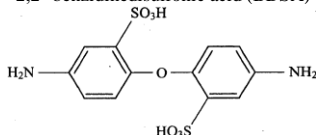
Field Code Changed

	<p>2,2',4,4',6,6'-biphenyl hexaacyl chloride (BHAC)</p> 	bar).	
<p>disulfonated bis[4-(3-aminophenoxy)phenyl]sulfone (S-BAPS)</p> 	<p>trimesoyl chloride (TMC)</p> 	<p>Greater flux with reduced rejection at lower TMC or higher S-BAPS concentration; 55 LMH with NaCl rejection of 87.9 % at 15.5 bar and 2,000 ppm NaCl; lower chlorination tolerance than MPD-TMC TFC.</p>	<p>[479] Field Code Changed Field Code Changed</p>
<p>ethylenediamine (EDA)  diethylenetriamine (DETA)  hyperbranched polyethyleneimine (PEI) </p>	<p>trimesoyl chloride (TMC);  terephthaloyl chloride (TPC) </p>	<p>Negatively charged surfaces for EDA-TMC and DETA-TMC; positively charged surfaces for PEI-TPC and PEI-TMC; PEI-TMC, DETA-TMC, PEI-TPC, EDA-TMC membranes had fluxes of ~38 LMH, 17.3 LMH, 12.4 LMH, and 4.7 LMH with varied rejections depending on different ions (1,000 ppm feed and 4 bar).</p>	<p>[125] Field Code Changed Field Code Changed</p>
<p><i>m</i>-phenylenediamine (MPD) </p>	<p>trimesoyl chloride (TMC);  5-isocyanato-isophthaloyl chloride (ICIC)  chloroformyloxisophthaloyl chloride (CFIC) </p>	<p>Decreasing skin layer thickness, roughness and chlorine stability, as well as increasing adsorption and hydrophilicity in the order of MPD-CFIC, MPD-TMC, MPD-ICIC; negatively charged membrane surface; 40 LMH, 48 LMH, 58 LMH and rejection of >98% for MPD-CFIC, MPD-TMC, and MPD-ICIC (2,000 ppm NaCl feed solution and 16 bar).</p>	<p>[132] Field Code Changed Field Code Changed</p>
<p><i>m</i>-phenylenediamine (MPD) </p>	<p>chloroformyloxisophthaloyl chloride (CFIC)  isophthaloyl chloride (IPC)  terephthaloyl chloride (TPC) </p>	<p>Improved separation by adding IPC or/and TPC in MPD-CFIC (~39 LMH and 99.45%), using hexane (38.8 LMH and 99.23%), optimizing curing (42.5 LMH and 99.46%) and post-treatment (41 LMH and 99.41%) (35,000 ppm NaCl feed solution and 55 bar).</p>	<p>[129] Field Code Changed Field Code Changed</p>

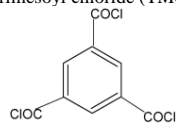
<p><i>m</i>-phenylenediamine-4-methyl (MMPD)</p>  <p><i>N,N'</i>-dimethyl-<i>m</i>-phenylenediamine (DMMPD)</p>  <p><i>m</i>-phenylenediamine (MPD)</p> 	 <p>chloroformylisophthaloyl chloride (CFIC)</p>  <p>trimesoyl chloride (TMC)</p>	<p>Improved chlorine stability up to 8000 ppm h; lower rejection ratio (~95%) and flux (~23 LMH) for MMPD-CFIC@CFIC-DMMPD, compared with MPD-TMC TFC (~36 LMH and 97%) (2,000 ppm NaCl feed and 15.5 bar).</p>	<p>[134]</p> <p>Field Code Changed</p> <p>Field Code Changed</p>
<p><i>m</i>-phenylenediamine-4-methyl (MMPD)</p>  <p><i>m</i>-phenylenediamine (MPD)</p> 	<p>cyclohexane-1,3,5-tricarboxyl chloride (HTC)</p>  <p>trimesoyl chloride (TMC)</p> 	<p>MMPD-HTC, MMPD-TMC, MPD-HTC, and MPD-TMC membrane had rejections of 97.5, 98.3, 98.2, and 99.2%, and fluxes of 53.2 LMH, 34.8 LMH, 89.6 LMH, and 52.6 LMH (1,500 ppm NaCl feed and 15 bar); improved rejection and reduced flux of MMPD-HTC by increasing reaction (10 s - 20 s), pH (7.5 -9.5), HTC concentration, curing temperature and time; MMPD-HTC had a chlorine resistance of ~3,000 ppm h and good stability over 3 months.</p>	<p>[480]</p> <p>Field Code Changed</p> <p>Field Code Changed</p>
<p>bisphenol A (BPA)</p> 	<p>trimesoyl chloride (TMC)</p> 	<p>Decreasing water permeance by increasing IP time and BPA concentration; more susceptible to humic acid foulant at pH = 3; lower fouling by TFC fabricated with 2w/v% BPA in 10 s IP.</p>	<p>[481]</p> <p>Field Code Changed</p> <p>Field Code Changed</p>
<p>4-aminobenzoylpiperazine (4-ABP)</p> 	<p>trimesoyl chloride (TMC)</p> 	<p>Decreasing flux and salt rejection at greater 4-ABP concentration and curing temperature; increasing flux but lower rejection at higher TMC concentration; NaCl rejection of ~20% and flux of 46 LMH for the TFC prepared with 1% 4-ABP, 0.25% TMC, cured at 70 °C for 15 min (1,500 ppm NaCl and 4 bar).</p>	<p>[482]</p> <p>Field Code Changed</p> <p>Field Code Changed</p>
<p><i>m</i>-phenylenediamine (MPD)</p>	<p>trimesoyl chloride (TMC)</p>	<p>Smoother and enhanced negatively charged at greater BDSA content;</p>	<p>[483]</p> <p>Field Code Changed</p> <p>Field Code Changed</p>



2,2'-benzidinedisulfonic acid (BDSA)

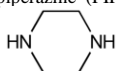


trimesoyl chloride (TMC)

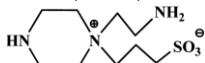


increased pure water flux from 22 LMH to 45 LMH with NaCl and MgCl₂ rejection of above 97.5% and 98.4% for TFC prepared with 0% to 10% BDSA in MPD solution (at 16 bar).

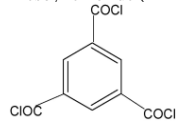
piperazine (PIP)



N-aminoethyl piperazine propane sulfonate (AEPPS)



trimesoyl chloride (TMC)

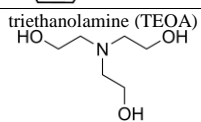


Increased size of nodular structures and hydrophilicity at greater AEPPS; improved flux from ~25.5 LMH to 46 LMH with slight decrease of NaCl rejection from 30% to 26% when AEPPS from 0 wt% - 1.05 wt% (1,000 ppm NaCl and 6 bar); improved antifouling property by adding AEPPS.

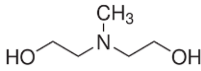
[135]

Field Code Changed

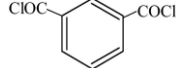
Field Code Changed



N-methyl-diethanolamine (MDEOA)



isophthaloyl chloride (IPC)



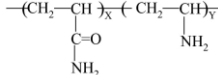
Best pure water flux (16 LMH) for TFC membrane fabricated at 3 w/v% LiBr in TEOA solution (6 bar); lower pure water flux but improved rejection when adding LiBr in MDEOA solution; more hydrophilic surface by adding LiBr.

[122]

Field Code Changed

Field Code Changed

polyamine polyvinylamine (PVAm)



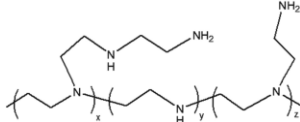
Rejection and water flux affected by PVAm and IPC concentration; good stability (~ 25 LMH and 93% rejection) for 90 days at 1,000 ppm MgSO₄ and 6 bar.

[484]

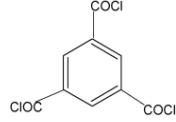
Field Code Changed

Field Code Changed

branched polyethyleneimine (PEI)



trimesoyl chloride (TMC)



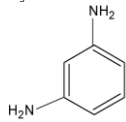
Composite hollow fibre; tightened skin layer, low pure water permeability and high rejection for composite with PEI of lower MW; higher pure water permeability and lower rejection when using high concentration PEI and low concentration TMC; performance with flux of 21.8 LMH and rejection of 96.7% (MgCl₂), 41.2% (NaCl), 54.2% (Na₂SO₄) (at 2 bar and 1,000 ppm solution).

[485]

Field Code Changed

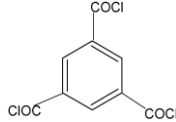
Field Code Changed

m-phenylenediamine (MPD)



o-aminobenzoic acid-triethylamine salt (o-ABA-TEA)

trimesoyl chloride (TMC)



Greater flux and comparable rejection by increasing amine salt concentration; performance affected by post-treatment; ≥98% rejection and flux of 52 LMH for the optimized membrane with 2.85 wt% o-ABA-TEA (15.5 bar and 2,000 ppm NaCl).

[127,

128,

160]

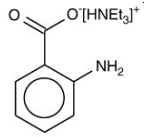
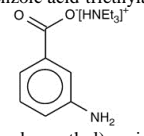
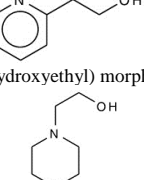
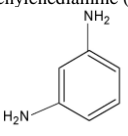
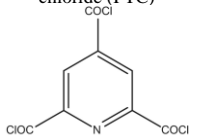
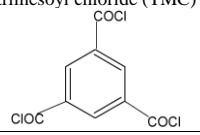
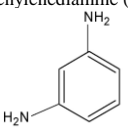
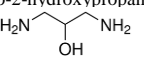
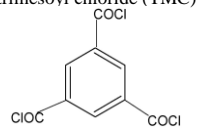
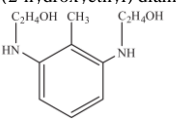
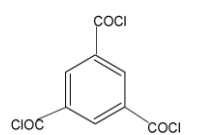
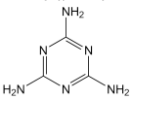
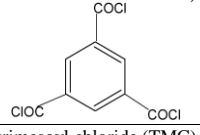
Field Code Changed

Field Code Changed

Field Code Changed

Field Code Changed

By introducing 1.0 wt% o-ABA-TEA, TFC had 75.4 LMH with 99.41% salt rejection under desalination of synthetic seawater at

 <p><i>m</i>-aminobenzoic acid-triethylamine salt</p>  <p>2-(2-hydroxyethyl) pyridine</p>  <p>4-(2-hydroxyethyl) morpholine</p>	<p>55.2 bar; improved antifouling property.</p>
<p><i>m</i>-phenylenediamine (MPD)</p> 	<p>2,4,6-pyridinetri-carboxylic acid chloride (PTC)</p>  <p>trimesoyl chloride (TMC)</p>  <p>A lower tendency towards bacterial attachment; best result of ~50 LMH and 92.5% rejection at 1,500 ppm and 13.8 bar.</p>
<p><i>m</i>-phenylenediamine (MPD)</p>  <p>1,3-diamino-2-hydroxypropane (DAHP)</p> 	<p>trimesoyl chloride (TMC)</p>  <p>Reduced ultrathin layer thickness and higher flux at 12.8% DAHP/MPD, whilst maintaining good rejection (96%-98%) (15 bar and 2,000 ppm NaCl).</p>
<p>bis-2,6-<i>N,N</i>-(2-hydroxyethyl) diaminotoluene</p> 	<p>trimesoyl chloride (TMC)</p>  <p>Increasing rejection with lower flux by increasing monomer concentration, and polymerization time; good stability to 200 ppm NaOCl for more than 50 h.</p>
<p>melamine</p> 	<p>trimesoyl chloride (TMC)</p>  <p>Reduced flux at higher concentration melamine, reaction time and curing temperature; better thermal and chlorine stability compared to PIP-TMC TFC membrane.</p>
<p><i>m</i>-phenylenediamine (MPD)</p>	<p>trimesoyl chloride (TMC)</p> <p>Improved hydrophilicity and antifouling without significantly</p>

[486]

Field Code Changed

Field Code Changed

[126]

Field Code Changed

Field Code Changed

[487]

Field Code Changed

Field Code Changed

[182]

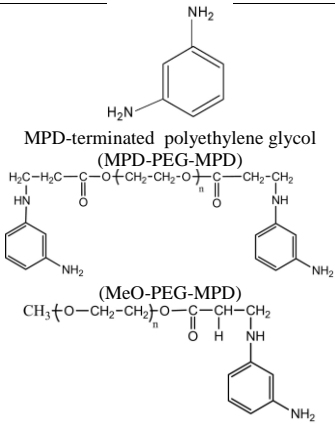
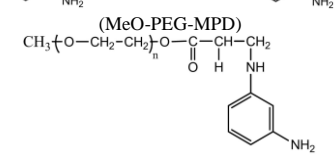
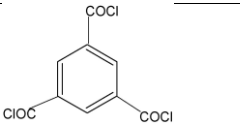
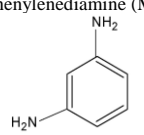
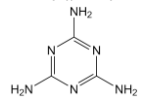
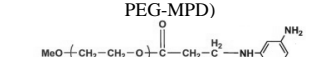
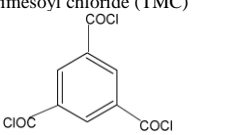
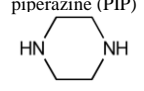
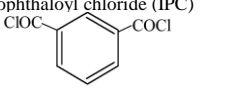
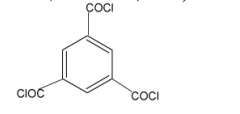
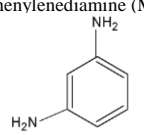
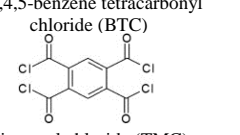
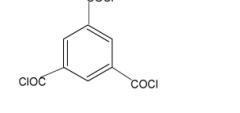
Field Code Changed

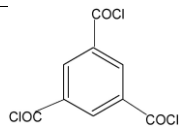
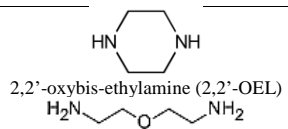
Field Code Changed

[162]

Field Code Changed

Field Code Changed

<p>MPD-terminated polyethylene glycol (MPD-PEG-MPD)</p>  <p>(MeO-PEG-MPD)</p> 		<p>affecting NaCl rejection (~95%).</p>	
<p><i>m</i>-phenylenediamine (MPD)</p>  <p>melamine</p>  <p>MPD-terminated polyethylene glycol (MeO-PEG-MPD)</p> 	<p>trimesoyl chloride (TMC)</p> 	<p>Enhanced overall antifouling property for TFC membrane prepared with 1:1:0.5 w/w ratio of MPD: melamine: MeO-PEG-MPD with flux of 38 LMH and rejection of 93% at 2,000 ppm NaCl and 14 bar.</p>	<p>[488] Field Code Changed Field Code Changed</p>
<p>piperazine (PIP)</p> 	<p>isophthaloyl chloride (IPC)</p>  <p>trimesoyl chloride (TMC)</p> 	<p>Water flux and rejection of 60.0 LMH and 51.8% for PIP-IPC at 20.7 bar and ~1,462 ppm NaCl; lower permeability, greater antifouling property and fouling reversibility of PIP-IPC than PIP-TMC.</p>	<p>[164] Field Code Changed Field Code Changed</p>
<p><i>m</i>-phenylenediamine (MPD)</p> 	<p>1,2,4,5-benzene tetracarbonyl chloride (BTC)</p>  <p>trimesoyl chloride (TMC)</p> 	<p>Optimized water flux and rejection: 31.9 LMH and 98.8% (at 15.5 bar and 2,000 ppm NaCl); improved chlorine resistance.</p>	<p>[229] Field Code Changed Field Code Changed</p>
<p>piperazine (PIP)</p>	<p>trimesoyl chloride (TMC)</p>	<p>Improved hydrophilicity, increased flux from 25.5 LMH to 41 LMH with slightly reducing rejection</p>	<p>[489] Field Code Changed Field Code Changed</p>



from 30% - 18% by increasing amount of 2,2'-OEL (7 bar and 2,000 ppm NaCl feed); good stability against fouling.

Table 2.

Polymer matrix	Inorganic filler	Preparation method	Properties (compared to parent polymeric membrane)	Ref.
PA	Ag	IP with dispersing Ag in MPD aqueous solution and using MWCNTs-incorporated PSf as support; cured at 60–70 °C.	Improved pure water flux (~20%) with comparable (88.1%) rejection when loading with 10 wt% Ag (2,000 ppm NaCl feed and 13.8 bar); enhanced surface hydrophilicity, antibacterial and antifouling properties.	[104]
PA/PES	TiO ₂ (20 ± 5 nm)	Phase inversion with TiO ₂ in NMP/1,4-dioxane solution of PAI/PEI.	Improved hydrophilicity and antifouling property; increasing rejection and pure water flux with TiO ₂ loading; good chlorine stability.	[311]
PA	TiO ₂ (20 nm)	Dip coating support in TiO ₂ ethanol solution, followed by IP and cured at 80 °C.	Greater hydrophilicity; increasing flux (21.7 LMH – 48.9 LMH) with slightly higher NaCl rejection (76% – 84%) than pristine one (12 LMH and 70%) (2,000 ppm NaCl feed); greater flux recovery and antibacterial property.	[490]
PA	AAPTS-TiO ₂ (~21 nm)	IP by dispersing functionalized TiO ₂ in MPD aqueous solution; cured at 70 °C.	Greater thermal stability; more hydrophilic and smoother; improved pure water fluxes (13 LMH – 27 LMH) than virgin one (12 LMH) at 2,000 ppm NaCl feed and 7.6 bar.	[295]
PVA	carboxylated TiO ₂ (~21 nm)	Dip coating PVDF support in PVA solution containing functionalized TiO ₂ ; crosslinked and dried at 110 °C.	Improved interfacial adhesion between filler and polymer; higher hydrophilicity; lower initial pure water fluxes but with good rejection and antifouling properties.	[329]
PA	ZnO	IP with dispersing ZnO in either TMC hexane solution or branched PEI aqueous solution; cured at 90 °C.	Improved fluxes (23 LMH – 40 LMH) with slightly lower NaCl rejection (50.1% – 57.2%) compared with the control (22 LMH and 58.4%) at 10 bar and 1,753 ppm NaCl; better ZnO distribution uniformity by dispersion in PEI aqueous phase.	[491]
PA	Silica (10-20 nm)	IP by dispersing silica in MPD/glycerol/NMP/SDS/TEA aqueous solution; cured at 80 °C.	Highest flux with 0.1 wt% of SiO ₂ (50 LMH) with rejection of >90% (44 bar and 11,000 ppm NaCl feed); greater hydrophilicity and roughness.	[492]
PA with sulfonated poly(arylene ether sulfone)	hyperbranched aromatic polyamide-grafted silica	IP; treated at 60 °C.	Comparable salt rejection (91%) and higher flux (78 LMH) than MPD-TMC PA membrane (27 LMH and 95%) at 32,000 ppm NaCl feed and 55 bar; enhanced chlorine stability.	[320]
PA with sulfonated poly(arylene ether sulfone)	hyperbranched aromatic polyamide-grafted silica	IP by dispersing silica in MPD/sulfonated poly(arylene ether sulfone)/TEA in aqueous solution; treated at 60 °C.	Higher water flux (34.5 LMH) with comparable salt rejection (97.7%) than MPD-TMC PA membrane (22.1 LMH and 98%) at 32,000 ppm NaCl feed and 55 bar; enhanced chlorine stability.	[493]
sulfonated poly(arylene ether sulfone)	mesoporous silica (100 nm)	IP with adding silica in TMC/cyclohexane solution; post-treatment.	Increasing rejection and decreasing flux up to 1 wt% SiO ₂ , followed by abrupt reduction of rejection and increase of flux; 32 LMH with 96.8% rejection for 1 wt% SiO ₂ cured at 70 °C (2,000 ppm NaCl and 15.5 bar).	[318]
PA	MCM-41 (100 nm)	IP with adding MCM-41 in TMC/hexane solution; treated at 80 °C.	More hydrophilic, negatively charged and rougher surface; better fluxes (33 LMH – 47 LMH) and comparable rejection (>97.5%) at 20.7 bar and 2,000 ppm NaCl feed.	[300]

FA	mesoporous silica (164 nm)	IP with adding silica in TMC/hexane solution; heat treatment.	Greater hydrophilicity; comparable rejection (>96%) and greater fluxes (35 LMH – 53 LMH) at 2,000 ppm NaCl feed and 16 bar.	[301]	Field Code Changed Field Code Changed
FA	ZIF-8 (~200 nm)	IP with dispersing ZIF-8 in TMC/hexane solution.	Increased flux and NaCl rejection (~51 LMH and 98.5% for 0.4 w/v% loading at 15.5 bar and 2,000 ppm NaCl feed solution); less crosslinked and more hydrophilic surface.	[340]	Field Code Changed Field Code Changed
CA/PEG	silica	Phase inversion of CA/PEG acetone solution with adding silica alkaline solution.	Better flux and rejection with adding silica; improved hydrophilicity, thermal and mechanical stability.	[494]	Field Code Changed Field Code Changed
FA	amine-functionalized EMT zeolite	IP with dispersing zeolite in aqueous solution; cured at 60 °C.	Better flux (37.8 LMH) and comparable rejection (98.8%) at 55 bar and 32,000 ppm NaCl feed.	[339]	Field Code Changed Field Code Changed
FA	octadecyltrichloro silane-modified NaA zeolite (100 nm)	IP with adding zeolite in TMC/hexane solution; cured at 60°C.	Better hydrophilicity; similar or greater fluxes (17.5 LMH – 41 LMH) and improved rejections (94% – 98.5%) (2000 ppm NaCl feed and 16 bar).	[302]	Field Code Changed Field Code Changed
FA	silicalite (50-110 nm)	IP with adding zeolite in TMC/hexane solution; heat treated at 65 °C.	Highest fluxes (9.9 LMH) and lowest rejection (50%) with 0.5 w/v% of zeolite in solution (at 2,000 ppm NaCl feed and 34.5 bar).	[287]	Field Code Changed Field Code Changed
FA	NaA zeolite (250 nm)	IP with dispersing zeolite in TMC/hexane solution and using zeolite-PSf or pure PSf; heat treated at 82 °C.	More stable flux; improved hydrophilic and more negatively charged smooth surface.	[103]	Field Code Changed Field Code Changed
FA	NaA zeolite (~250 nm)	IP with dispersing zeolite (0.2 wt%) in TMC/Isopar-G solution; post-treatment.	Post-treatment changed molecular structure of membranes; comparison with commercially SWRO membrane.	[305]	Field Code Changed Field Code Changed
FA	NaX zeolite (40-150 nm)	IP with dispersing zeolite in TMC/hexane solution; heat cured at 70 °C.	Smoother, more hydrophilic, and thinner membrane with larger pore sizes; improved fluxes (8.8 LMH – 13.3 LMH) and comparable rejection (~95%) at 12 bar and 2,000 ppm NaCl feed.	[306]	Field Code Changed Field Code Changed
FA	NaA zeolite (70-80 nm)	IP with dispersing zeolite in TMC/hexane or MPD/aqueous solution.	Greater fluxes (23 LMH – 33 LMH) and rejection (~97.5%) when loading of zeolite was \geq 0.025 w/v% in organic phase (at 2,000 ppm NaCl feed and 16 bar).	[307]	Field Code Changed Field Code Changed
FA	NaY zeolite (~250 nm)	Pre-seeding assisted IP with dispersing zeolite in TMC hexane/ethanol solution.	Compact and flat surface morphology; higher flux (17.3 LMH – 37.3 LMH) and comparable salt rejection (87.8% - 97.6%) with loading of 0.05 wt% - 0.6 wt% at 15 bar and 2,000 ppm NaCl feed.	[308]	Field Code Changed Field Code Changed
FA	NaY zeolite (~100-200 nm)	IP by dispersing zeolite in MPD/CSA-TEA/SLS aqueous solution; post-treatment.	Increasing flux from 39.6 LMH without zeolite to 74.2 LMH with 0.15 wt% zeolite; rejection \geq ~98%; 85.9 LMH with 98.4% rejection achieved by optimizing post-treatment (at 2,000 ppm NaCl feed and 15.5 bar).	[337]	Field Code Changed Field Code Changed
FA	NaA zeolite and silicalite-1 (50-150 nm)	IP with dispersing zeolite in TMC/hexane; heat cured at 60 °C.	Improved hydrophilicity; increasing flux from 20 LMH (without zeolites) to 33.9 LMH (NaA) and 66.6 LMH (silicalite-1) with >95% rejection (16 bar and 2,000 ppm NaCl feed); excellent acid and multivalent ion resistance by silicalite-1.	[338]	Field Code Changed Field Code Changed
FA	zwitterion-functionalized CNTs	IP on PES layer after depositing of SWCNTs <i>via</i> vacuum filtration.	Increasing water flux (23.8 LMH – 48.5 LMH) and slightly changed rejection ratio (>93%) as increasing fraction of CNTs, compared with 11.5 LMH and 97.6% of pristine membrane (1,000 ppm Na ⁺ feed and 36.5 bar).	[352]	Field Code Changed Field Code Changed

PA	acid-modified CNTs	IP with dispersing CNTs (0.002 wt %) in MPD aqueous solution; treated at 100 °C.	Higher water flux (47 LMH – 85 LMH) and variable salt rejection (5% – 92%) in relative to the virgin membrane (~37 LMH and 90%) at 15.5 bar and 2,000 ppm NaCl feed solution; membrane separation performance affected by functionalization of CNTs; greater stability.	[349]	Field Code Changed Field Code Changed
polyester	acid-modified MWCNTs	Improved IP with dispersing MWCNTs in TEOA-surfactant aqueous solution; post-treated at 60 °C.	Higher roughness and hydrophilicity; highest pure water flux and rejection with 0.5 mg/mL MWCNTs; good stability in long-term separation.	[315], [316]	Field Code Changed Field Code Changed Field Code Changed
PES	TiO ₂ coated MWCNTs (diameter = 25 nm; length = 0.5-1 µm)	Phase inversion with dispersing TiO ₂ -coated MWCNTs in PES/PVP/DMAc.	Greater porosity, hydrophilicity, and pure water flux (4.35 LMH – 5.66 LMH) with addition of fillers (0.1 wt% – 1 wt%), compared with bare membrane (3.71 LMH at 5 bar); improved antifouling property.	[312]	Field Code Changed Field Code Changed
PES	acid-modified MWCNTs	Phase inversion with dispersing MWNTs in PES/PVP/DMAc.	Less roughness, better fluxes and rejection, improved antifouling property by adding MWCNTs; best antifouling when 0.04 wt% MWCNTs.	[317]	Field Code Changed Field Code Changed
PAA/PAH	acid-modified MWCNTs	LbL assembly with dispersing MWCNT in PAA aqueous solution; cured at 180 °C under vacuum.	Improved chlorine stability and lower salt rejection (~90% with flux of 2 LMH – 4 LMH at 15.5 bar and 2,000 ppm) than the PA membrane.	[314]	Field Code Changed Field Code Changed
PA	acid-modified MWCNTs	IP with dispersing MWCNTs in MPD aqueous solution; cured at 60 °C.	More hydrophilic surface, greater fluxes (25 LMH – 71 LMH) and lower rejection (94% – 81.5%) with increasing loading of MWNTs (0 w/v% – 0.1 w/v%) (16 bar and 2,000 ppm).	[296]	Field Code Changed Field Code Changed
PA	MWCNTs modified with acid and diisobutyl peroxide	IP with dispersing MWCNTs in MPD aqueous solution; cured at 60 °C.	Higher flux (15 LMH – 28 LMH) with slight decreased rejection (95% - 90%), at greater amount of MWCNTs (0% - 0.1%) (2,000 ppm NaCl and 16 bar); improved hydrophilicity, better antifouling and chlorine stability.	[348]	Field Code Changed Field Code Changed
PA	poly(methyl methacrylate)-modified MWCNTs	IP with dispersing MWCNTs in TMC/toluene solution; cured at 80 °C.	Improved pure water flux and NaCl rejection by adding MWCNTs up to 0.67g/L MWCNTs followed by a drop; best with 62% flux improvement over the TFC membrane.	[495]	Field Code Changed Field Code Changed
PA	hydrophilized ordered mesoporous carbon	IP with dispersing carbon in MPD aqueous solution; cured at 60–70 °C.	Greater hydrophilicity; decreasing NaCl rejection from 68.2% to 45% with 0 wt% -6 wt% carbon; increasing pure water flux till with >5 wt% carbon followed by a decrease.	[298]	Field Code Changed Field Code Changed
PA	aluminosilicate SWNTs (diameter ~ 2.7 nm; length = 150 nm)	IP with dispersing aluminosilicate SWNTs in TMC/hexane solution.	Increasing pure water flux from 7.5 LMH to 16 LMH when SWNTs loading from 0 w/v% to 0.2 w/v% at 12 bar; slightly higher NaCl rejection of ~96% with SWNTs.	[496]	Field Code Changed Field Code Changed
PA	acid-functionalized CNTs, GO or mixture	IP with dispersing CNTs, GO or mixture in MPD aqueous solution; heated at 100 °C.	Best performance for PA membranes with CNTs (44.2 LMH and 96.8%), GO (39.2 LMH and 97.0%), and CNTs/GO (59.0 LMH and 96.2%) when using 0.001 wt%, 0.001 wt%, and 0.02 wt% carbon nanomaterials in MPD solution (15.5 bar and 2,000 ppm NaCl); improved mechanical strength, durability, and chlorine resistance.	[291]	Field Code Changed Field Code Changed
PA	halloysite nanotubes (inner	IP with dispersing halloysite in TMC/cyclohexane solution; cured at	Improved hydrophilicity; increasing flux from 19 LMH (TFC) to 36 LMH (TFN	[497]	Field Code Changed Field Code Changed

	diameter: 5 nm - 15 nm)	90 °C.	with 0.05 w/v% halloysite) and slight change of rejection from 97.2% to 95.6% at 15 bar and 2,000 ppm NaCl; improved antifouling capacity.		
PA	amino - functionalized titanate nanotubes (OD =5–25 nm)	IP with dispersing titanate in TMC/cyclohexane solution; cured at 90 °C.	Improve fluxes (26 LMH – 58 LMH) and comparable rejection (>85%) (with loading of 0.01 w/v% - 0.1 w/v%) at 2,000 ppm NaCl feed and 15 bar; good antifouling property.	[498]	Field Code Changed Field Code Changed
PA	GO	IP with dispersing GO in MPD aqueous solution; cured at 60 °C.	Improved flux up to 25 LMH followed by a decline of flux when GO loading > 0.20 wt%; ~90% rejection at 15 bar and 2,000 ppm NaCl; excellent antifouling properties towards BSA and humic acid.	[499]	Field Code Changed Field Code Changed
PA	GO	IP with dispersing GO in MPD aqueous solution.	Reduced roughness and thickness; increased hydrophilicity and anti-biofouling property; good chlorination stability; improved flux from 9 LMH (control) to 16.6 LMH (38 ppm GO in MPD solution) with high rejection ratio of >99% at 2,000 ppm NaCl feed and 15.5 bar.	[358]	Field Code Changed Field Code Changed
PA	GO	IP with dispersing GO in MPD aqueous solution; cured at 70 °C.	Increasing flux with sacrificed salt rejection; strong antibacterial activity.	[500]	Field Code Changed
PA	TiO ₂ -decorated rGO	IP with dispersing TiO ₂ /rGO in MPD/CSA-TEA aqueous solution; cured at 70 °C.	Reduced roughness and higher hydrophilicity; improved chlorine resistance; increasing flux from 43 LMH to 51 LMH with rejection of >98.5% when adding 0.002 wt% - 0.02 wt% TiO ₂ /rGO (15 bar and 2,000 ppm NaCl feed).	[359]	Field Code Changed Field Code Changed Field Code Changed
PA	POSS	IP with dispersing POSS in MPD aqueous solution.	Improved water flux (44.6 LMH) and rejection (99.6%) compared with the PA (33.7 LMH and 99.0%) at 32,000 ppm NaCl feed and 55 bar.	[292]	Field Code Changed Field Code Changed
PA	POSS	IP with dispersing POSS in either TMC/hexane solution or MPD aqueous solution.	Tailorable membrane chemistry and performance by varying types and amount of POSS.	[293]	Field Code Changed Field Code Changed
CA	CA-anchored POSS	Phase inversion with CA-anchored POSS/CA/acetone/formamide solution.	Higher flux (2 LMH – 9 LMH) and lower salt rejection (9% – 15%) at 2,000 ppm NaCl and 10 bar when 0.5 wt% - 5wt% CA-POSS; better compaction resistance and lower mechanical strength.	[319]	Field Code Changed Field Code Changed

Table 3.

Support	Structure	Performance				Testing condition		Ref.
		AL-FS (FO)		AL-DS (PRO)		Feed solution	Draw solution	
		Water flux (LMH)	Salt flux (gMH)	Water flux (LMH)	Salt flux (gMH)			
PSf	flat sheet	9.5/12.0	2.4/4.9	18.1/20.5	6.3/5.9	10 mM NaCl	0.5 M NaCl	[29] Field Code Changed
PSf	flat sheet	20.1	2.0	33.1	2.6	DI water	0.5 M NaCl	[405] Field Code Changed
PSf/SPEK	flat sheet	35	7	50	9	DI water	2.0M NaCl	[393] Field Code Changed
PES/PESU-co-sPPSU	flat sheet	21.0	2.2	33	2.8	DI water	2.0 M NaCl	[399] Field Code Changed
sPPSU	flat sheet	48	7.6	54	8.8	DI water	2.0 M NaCl	[501] Field Code Changed
hydrolysed CTA (further modified by linking molecule)	flat sheet	–	–	2.4-6.7	8.0-47.8	DI water	1.5 M NaCl	[413, 414] Field Code Changed
PDA-modified PSf	flat sheet	8.2	1.4	24	1.8	DI water	2.0 M NaCl	[411] Field Code Changed
PSf/PES	flat sheet	27.6	37.5	–	–	DI water	2.0 M NaCl	[502] Field Code Changed
PES/SPSf ⁽¹⁾	flat sheet	26.0	8.3	47.5	12.4	DI water	2.0 M NaCl	[398] Field Code Changed
carboxylated PSf	flat sheet	18	2.2	27	5.5	DI water	1.0 M MgCl ₂	[403] Field Code Changed
PSf-PET fabric	flat sheet	0.5-25	95.8-99.3 ⁽²⁾	–	–	DI water	1.0 M NaCl	[397] Field Code Changed
PSf-PET fabric	flat sheet	18.2	97.4% ⁽³⁾	–	–	DI water	1.5 M NaCl	[378] Field Code Changed
PSf-PET fabric	flat sheet (co-casting)	60.3	17.6	31.1	8.5	DI water	1.0 M NaCl	[404] Field Code Changed
PSf/silica (3 wt%)-PET fabric	flat sheet (co-casting)	31.0	7.4	60.5	16.0	DI water	1.0 M NaCl	[406] Field Code Changed
PSf/TiO ₂ (0.5 wt%)	flat sheet	17.1	2.9	31.2	6.7	10 mM NaCl	0.5 M NaCl	[416] Field Code Changed
PSf/ rGO-modified graphitic carbon nitride (0.5 wt%)	flat sheet	41.4	9.6	–	–	DI water	2.0 M NaCl	[422] Field Code Changed
PSf/zeolite (0.5 wt%)	flat sheet	40	28	86	57	DI water	2 M NaCl	[420] Field Code Changed
PES/MWCNTs (2.0 wt%)	flat sheet	–	–	12	94.7(%)	10 mM NaCl	2 M glucose	[419] Field Code Changed
PVDF nanofiber	flat sheet	11.6/28	3.5/12.9	30.4/47.6	6.4/21.6	DI water	1.0 NaCl	[384] Field Code Changed
PETA nanofibre-PSf	flat sheet	12.9	96.8 ⁽⁴⁾	–	–	DI water	1.0 M NaCl	[381] Field Code Changed
CA/PAN nanofiber-PET fabric	flat sheet	27.6	3.85	43	1.7	DI water	1.5 M NaCl	[380] Field Code Changed
PETA/PVA nanofiber	flat sheet	–	–	47.2	9.5	DI water	0.5 M NaCl	[379] Field Code Changed
polyketone	flat sheet	12.6-29.3	2.0-3.8	22.6-41.5	2.8-5.0	DI water	0.6 M NaCl	[395] Field Code Changed
PAN	flat sheet	9.25/9.25	5.8/6.4	11.6/13.9	5.8/6.4	DI water	0.5 M NaCl	[396] Field Code Changed
nylon 6,6 microfiltration membrane	flat sheet	6	0.7	21.5	0.8	DI water	1.5 M NaCl	[401, 412] Field Code Changed
CAP	flat sheet	80.1	10.0	128.8	19.4	DI water	2.0 M NaCl	[408] Field Code Changed
CAP ⁽¹⁾	flat sheet	–	–	31.8/35.0	1.6/1.9	DI water	2.0 M NaCl	[400] Field Code Changed
PEI/PAA-coated hydrolyzed PAN-PET fabric	flat sheet	24.6	2.4	32.9	3.8	DI water	0.5 M NaCl	[503] Field Code Changed
hydroxyl functionalized PTA-POD	flat sheet	37.5	5.5	78.4	12.3	DI water	1.0 M NaCl	[394] Field Code Changed
PES	hollow fibre	16.7-18.7	1.2-2.0	43.6-49.4	2.8-4.0	DI water	0.5 M NaCl	[391] Field Code Changed
PES	hollow fibre	–	–	42.6	4.0	DI water	0.5 M NaCl	[390] Field Code Changed
PES	hollow fibre	5/14	2.1/1.8	12.9/32.2	5.0/3.5	DI water	0.5 M NaCl	[386] Field Code Changed
PES	hollow fibre	32.1-	6.2-9.9	57.1-65.1	6.9-12.3	DI water	2.0 M NaCl	[389] Field Code Changed

34.5									
PES	hollow fibre (double-skinned) ⁽⁵⁾	14.2-17.3	3.5-4.2	32.7-38.4	3.6-4.0	DI water	0.5 M NaCl	[430]	Field Code Changed
PAI	hollow fibre (double-skinned) ⁽⁵⁾	16.9	16	41.3	5.2	DI water	2.0 M NaCl	[429]	Field Code Changed
Matrimid®	hollow fibre (tri-bore)	11.8	2.5	50.5	3.5	DI water	2.0 M NaCl	[387]	Field Code Changed

⁽¹⁾ TFC membranes were made of PPD-TMC PA active layer; others in Table 3 were fabricated from MPD-TMC IP.

⁽²⁾ NaCl salt rejection % in RO at 27.6 bar and 50 mM NaCl solution.

⁽³⁾ NaCl salt rejection % in RO at a pressure drop of 27.2 bar and 50 mM NaCl feed solution.

⁽⁴⁾ NaCl salt rejection % in RO at 13.8 bar and 50 mM NaCl feed solution.

⁽⁵⁾ Double-skinned FO hollow fibres were made of two selective layers: RO layer (MPD-TMC) and NF layer (PAI-PEI or crosslinked PSS/PAH).

Table 4. Summary of commercially available RO and FO membranes developed thus far.

Membrane	Advantages	Disadvantages	Application
CA asymmetric	<ul style="list-style-type: none"> • Low cost; • Chlorine tolerance. 	<ul style="list-style-type: none"> • Limited chemical resistance; • Susceptibility to biodegradation; • Narrow pH and temperature operating range; • Low permeability. 	RO and FO
PA TFC	<ul style="list-style-type: none"> • Wide operating pH and temperature range; • High flux and salt retention; • Good structure durability and mechanical strength; • Wide application in desalination. 	<ul style="list-style-type: none"> • Limited chlorine and fouling resistance. 	RO and FO
zeolite-PA TFN	<ul style="list-style-type: none"> • As above to PA TFC; • Reduced feed pressure required. 	<ul style="list-style-type: none"> • As above to PA TFC; • High cost; • Improvement needed for removal of some pollutants, e.g. boron. 	RO
Aquaporin	<ul style="list-style-type: none"> • High permeability and good rejection. 	<ul style="list-style-type: none"> • High cost; • Limited data available, e.g. regarding to its long term operation. 	FO